Dcp2 C-terminal *Cis*-Binding Elements Control Selective Targeting of the Decapping Enzyme by Forming Distinct Decapping Complexes

Feng He[1], Chan Wu[1], and Allan Jacobson[1]

[1]Department of Microbiology and Physiological Systems

University of Massachusetts Medical School

368 Plantation Street

Worcester, MA 01655

Running title: Regulation of mRNA decapping target specificity

Keywords: mRNA decay, NMD, Dcp1, Dcp2, Edc3, Upf1, Pat1, Xrn1

Correspondence
feng.he@umassmed.edu
allan.jacobson@umassmed.edu

Highlights

Loss of Dcp2 *cis*-binding elements causes selective stabilization of distinct decapping substrates

Dcp2 *cis*-binding elements promote the assembly of target-specific decapping complexes *in vivo*

Xrn1 binds to Dcp2, and both Edc3 and Xrn1 are common components of multiple decapping complexes

Upf1, Edc3, and Pat1 function as unique targeting subunits of the yeast holo-decapping enzyme

SUMMARY

A single Dcp1-Dcp2 decapping enzyme targets diverse classes of yeast mRNAs for decapping-dependent 5' to 3' decay, but the molecular mechanisms controlling selective mRNA targeting by the enzyme remain elusive. Through extensive genetic analyses we uncover *cis*-regulatory elements in the Dcp2 C-terminal domain that control selective targeting of the decapping enzyme by forming distinct decapping complexes. Two Upf1-binding motifs target the decapping enzyme to NMD substrates, and a single Edc3-binding motif targets both Edc3 and Dhh1 substrates. Pat1-binding leucine-rich motifs target Edc3 and Dhh1 substrates under selective conditions. Although it functions as a unique targeting component of specific complexes, Edc3 is a common component of multiple complexes. Xrn1 also has a specific Dcp2 binding site, allowing it to be directly recruited to decapping complexes. Collectively, our results demonstrate that Upf1, Edc3, and Pat1 function as regulatory subunits of the holo-decapping enzyme, controlling both its targeting specificity and enzymatic activation.

INTRODUCTION

Decapping, the removal of mRNA 5' cap structures, is a fundamental step in eukaryotic mRNA turnover that commits a transcript to complete 5' to 3' exoribonucleolytic digestion by Xrn1 (Grudzien-Nogalska and Kiledjian, 2017; Parker, 2012). Decapping plays a key role in general 5' to 3' mRNA decay (Decker and Parker, 1993), nonsense-mediated mRNA decay (NMD) (He and Jacobson, 2001), AU-rich element-mediated mRNA decay (Fenger-Gron et al., 2005; Pedro-Segura et al., 2008), microRNA-mediated gene silencing (Behm-Ansmant et al., 2006; Rehwinkel et al., 2005) and transcript-specific degradation (Badis et al., 2004; Dong et al., 2007). In yeast, mRNA decapping is carried out by a single enzyme comprised of the Dcp1 regulatory subunit and the Dcp2 catalytic subunit. Dcp1 is a small EVH domain protein (Beelman et al., 1996; She et al., 2004) and Dcp2 is a 970-amino acid protein containing a highly conserved catalytic domain at its N-terminus and a largely disordered C-terminal domain embedded with multiple regulatory elements (Charenton et al., 2017; Dunckley and Parker, 1999; Gaudon et al., 1999; He and Jacobson, 2015).

In addition to the Dcp1-Dcp2 decapping enzyme, yeast mRNA decapping also requires several specific decapping activators including Upf1, Pat1, Lsm1, Dhh1, Scd6, Edc1, Edc2, and Edc3 (Parker, 2012). Upf1 is required for nonsense-containing mRNAs (He and Jacobson, 2001; He et al., 2003). Pat1, Lsm1, and Dhh1 were originally thought to be required for general mRNA decay (Bouveret et al., 2000; Coller et al., 2001; Fischer and Weis, 2002; Hatfield et al., 1996; Tharun et al., 2000), but recent evidence indicates that they each target a specific subset of yeast mRNAs (He et al., 2018). Scd6 targets a limited number of specific transcripts for decapping (Zeidan et al., 2018). Edc3 was also originally thought to be required for general mRNA decapping (Kshirsagar and Parker, 2004), but this factor exhibits exquisite substrate specificity and appears to target just two transcripts, *YRA1* pre-mRNA and *RPS28B* mRNA (Badis et al., 2004; Dong et al., 2007). Edc1 and Edc2 were isolated as high-copy suppressors of *dcp1* and *dcp2* mutations (Dunckley et al., 2001), and these two factors can stimulate mRNA decapping *in vitro* (Borja et al., 2011; Steiger et al., 2003), but they do not appear to be required for mRNA decapping in vivo. Whether Edc1 and Edc2 may also target specific mRNAs has not been investigated. Several specific functions, including translation repression, decapping enzyme activation, and codon optimality sensing have been proposed for these decapping activators (Coller and Parker, 2005; Nissan et al., 2010; Radhakrishnan et al., 2016) , but each of these proposed functions is subject to sufficient controversy to render their actual roles largely unknown (Arribere et al., 2011; He and Jacobson, 2015; Sweet et al., 2012; Webster et al., 2018).

Mechanistic investigations of mRNA decapping over the last two decades have mostly used biochemical and structural approaches and focused on the catalytic mechanisms of the decapping enzyme (Charenton and Graille, 2018; Valkov et al., 2017). These studies

provided significant insights into the structures of the Dcp1-Dcp2 decapping enzyme (She et al., 2006; She et al., 2004; She et al., 2008), its conformational dynamics (Floor et al., 2012; Wurm et al., 2017), cap- and RNA-binding properties (Deshmukh et al., 2008; Floor et al., 2010), and catalytic mechanisms (Aglietti et al., 2013). These experiments also revealed binding patterns of Edc1, Edc3, and Pat1 to the decapping enzyme and suggested potential functions of these factors in enzymatic activation (Charenton et al., 2017; Charenton et al., 2016; Fromm et al., 2012; Mugridge et al., 2018; Paquette et al., 2018; Valkov et al., 2016); Paquette et al., 2018; Valkov et al., 2016). However, these biochemical and structural studies all used C-terminally truncated Dcp2, isolated peptides or domains from the decapping activators, and generic mRNA substrates. Thus, the proposed mechanisms for decapping activation that emerged from these studies likely need additional validation. Further, these experiments did not address how the decapping enzyme is targeted to different substrate mRNAs.

Our recent genetic experiments demonstrated that the Dcp2 C-terminal domain plays a crucial role in the control of mRNA decapping (He et al., 2018; He and Jacobson, 2015). This domain contains an inhibitory element (IE) and a set of specific linear binding elements for several decapping activators, including Edc3 (E3), Upf1 (U1$_1$, U1$_2$) and Pat1 (L$_1$-L$_9$) (Figure 1A). Here we have generated specific *DCP2* deletions that eliminated either a single element or combinations of different elements and analyzed the consequences of these deletions on Dcp2 interactions with specific decapping activators and decay of different decapping substrates. Our experiments uncover the molecular mechanisms that control the selective targeting of the yeast decapping enzyme and reveal the functional contributions of Upf1, Edc3, and Pat1 in decapping of their respective mRNA targets.

RESULTS

Loss of Both Upf1-binding Motifs Eliminates Upf1's Binding to Dcp2 and Causes Selective Partial Stabilization of NMD Substrates

Wild-type (WT) Dcp2 exhibited a strong two-hybrid interaction with Upf1. Deletion of either the first (U1D1) or the second (U1D2) Upf1-binding motif had no discernible effect on Upf1's binding to Dcp2, but loss of both Upf1-binding motifs (U1D1-U1D2) eliminated Upf1 binding to Dcp2 (Figure 1B). In contrast, loss of both Upf1-binding motifs affected neither Edc3 nor Pat1 binding to Dcp2 (Figure 1B). These results indicate that the two Upf1-binding motifs are redundant and either can promote independent Upf1 binding to Dcp2.

5

WT yeast expressed low levels of NMD substrates, including the *CYH2* pre-mRNA and the *ade2-1, can1-100*, and *trp1-1* mRNAs. Loss of either the first or the second Upf1-binding motif had no significant effect on the levels of accumulation for each of these NMD substrates. However, loss of both Upf1-binding motifs caused approximately two- to three-fold increases in the levels of these transcripts (Figures 1C and S2, *HA-dcp2* alleles containing U1D1-U1D2). These increases were much smaller in magnitude than those caused by deletion of *UPF1*, which usually led to >10-fold increases for these transcripts. Loss of both Upf1-binding motifs did not affect the levels of the Edc3, Dhh1, Pat1/Lsm1, and Pat1/Lsm1/Dhh1 substrates (Figures 1C and S2). This selective stabilization of nonsense-containing mRNAs indicates that the two Upf1-binding motifs control targeting of the decapping enzyme to NMD substrates. In addition, the two motifs have independent activities and are functionally redundant in promoting NMD. The partial stabilization of NMD substrates caused by loss of both Upf1-binding motifs suggests that decapping is not a major rate-limiting step in the overall NMD pathway. It also appears that NMD substrates can be degraded by an alternative route in the absence of active recruitment of the decapping enzyme by Upf1.

Loss of the Edc3-binding Motif Eliminates Edc3 Binding to Dcp2 and Causes Selective Stabilization of Both Edc3 and Dhh1 Substrates

WT Dcp2 also exhibited strong two-hybrid interaction with Edc3. Loss of E3 (E3D) did not affect the binding of Upf1 or Pat1 to Dcp2 but eliminated Edc3 binding to Dcp2 (Figure 1B), indicating that the E3 motif promotes selective binding of Edc3 to the decapping enzyme. Loss of the E3 motif did not affect the levels of NMD and Pat1/Lsm1 substrates, but did lead to stabilization of the Edc3 substrates, *RPS28B* mRNA and *YRA1* pre-mRNA, to different extents (Figures 1C and S2, *HA-dcp2-E3D*). Compared to their fold increases in *edc3Δ* cells, loss of the Edc3-binding motif caused complete stabilization of *RPS28B* mRNA (~2-fold increases in both E3D and *edc3Δ* cells), but only partial stabilization of *YRA1* pre-mRNA (3-fold increase in E3D vs. 9-fold increase in *edc3Δ* cells). The different effects of loss of the E3 motif may be indicative of different roles of Edc3 in decapping of these transcripts. Decapping of *RPS28B* mRNA is likely rate-limiting and totally dependent on Edc3-mediated recruitment of the decapping enzyme. The sole function of Edc3 in *RPS28B* mRNA decay would thus be to recruit the decapping enzyme and, when this recruitment is blocked by E3 deletion, *RPS28B* mRNA is not likely degraded by an alternative pathway. In contrast, Edc3-mediated recruitment of the decapping enzyme may contribute only partially to the overall decapping process of *YRA1* pre-mRNA and Edc3 may play an additional role in the decay of this transcript. Also, when Edc3-mediated recruitment of the decapping enzyme is blocked by E3 deletion, *YRA1* pre-mRNA appears to be degraded by an alternative route, albeit less efficiently. Both possibilities were validated by experiments described below.

6

Although deletion of *EDC3* did not affect the levels of Dhh1 substrates, loss of the E3 motif caused partial stabilization of these mRNAs (Figures 1C and S2, compare *edc3Δ* vs *HA-dcp2-E3D*; He et al., 2018). This result indicates that, in addition to Edc3 substrates, E3 also controls targeting of the decapping enzyme to Dhh1-regulated mRNAs. Given the disparate mRNA decay phenotypes caused by *edc3Δ* and E3D for Dhh1 substrates, the E3-mediated targeting the decapping enzyme to Dhh1 substrates is unlikely to be carried out solely via interaction with Edc3. At least in the absence of Edc3, one additional factor may bind E3 and target the decapping enzyme to Dhh1-regulated mRNAs. A role for E3 in the decapping of Dhh1 substrates may appear surprising, but physical interactions between Edc3 and Dhh1 have been reported (He and Jacobson, 2015; Sharif et al., 2013). The partial stabilization of Dhh1 substrates caused by loss of E3 can be explained similarly as described above for *YRA1* pre-mRNA.

The *dcp2 E3D* allele contains a deletion of a conserved 37-codon segment that we identified previously as encoding the Edc3-binding element (He and Jacobson, 2015). Phylogenetic sequence analysis suggested that this segment may encode composite binding elements (Figure S1A). To further map this region, we generated two smaller deletions in the originally defined element. E3D1 eliminates the first part of the element (17 amino acids, E3-1) and E3D2 eliminates the second part (20 amino acids, E3-2). Loss of E3-2 did not affect Edc3 binding to Dcp2, but loss of E3-1 eliminated Edc3's binding to Dcp2 (Figure 1B), indicating that Edc3 binds to the conserved 17-amino acid segment. Loss of E3-1 also caused complete stabilization of *RPS28B* mRNA and partial stabilization of *YRA1* pre-mRNA and Dhh1-regulated mRNAs (Figures 1D and S1C), suggesting that the E3-1 element controls selective targeting of the decapping enzyme to both Edc3 and Dhh1 substrates.

Loss of the Pat1-binding Motifs Eliminates Pat1 Binding to Dcp2, but Has No Effect on Levels of Pat1/Lsm1-regulated mRNAs

We next focused on the nine helical leucine-rich motifs L_1 to L_9, each of which, except L_8, was shown to bind Pat1 in yeast two-hybrid and GST-pulldown assays (Charenton et al., 2017; He and Jacobson, 2015). However, whether these eight motifs are all engaged in Pat1 binding and whether they promote independent or collaborative binding of Pat1 to Dcp2 in the context of full-length protein is unknown. WT Dcp2 exhibited strong two-hybrid interaction with Pat1 and loss of the first five leucine-rich motifs (L_1 to L_5) eliminated this interaction (Figure 2A, alleles LD1-5 to LD1-9). In contrast, loss of the last four leucine-rich motifs (L_9 to L_6) did not affect Pat1 binding to Dcp2 (Figure 2A, allele L9-6). Consecutive deletions between L_1 and L_5 from either the N-terminus or the C-terminus yielded graded responses for Pat1 binding. From the N-terminus, loss of L_4 weakened and further loss of L_5 eliminated Pat1 binding (Figure 2A, alleles L1-4 and L1-5). From the

C-terminus, loss of L_4 and L_3 greatly weakened and further loss of L_2 eliminated Pat1 binding (Figure 2A, alleles LD9-4, LD9-3, and LD9-2). None of the leucine-rich element deletions affected the binding of Edc3 or Upf1 to Dcp2 (Figure 2A). These results indicate that in the context of full-length Dcp2, leucine-rich motifs L_1 to L_5 control the selective binding of Pat1 to Dcp2, most likely with a contribution from each motif, in contrast to the proposed mode for Pat1 binding to Dcp2 based on structural data (Charenton et al., 2017).

Consistent with the selective targeting of the decapping enzyme by both the Edc3 and Upf1-binding motifs, none of the leucine-rich element deletions affected the levels of the Edc3, Dhh1, or NMD substrates (Figures 2B and S3C). Surprisingly, none of the leucine-rich element deletions altered the levels of Pat1-regulated mRNAs, including both Pat1/Lsm1 and Pat1/Lsm1/Dhh1 substrates (Figures 2B and 2C). This indicates that Pat1-mediated targeting of the decapping enzyme does not make a significant contribution to the overall decay of Pat1-regulated transcripts, raising a question of the role of Pat1 in decapping. Because loss of Pat1 causes significant stabilization of both the Pat1/Lsm1 and Pat1/Lsm1/Dhh1 substrates (Figure 2B) (He et al., 2018), one possible explanation for this surprising observation is that decapping is not rate-limiting for Pat1-regulated mRNAs, and Pat1 performs an unidentified major function upstream, independent of its role in the recruitment and activation of the decapping enzyme (Lobel et al., 2019; Nissan et al., 2010).

In the Absence of Active Recruitment of the Decapping Enzyme, Different Decapping Substrates Are Still Degraded by Decapping-dependent 5' to 3' Decay

As described above, the Upf1-, Edc3-, and Pat1-binding motifs in Dcp2 promote selective binding of these factors to the decapping enzyme. Yet, loss of both Upf1-binding motifs in Dcp2 led to only partial stabilization of NMD substrates and loss of the Edc3-binding motif resulted in partial stabilization of Edc3 and Dhh1 substrates except for the *RPS28* mRNA. Further, loss of the Pat1-binding motifs did not cause significant stabilization of Pat1/Lsm1 or Pat1/Lsm1/Dhh1 substrates. The little or no effect of these deletions on different decapping substrates raised a question of decay mechanism for these mRNAs in the absence of active decapping enzyme recruitment. We considered two likely possibilities for their decay in the absence of active recruitment of the decapping enzyme: degradation by a 3' to 5' exosome-dependent decay mechanism or decapping by an alternative route but overall degradation by decapping-dependent 5' to 3' decay. To distinguish between these possibilities, we generated double mutant cells that combine the *dcp2 cis* element deletions U1D1-U1D2, E3D or E3D1, and LD1-9 with deletions of key genes required for 5' to 3' decay (*XRN1*) or 3' to 5' decay (*SKI2* or *SKI7*) and analyzed

8

the mRNA decay phenotypes of different decapping substrates in the resulting "double" mutant cells (Figure 3A).

In *dcp2-U1D1-U1D2* cells, deletion of *SKI2* or *SKI7* did not cause additional stabilization of the NMD substrates (*CYH2* pre-mRNA and *can1-100* mRNA) whereas deletion of *XRN1* caused substantial stabilization of these transcripts (Figure 3B). Similarly, deletion of *SKI2* or *SKI7* did not cause additional stabilization of both Edc3 and Dhh1 substrates, e.g., *YRA1* pre-mRNA, *EDC1,* and *SDS23* mRNAs, in *dcp2-E3D* or *E3D1* cells, but deletion of *XRN1* caused substantial stabilization of each of these transcripts (Figures 3B and S4). Deletions of *SKI2* or *SKI7* also did not cause discernible stabilization of the Pat1/Lsm1 substrates, *BUR6*, *DIF1*, and *LSM3* mRNAs, in *dcp2-LD1-9* cells, but deletion of *XRN1* stabilized these mRNAs substantially (Figure 3C). In each case, deletion of *XRN1* in the respective *dcp2 cis* element mutant cells yielded similar fold increases in transcript levels as those caused by *XRN1* deletion in *DCP2* WT cells (Figures 3B and 3C). These results indicate that in the absence of active recruitment of the decapping enzyme, the decapping substrates examined here, including the NMD, Edc3, Dhh1, and Pat1/Lsm1 substrates, are not degraded by exosome-dependent 3' to 5' decay, but are all still degraded by decapping-dependent 5' to 3' decay. This indicates that these decapping substrates can all be decapped by an alternative route when the normal Dcp2 *cis*-element-mediated active recruitment of the decapping enzyme is blocked.

In the Absence of Active Edc3 Recruitment of the Decapping Enzyme, Edc3 and Dhh1 Substrates Are Degraded by Pat1-mediated Decay

The experiments of Figure 3 demonstrated that different decapping substrates can all be decapped by an alternative route when recruitment of the decapping enzyme to these mRNAs was blocked by specific *dcp2 cis*-element deletions. To determine whether the Edc3-, Upf1-, and Pat1-mediated decapping pathways have redundant activities or may function as backup systems for each other, we constructed a third set of *dcp2* alleles harboring different combinations of element deletions that eliminate the binding of Edc3 (E3D or E3D1), Upf1 (U1D1-U1D2), and Pat1 (LD1-8, LD1-9, or LD9-2) to Dcp2 (Figure 4A). In addition, we also included two inconsequential Upf1-binding element deletions (U1D1 or U1D2) and one partially functional Pat1-binding element deletion (LD9-3) in this set.

Each of these alleles yielded the expected binding patterns of Edc3, Upf1, and Pat1 to Dcp2 except the four alleles that contain single Upf1-binding motif deletions (Figure 4A, alleles E3D-U1D1-LD1-9, E3D-U1D2-LD1-9, E3D1-U1D1-LD1-9, E3D1-U1D2-LD1-9). The mutant Dcp2 proteins generated from these four alleles showed no two-hybrid interaction with Upf1 (Figure 4A), but appeared fully functional in NMD (see below). As both Upf1-binding motifs border the leucine-rich motifs, we suspect that the LD1-9

deletion may indirectly affect the conformation of these two binding motifs and diminish Upf1 binding to Dcp2.

Although none of the leucine-rich element deletions affected the decay of Edc3 and Dhh1 substrates (Figure 2B), combining the leucine-rich element deletions LD1-8, LD1-9, LD9-3, and LD9-2 with the Edc3-binding element deletions E3D or E3D1 caused additional substantial stabilization of the Edc3 substrate *YRA1* pre-mRNA and the Dhh1 substrates *EDC1*, *SDS23*, and *HXT6* mRNAs (Figures 4B and S6). None of the combinations of these element deletions affected the Pat1/Lsm1 substrates or the NMD substrates (Figures 4B and S6). These results indicate that in the absence of active recruitment of the decapping enzyme by Edc3, both Edc3 and Dhh1 substrates are degraded by the Pat1-mediated decay pathway, suggesting that Pat1-mediated decapping serves as a backup or fail-safe system in the decay of Edc3 and Dhh1-regulated mRNAs. We also noticed a subtle functional difference for these *dcp2* alleles. In otherwise the same deletion context, cells harboring E3D1 consistently had lower transcript levels than those harboring E3D for Edc3 and Dhh1 substrates (Figure 4B). These differences could be indicative of E3-2 element function in decay of these mRNAs, as E3D eliminates both E3-1 and E3-2 elements and E3D1 eliminates only the E3-1 element. Similarly, cells harboring LD9-3 also had consistently lower transcript levels than those harboring LD9-2 for both Edc3 and Dhh1 substrates, suggesting that LD9-3 deletion maintains more function of Dcp2 than that of LD9-2 in decay of these mRNAs. Consistent with this interpretation, LD9-3 weakens but LD9-2 eliminates Pat1 binding to Dcp2 (Figure 4A, compare alleles E3D-LD9-2 to E3D-LD9-3, and E3D1-LD9-2 to E3D1-LD9-3).

Combing the leucine-rich element deletion LD1-9 with the Upf1-binding element deletion U1D1-U1D2 did not cause additional stabilization of the NMD substrates *CYH2* pre-mRNA, *can1-100*, and *ade2-1* mRNAs (Figures 4C and S8, allele U1D1-U1D2-LD1-9 compared to allele U1D1-U1D2 in Figure 1B). Further combining the Edc3-binding motif deletions E3D or E3D1 also did not cause additional stabilization of the *CYH2* pre-mRNA and *can1-100* mRNA, but did appear to cause small but significant increases in *ade2-1* mRNA levels (Figures 4C and S8, compare allele U1D1-U1D2-LD1-9 to alleles E3D-U1D1-U1D2-LD1-9 and E3D1-U1D1-U1D2-LD1-9). These results indicate that Pat1-mediated decapping does not function as a backup system for NMD substrates in the absence of Upf1-mediated recruitment of the decapping enzyme. However, Edc3-mediated decapping may function as a backup system for some nonsense-containing mRNAs. Further, the combination of element deletions E3D-U1D1-U1D2-LD1-9 eliminates all the binding motifs of known decapping activators in Dcp2, yet this combination of deletions still did not have any significant effect on the levels of accumulation of the Pat1/Lsm1 substrates (Figures 4C and S8). This result indicates that neither Edc3-mediated decapping nor Upf1-mediated decapping functions as a backup

system in decay of Pat1/Lsm1 substrates, raising the possibility that Pat1/Lsm1 substrates can be decapped without the function of any decapping activators.

The combination of element deletions U1D1-U1D2-LD1-9 created a *dcp2* allele harboring a lonely Edc3-binding motif. This *dcp2* allele had the activity of WT *DCP2* in promoting the decay of both Edc3 and Dhh1 substrates (Figures 4C and S8, compare U1D1-U1D2-LD1-9 to WT). Similarly, the combination of deletions E3D-U1D2-LD1-9 and E3D1-U1D2-LD1-9 created two *dcp2* alleles harboring a lonely Upf1-binding motif $U1_1$, and the combination of deletions E3D-U1D1-LD1-9 and E3D1-U1D1-LD1-9 created two *dcp2* alleles harboring a lonely Upf1-binding motif $U1_2$. Each of these four *dcp2* alleles had the activity of WT *DCP2* in promoting NMD (Figures 4C and S8, compare alleles E3D-U1D2-LD1-9, E3D1-U1D2-LD1-9, E3D-U1D1-LD1-9, and E3D1-U1D1-LD1-9 to WT). These results indicate that the Edc3-binding motif and each of the Upf1-binding motifs can function independently of other elements and promote specific mRNA decay activities.

Edc3 Carries out One Additional Function Upstream of Recruitment of the Decapping Enzyme in Decay of Both Edc3 and Dhh1 Substrates

Except for *RPS28B* mRNA, loss of the Dcp2 Edc3-binding motif, both Upf1-binding motifs, or the Pat1-binding motifs caused only partial stabilization, or no stabilization, of Edc3, NMD, and Pat1/Lsm1 substrates. In contrast, loss of the corresponding specific binding factors Edc3, Upf1, or Pat1 all resulted in substantial stabilization of their targeted mRNAs (see above). These results strongly suggest that Edc3, Upf1, or Pat1-mediated recruitment of the decapping enzyme is not rate-limiting to the overall decay process and each of these decapping activators most likely carries out an additional major function upstream of the recruitment of the decapping enzyme in decay of the respective targeted mRNAs. To test this idea further, we constructed double mutant strains containing *dcp2 cis* deletions E3D or E3D1 and deletion of *EDC3* and analyzed the decay phenotypes of Edc3 and Dhh1 substrates in the resulting strains. Because E3D and E3D1 both eliminate Edc3 binding to Dcp2, we reasoned that any additional stabilization caused by *EDC3* deletion of specific mRNAs in E3D or E3D1 cells is likely due to loss of an extra function of Edc3.

Deletion of *EDC3* caused additional 7-8-fold stabilization of the Edc3 substrate *YRA1* pre-mRNA in E3D or E3D1 cells (Figures 4D and S9). Deletion of *EDC3* also caused additional stabilization of the Dhh1 substrates *EDC1* and *SDS23* mRNAs and the Pat1/Lsm1/Dhh1 substrates *HSP12* and *HXT6* mRNAs (Figure 4E). These results provide evidence that Edc3 is directly involved in the decay of Dhh1-regulated mRNAs, and demonstrate that besides recruiting the decapping enzyme, Edc3 indeed carries out an additional function in decay of both Edc3 and Dhh1 substrates.

11

Dcp2 *Cis*-Binding Elements Promote the Assembly of Distinct Decapping Complexes in Yeast Cells

The experiments described above indicate that the Dcp2 C-terminal *cis*-binding elements promote independent binding of Edc3, Upf1, and Pat1 to Dcp2 and control the selective targeting of the decapping enzyme to different decapping substrates. These results and our earlier observation that different decapping activators each target a specific subset of yeast mRNAs (He et al., 2018) strongly suggest that different Dcp2 *cis*-binding elements promote the assembly of distinct decapping complexes. To test this idea, we explored two-hybrid interactions that are bridged through Dcp2 between Dcp1 and Edc3, Upf1, Pat1, or Dhh1 (Figure 5A) (He and Jacobson, 2015) and dissected the molecular basis for each of these bridged interactions. We constructed two sets of yeast two-hybrid tester strains and analyzed each of the bridged interactions in these strains. One set of strains contains single deletions of *EDC3*, *UPF1*, *PAT1*, and *SCD6* or a previously described *dcp2-N245* truncation that eliminates the entire Dcp2 C-terminal domain (He and Jacobson, 2015). This set of strains also contains double mutants that combine *EDC3* deletion either with deletions of *UPF1*, *PAT1*, and *SCD6* or with the *dcp2-N245* truncation. The second set of strains contains different C-terminal truncations of Dcp2 in both *EDC3* and *edc3Δ* backgrounds. Each of these Dcp2 truncations eliminates a distinct set of its *cis*-binding elements.

As shown in Figure 5A, Dhh1 exhibited strong two-hybrid interaction with Dcp1 in WT cells. Deletions of *UPF1*, *PAT1*, or *SCD6* did not affect the Dhh1:Dcp1 interaction. In contrast, loss of the entire C-terminal domain of Dcp2 or deletion of *EDC3* eliminated Dhh1:Dcp1 interaction. These results indicate that the Dhh1:Dcp1 interaction observed in WT cells requires both the Dcp2 C-terminal domain and Edc3, suggesting that this interaction occurs in a Dcp1-Dcp2-Edc3-Dhh1 complex. Further, in a WT *EDC3* background, Dcp2 C-terminal truncations maintaining the E3 motif left the Dhh1:Dcp1 interaction intact. In contrast, the Dcp2 C-terminal truncation eliminating the E3 motif abolished the Dhh1:Dcp1 interaction (Figure 5B). These results show that the observed Dhh1:Dcp1 interaction also requires an intact Dcp2 E3 motif, indicating that the Dcp2 Edc3-binding motif promotes assembly of the Dcp1-Dcp2-Edc3-Dhh1 decapping complex in vivo (Figure 5D). In an *edc3Δ* background, Dhh1 exhibited no interaction with Dcp1 (the slight blue color of the transformants was due to self-activation of Gal4(DB)-Dhh1 fusion protein) (Figure 5B) (He and Jacobson, 2015), indicating that Dhh1 assembles into the Dcp1-Dcp2-Edc3-Dhh1 via association with Edc3, consistent with the physical interaction between these two factors (He and Jacobson, 2015; Sharif et al., 2013).

In WT cells, Upf1 also exhibited strong two-hybrid interaction with Dcp1 (Figure 5A). Deletions of *UPF1*, *PAT1*, or *SCD6* did not affect Upf1:Dcp1 interaction. In contrast,

deletion of *EDC3* diminished and loss of the entire C-terminal domain of Dcp2 eliminated Upf1:Dcp1 interaction. These results indicate that Upf1:Dcp1 interaction in WT cells requires the C-terminal domain of Dcp2 and is enhanced by the presence of Edc3, suggesting that this interaction occurs in a Dcp1-Dcp2-Edc3-Upf1 complex. In a WT *EDC3* background, Dcp2 C-terminal truncations eliminating the second Upf1-binding motif $U1_2$ did not affect Upf1:Dcp1 interaction (Figure 5B, alleles N630 and N475); however, further eliminating the first Upf1-binding motif $U1_1$ abolished Upf1:Dcp1 interaction (Figure 5B, alleles N400, N300 and N245). In an *edc3Δ* background, Upf1 interacted weakly with Dcp1 and Dcp2 C-terminal truncations eliminating the second Upf1-binding motif $U1_2$ abolished Upf1:Dcp1 interaction (Figure 5B, compare alleles N771 to N630). These results indicate that the Upf1-binding motifs $U1_1$ and $U1_2$ can both promote the assembly of Upf1-containing decapping complexes and that Edc3 enhances the binding of Upf1 to the $U1_1$ motif to promote assembly of the Dcp1-Dcp2-Edc3-Upf1 decapping complex in vivo (Figure 5D).

In contrast to Dhh1 and Upf1, Pat1 exhibited only weak two-hybrid interaction with Dcp1 in WT cells (Figure 5A). Deletions of *UPF1*, *PAT1*, or *SCD6* did not alter Pat1:Dcp1 interaction, but loss of the entire Dcp2 C-terminal domain eliminated Pat1:Dcp1 interaction (Figure 5A). Interestingly, deletion of *EDC3* enhanced Pat1:Dcp1 interaction (Figure 5A). These results indicate that Pat1 can associate with the Dcp1-Dcp2 decapping enzyme both in the presence and absence of Edc3. Eliminating different leucine-rich motifs between L_2 and L_9 by progressive Dcp2 C-terminal truncations did not significantly alter the respective Pat1:Dcp1 interaction strength in *EDC3* and *edc3Δ* backgrounds. However, further eliminating the leucine-rich motif L_1 abolished Pat1:Dcp1 interaction in an *EDC3* background and greatly diminished Pat1:Dcp1 interaction in an *edc3Δ* background (Figure 5B). These results show that Pat1:Dcp1 interaction requires the L_1 motif in Dcp2 regardless of the cellular status of Edc3, suggesting that this motif may promote assembly of several different decapping complexes including a Dcp1-Dcp2-Edc3-Pat1 complex (Figure 5D).

Edc3 Is a Common Component of Multiple Decapping Complexes

To further validate our conclusion that Dcp2 *cis*-binding elements promote assembly of distinct decapping complexes and to explore the assembly dynamics of these complexes, we examined whether Dcp2 bridges interactions between Edc3 and Upf1 or Pat1. As shown in Figure 5A, in contrast to the Upf1:Dcp1 interaction, Upf1 did not show two-hybrid interaction with Edc3 in WT cells. Upf1 also did not show interaction with Edc3 in *upf1Δ*, *pat1Δ*, or *scd6Δ* cells. Surprisingly, Upf1 exhibited strong two-hybrid interaction with Edc3 in *edc3Δ* cells. Deletions of *UPF1*, *PAT1*, or *SCD6* in *edc3Δ* cells did not alter this strong Upf1:Edc3 interaction; however, deletion of the entire Dcp2 C-terminal domain in *edc3Δ*

cells eliminated Upf1:Edc3 interaction. These results indicate that Dcp2 bridges an interaction between Upf1 and Edc3 and that this bridged Upf1:Edc3 interaction is inhibited by endogenous Edc3. In an $edc3\Delta$ background, eliminating the second Upf1-binding motif $U1_2$ in Dcp2 by C-terminal truncation abolished the Upf1:Edc3 interaction (Figure 5C, compare alleles N771 and N630). This result shows that the Upf1:Edc3 interaction requires the $U1_2$ motif in Dcp2 and that this motif can promote assembly of a Dcp1-Dcp2-Edc3-Upf1 decapping complex in vivo, with Upf1 binding to the Dcp2 $U1_2$ motif (Figure 5E).

Similar to the Upf1:Edc3 interaction, Pat1 also did not show two-hybrid interaction with Edc3 in WT cells, deletion of *EDC3* promoted Pat1:Edc3 interaction, and deletion of the entire C-terminal domain of Dcp2 eliminated Pat1:Edc3 interaction in $edc3\Delta$ cells (Figure 5A). These results indicate that Dcp2 also bridges an interaction between Pat1 and Edc3 and that this bridged interaction is inhibited by endogenous Edc3. In an $edc3\Delta$ background, eliminating different leucine-rich motifs between L_3 and L_9 did not affect Pat1:Edc3 interaction; however, further eliminating the L_2 motif abolished Pat1:Edc3 interaction (Figure 5C). This result shows that Pat1:Edc3 interaction requires the L_2 motif in Dcp2 and that this motif can promote assembly of a Dcp1-Dcp2-Edc3-Pat1 decapping complex *in vivo*, with Pat1 binding to the Dcp2 L_2 motif (Figure 5E).

Our two-hybrid analyses of the bridged molecular interactions between Upf1 and Dcp1 or Edc3 revealed two distinct Upf1-containing decapping complexes with the same composition but different configurations. Similarly, analyses of the bridged molecular interactions between Pat1 and Dcp1 or Edc3 also revealed two distinct Pat1-containing decapping complexes of the same composition but different configurations (Figures 5D and E). These complexes share Dcp1, Dcp2, and Edc3 with Upf1 binding to either $U1_1$ or $U1_2$, or with Pat1 binding to either L_1 or L_2 in Dcp2. We suspect that the binding site preference for Upf1 and Pat1 in these decapping complexes is likely caused by the constraint of configurations of the Gal4 DNA-binding and activation domains fused to the respective binding partners. Nevertheless, these results indicate that Upf1 and Pat1 can both bind to two different binding motifs in Dcp2, raising the possibility that different Upf1 and Pat1-binding motifs in Dcp2 may control structural transitions of specific decapping complexes.

Our observation that endogenous Edc3 can completely inhibit the bridged molecular interactions between Edc3 and Upf1 or Pat1 is intriguing (Figure 5A). It indicates that free Edc3-binding sites from Dcp2 molecules are limiting and suggests that the entire pool of Dcp2 molecules are likely to be stably bound by endogenous Edc3. Consistent with this interpretation, as demonstrated above, Edc3 exists as a common component of multiple decapping complexes.

Xrn1 Binds to an Internal Fragment of Dcp2 and Is Recruited to the Decapping Complex by Dcp2

To assess potential coupling between decapping and 5' to 3' exoribonucleolytic decay, we tested two hybrid interactions between Xrn1 and all known decapping factors. Xrn1 interacted with Dcp1, Edc3, Pat1, and Upf1 (Figure 6A). Xrn1 did not interact with full-length Dcp2, but interacted with a 726-amino acid C-terminal Dcp2 fragment Dcp2-ND244 (Figure 6A), suggesting that Xrn1 binding to Dcp2 may be dependent on a specific Dcp2 conformation. Deletions of *EDC3*, *UPF1*, or *PAT1* and elimination of the entire C-terminal domain of Dcp2 did not affect binding of Xrn1 to Dcp2-ND244 or Pat1 (Figure 6C), suggesting that Xrn1 may bind to Dcp2 and Pat1 directly. To identify the Xrn1 binding region of Dcp2, we analyzed Xrn1 interactions with a panel of Dcp2 fragments (Figure S10A). In contrast to the binding of Edc3, Upf1, and Pat1 to Dcp2, Xrn1 binding to Dcp2 required a large Dcp2 fragment with the minimal Xrn1 binding region encompassing an internal fragment from aa 316 to 575 (Figure 6D).

In contrast to the Xrn1:Dcp2-ND244 and Xrn1:Pat1 interactions, the Xrn1:Dcp1, Xrn1:Edc3, and Xrn1:Upf1 interactions are all bridged by Dcp2. As shown in Figure 6B, deletions of *UPF1*, *PAT1*, or *SCD6* did not significantly affect Xrn1:Dcp1 interaction. However, elimination of the Dcp2 C-terminal domain or deletion of *EDC3* abolished Xrn1:Dcp1 interaction, suggesting that Xrn1:Dcp1 interaction is bridged by Dcp2 and influenced by Edc3, and occurs in a Dcp1-Dcp2-Edc3-Xrn1 complex (Figure 6F). In support of the latter conclusion, Xrn1:Dcp1 interaction is also dependent on an intact Xrn1 binding site in Dcp2. In an *EDC3* background, loss of partial Xrn1-binding region by Dcp2 C-terminal truncation abolished Xrn1:Dcp1 interaction (Figure 6E, compare alleles N630 and N475). Deletions of *EDC3*, *UPF1*, *PAT1*, or *SCD6* did not affect Xrn1:Edc3 interaction, but elimination of the entire Dcp2 C-terminal domain abolished Xrn1:Edc3 interaction (Figure 6B), indicating that this interaction is bridged by Dcp2. As additional support for this conclusion, in both *EDC3* and *edc3Δ* backgrounds, Xrn1:Edc3 interaction requires an intact Xrn1 binding site in Dcp2, as loss of partial Xrn1-binding region eliminates Xrn1:Edc3 interaction (Figure 6E, compare alleles N630 and N475). In contrast to Upf1:Edc3 and Pat1:Edc3 interactions, Xrn1:Edc3 interaction was not inhibited by endogenous Edc3. We suspect that the observed Xrn1:Edc3 interaction may involve dimerization of exogenous Edc3 with endogenous Edc3 bound to Dcp2 in a decapping complex. Elimination of the Dcp2 C-terminal domain and deletion of *EDC3* both abolished Xrn1:Upf1 interaction (Figure 6B), indicating that this interaction is bridged by Dcp2 and occurs in a Dcp1-Dcp2-Edc3-Xrn1-Upf1 complex (Figure 6F). Consistent with being an interaction bridged by Dcp2, Xrn1:Upf1 interaction required the second Upf1-binding motif $U1_2$ in Dcp2, as loss of the $U1_2$ motif by Dcp2 C-terminal truncation eliminated Xrn1:Upf1 interaction (Figure 6E, compare alleles N771 and N630).

Collectively, our two-hybrid analyses show that Xrn1 binds to an internal fragment of Dcp2 and is recruited to the decapping complex by Dcp2. These results indicate that two important events in 5' to 3' mRNA decay, Dcp2-mediated decapping and Xrn1-mediated 5' to 3' exoribonucleolytic digestion, are physically coupled in vivo, suggesting that in addition to controlling the selective targeting of the decapping enzyme to different decapping substrates, the C-terminal domain of Dcp2 also controls efficient 5' to 3' exonucleolytic decay, ensuring that decapped mRNAs are degraded in a timely manner.

DISCUSSION

C-terminal *Cis*-Binding Motifs Promote Independent Binding of Edc3, Upf1, and Pat1 to Dcp2 and Control Selective Targeting of the Decapping Enzyme to Distinct Substrate mRNAs

The yeast decapping enzyme targets thousands of mRNAs for decapping-dependent decay (Celik et al., 2017; He et al., 2018) and the genetic experiments described here elucidate the mechanistic basis for the enzyme's selective targeting of specific subgroups of those mRNAs. Dcp2's large C-terminal domain encompasses multiple regulatory elements that serve as binding sites for proteins heretofore thought of as "decapping activators" and our systematic deletion of those sites has defined their roles. Loss of both Upf1-binding motifs eliminated Upf1 binding to Dcp2 and caused selective partial stabilization of NMD substrates; loss of the Edc3-binding motif eliminated Edc3-binding to Dcp2 and caused selective partial or complete stabilization of Edc3 substrates, as well as selective partial stabilization of Dhh1 substrates (Figures 1C and 1D). Further, deletions of the leucine-rich Pat1-binding motifs eliminated Pat1 binding to Dcp2 and, when these deletions were combined with deletions of the Edc3-binding motif, caused selective additional stabilization of Dhh1 substrates (Figure 4B).

Our observation that loss of the Edc3-binding motif caused selective stabilization of Dhh1 substrates uncovers a new direct role of Edc3 in selective targeting of the decapping enzyme to Dhh1-regulated mRNAs. This role is not totally unexpected since Edc3 interacts directly with Dhh1 (He and Jacobson, 2015; Sharif et al., 2013), Dhh1 association with the decapping enzyme is dependent on Edc3 (Figure 5A), and deletion of *EDC3* causes additional stabilization of Dhh1-regulated mRNAs in *dcp2-E3D* and *dcp2-E3D1* cells (Figure 4D). In contrast to Dcp2 *cis*-element E3D or E3D1 deletions, *trans* deletion of *EDC3* had no discernible effect on Dhh1 substrates (Figures 1B and 4B), a result suggesting that at least one additional factor binds to the Edc3-binding motif and can target the decapping enzyme to Dhh1-regulated mRNAs. Surprisingly, given the multiple proposed roles for Pat1 in mRNA decapping (Charenton et al., 2017; Lobel et al., 2019; Nissan et al., 2010), we found that loss of the Pat1-binding motifs had no effect on Pat1/Lsm1 substrates or any other decapping substrates (Figure 2B). We propose that

16

Pat1 binding to the leucine-rich motifs in the Dcp2 C-terminal domain still controls the selective targeting of the decapping enzyme to Pat1/Lsm1 substrates and may even enhance the decapping rates of the targeted mRNAs, but the Pat1-mediated decapping step is likely not rate-limiting for decay of Pat1/Lsm1 substrates.

Dcp2 C-terminal *Cis*-Binding Motifs Promote Assembly of Distinct Target-specific Decapping Complexes In Vivo

Consistent with our observation that Dcp2 *cis*-binding elements control the selective targeting of the decapping enzyme to different decapping substrates, our two-hybrid experiments reveal that the same elements can promote in vivo assembly of distinct target-specific complexes. The Edc3-binding motif E3 can promote the assembly of a Dhh1-containing Dcp1-Dcp2-Edc3-Dhh1 complex, the two Upf1-binding motifs $U1_1$ and $U1_2$ can promote assembly of two distinct Upf1-containing Dcp1-Dcp2-Edc3-Upf1 complexes of the same composition but different configurations with Upf1 binding either to the $U1_1$ or $U1_2$ motifs, and the Pat1-binding motifs L_1 and L_2 can promote assembly of two distinct Pat1-containing Dcp1-Dcp2-Edc3-Pat1 complexes of the same composition but different configurations with Pat1 binding either to the L_1 or L_2 motifs (Figures 5D and 5E). Based on several observations, including: 1) Edc3 associates with itself (Decker et al., 2007; He and Jacobson, 2015), 2) Edc3 targets two specific transcripts *RPS28B* mRNA and *YRA1* pre-mRNA for decapping-dependent decay (Badis et al., 2004; Dong et al., 2007), and 3) Edc3 binds to the 3'-UTR decay-inducing element of *RPS28B* mRNA as a dimer (He et al., 2014), we postulate that the Edc3-binding motif can promote assembly of at least one additional decapping complex, a Dcp1-Dcp2-Edc3-Edc3 complex containing Edc3 as a homodimer. Because Edc3 is directly involved in decay of Dhh1 substrates (Figure 4D), we speculate that the Dcp1-Dcp2-Edc3-Dhh1 complex likely also contains Edc3 as a dimer. Collectively, our results indicate that the *cis*-binding elements located in the Dcp2 C-terminal domain promote assembly of multiple decapping complexes with distinct composition and substrate specificities. Edc3 appears to be both a common core component of multiple decapping complexes and a unique targeting component of specific decapping complexes.

Our observation that Edc3 is a common component of multiple decapping complexes raises the intriguing issue of Edc3 function in these complexes. Numerous biochemical and structural studies, all using C-terminally truncated Dcp2 fragments and just the Lsm domain of Edc3, suggested that Edc3 promotes catalysis by the decapping enzyme, probably by enhancing substrate binding (Charenton et al., 2016; Fromm et al., 2012; Mugridge et al., 2018; Nissan et al., 2010). Our genetic experiments challenge this proposed function for Edc3 and suggest that the core Edc3 component of each decapping complex may inhibit the enzymatic activity or substrate binding of the decapping enzyme,

consistent with the existence of an inhibitory element in the Dcp2 C-terminus (He and Jacobson, 2015; Paquette et al., 2018). In addition, our genetic experiments also reveal that the core Edc3 component must carry out two additional important functions in mRNA decapping. One function is to provide the decapping enzyme with a set of unique Edc3 binding surfaces or modules and thus endow the decapping enzyme with Edc3 targeting specificity. Consistent with this proposition, eliminating Edc3 binding to Dcp2 caused selective stabilization of both Edc3 and Dhh1 substrates (Figures 1C and 1D). Another Edc3 function appears to be promotion of the assembly of additional specific decapping complexes, an example of which is the Dcp1-Dcp2-Edc3-Upf1 complex. In support of this notion deletion of *EDC3* diminishes the Dcp2-bridged Dcp1:Upf1 interaction and triggers a switch of Upf1 binding from the $U1_1$ to the $U1_2$ motif in Dcp2 (Figures 5A and 5B). Our proposition that Edc3 exists both as a common core component of multiple decapping complexes and as a unique targeting component of specific decapping complexes provides a unified theory for explaining the apparently contradictory proposed functions for Edc3, i.e., that Edc3 functions as a general decapping activator (Kshirsagar and Parker, 2004) or as a transcript-specific decapping activator (Badis et al., 2004; Dong et al., 2007).

Edc3, Upf1, and Pat1-mediated Active Recruitment of the Decapping Enzyme Makes Distinct Contributions to the Overall Decay of the Respective Targeted mRNAs

Our genetic analyses of Dcp2 *cis* element mutants revealed the relative mRNA decay contributions of specific factor-mediated decapping enzyme recruitment events and provided significant insights into the decay mechanisms for different decapping substrates. For the Edc3 substrate *RPS28B* mRNA, loss of the Edc3-binding motif by E3D or E3D1 in Dcp2 caused complete mRNA stabilization relative to deletion of *EDC3* itself (Figures 1C and 1D). For the Edc3 substrate *YRA1* pre-mRNA, and all the tested Dhh1 substrates, loss of the Edc3-binding site caused only partial stabilization relative to the respective *EDC3* or *DHH1* deletions (Figures 1C and 4B). Additional loss of the Pat1-binding motifs caused further stabilization of the latter Edc3 and Dhh1 substrates (Figure 4B). These results indicate that both Edc3 and Dhh1 substrates can be targeted by Pat1-mediated recruitment of the decapping enzyme. However, since loss of the Pat1-binding motifs alone had no effect on these Edc3 and Dhh1 substrates (Figure 2B), it appears that Pat1-mediated recruitment of the decapping enzyme merely functions as a backup system in the decay of Edc3 and Dhh1-regulated mRNAs. Because the combined deletions of the Edc3- and Pat1-binding motifs caused substantial stabilization of the Edc3 and Dhh1 substrates (Figure 4B), our results indicate that decapping is rate-limiting for both Edc3 and Dhh1 substrates, suggesting that the major functions of Edc3 or Pat1 in decay of these mRNAs is recruiting the decapping enzyme.

For NMD substrates, loss of both Upf1-binding motifs caused only marginal stabilization (2-3-fold), but deletion of *UPF1* caused substantial stabilization (>10-fold) (Figure 1C). These results indicate that Upf1-mediated recruitment of the decapping enzyme only makes a minor contribution to the overall decay of NMD substrates, suggesting that decapping is not a major rate-limiting step in NMD, active recruitment of the decapping enzyme to NMD substrates may be dispensable, and Upf1 must carry out one additional major function upstream of the recruitment of the decapping enzyme. Consistent with these ideas, in the absence of active recruitment of the decapping enzyme by Upf1, NMD substrates are still degraded by decapping-dependent pathway (Figure 3B). In addition, further deletions of the Edc3- and Pat1-binding motifs do not have significant effects on NMD substrates (Figure 4C), and in fact, even eliminating the entire C-terminal domain only caused marginal stabilization of NMD substrates (He and Jacobson, 2015).

For Pat1/Lsm1 substrates, loss of the Pat1-binding motifs had no effect, but deletion of *PAT1* caused substantial stabilization (Figure 2B). These results indicated that the Pat1-mediated recruitment of the decapping enzyme does not make a significant contribution to the overall decay of Pat1/Lsm1 substrates, suggesting that decapping is not rate-limiting in decay of the Pat1/Lsm1 substrates, active recruitment of the decapping enzyme to the Pat1/Lsm1 substrates may be dispensable, and Pat1 must carry out one additional major function upstream of the recruitment of the decapping enzyme. In support of this conclusion, in the absence of active recruitment of the decapping enzyme by Pat1, Pat1/Lsm1 substrates are still degraded by the decapping-dependent pathway (Figure 3C). Importantly, eliminating all the known-binding motifs in the Dcp2 C-terminal domain also did not have any effect on the decay Pat1/Lsm1 substrates (Figure 4C).

Dcp2 Directly Recruits the 5' to 3' Exoribonuclease Xrn1 to the Decapping Complexes

Our two-hybrid experiments revealed that the 5' to 3' exoribonuclease Xrn1 binds to Dcp2 and is directly recruited to decapping complexes by Dcp2. This conclusion is supported by several new observations. First, Xrn1 binds to a specific internal Dcp2 fragment (Figures 6D and S10B). Second, Xrn1 also interacts with both Dcp1 and Edc3, two other core components of the decapping enzyme, and each of the interactions requires the Dcp2 C-terminal domain as well as an intact Xrn1-binding region in this domain (Figures 6B and 6E). Third, Xrn1 is a common component of both the Dcp1-Dcp2-Edc3-Edc3-Xrn1 and Dcp1-Dcp2-Edc3-Upf1-Xrn1 complexes (Figure 6F). Finally, Xrn1's recruitment to the decapping complexes requires prior Edc3 binding to Dcp2, as deletion of *EDC3* eliminated both Dcp1:Xrn1 and Upf1:Xrn1 interactions (Figure 6B).

Our observation that Xrn1 is directly recruited by Dcp2 to decapping complexes suggests that decapping and 5' to 3' exoribonucleolytic decay are physically and mechanistically

linked. This coupling appears to be conserved over eukaryotic evolution, but the mechanism of this coupling may differ for different organisms, e.g., *D. melanogaster* Xrn1 binds to Dcp1 (Braun et al., 2012) and human Xrn1 binds to Edc4 in its respective decapping complex (Chang et al., 2019). Xrn1 binding to decapping complexes likely ensures immediate 5' to 3' exoribonucleolytic degradation of decapped transcripts and may also serve to inhibit the catalytic activity or substrate binding of the decapping enzyme until the enzyme is targeted to substrate mRNAs. Consistent with this idea, Xrn1 binding to Dcp2 requires the inhibitory element (Figure 6D) and overexpression of Xrn1 in *D. melanogaster* cells can inhibit the decapping of different reporter mRNAs (Braun et al., 2012).

Based on the observation that the same Pat1 C-terminal extension binds to multiple helical leucine-rich motifs in Dcp2 and a single such motif in Xrn1, Pat1 was proposed to coordinate the decapping and exonucleolytic decay events in general 5' to 3' mRNA decay by first recruiting the decapping enzyme and then Xrn1 to targeted mRNAs (Charenton et al., 2017). This Pat1-mediated sequential coupling model of decapping and 5' to 3' exonucleolytic decay is at odds with our result that Xrn1 is directly recruited by Dcp2 to the decapping complexes. Our previous observation that Pat1 targets only a subset of yeast transcripts (He et al., 2018), and our new results that loss of the Pat1-binding motifs had no effect on all tested decapping substrates yet loss of the Edc3- and Upf1-binding motifs each yielded specific effects also challenge the broad application of this Pat1-mediated coupling model. Thus, the observed Pat1:Xrn1 interaction may not serve to recruit Xrn1 to the decapped transcripts, but instead may serve to dissociate Xrn1 from the decapping complexes after Pat1-mediated decapping.

A New Model for Control of mRNA Decapping

Our genetic data suggest a new model for control of mRNA decapping in yeast (Figure 7) whose main features include: *cis*-regulatory elements located in the Dcp2 C-terminal domain control selective targeting of the decapping enzyme by forming distinct multi-component decapping complexes; the Dcp1 and Dcp2 subunits are shared common components of all decapping complexes; Edc3 functions as a shared common component of multiple decapping complexes, but is also a unique targeting component of dimeric Edc3-containing complexes; Xrn1 associates with Dcp2 after the binding of Edc3 to Dcp2 and is a component of multiple or perhaps all targeting complexes; Upf1 and Pat1 each function as unique targeting components in their respective Upf1- or Pat1-containing complexes; the targeting components Edc3, Upf1, and Pat1 each have at least two separate binding modules, one for the Dcp1-Dcp2-Edc3 core complex and another for their targeted mRNPs; and the final assembly and decapping activation of the target-

specific decapping complexes occurs on a to-be-degraded mRNP and the decapping event is coupled with immediate 5' to 3' degradation by Xrn1.

Target-specific decapping complexes other than those specific for NMD, Edc3, Dhh1, and Pat1 substrates must exist in yeast cells. Our genetic data suggested that one additional factor other than Edc3 also can bind to the Edc3-binding motif and target the decapping enzyme to Dhh1 substrates. In addition, the leucine-rich motifs L5 to L9 originally proposed for Pat1 binding in fact do not bind Pat1 in the context of full-length Dcp2, suggesting that they may bind other factors. Further, loss of all the known factor-binding motifs in Dcp2 does not have any discernible effect on decapping of Pat1/Lsm1 substrates, raising the possibility that these mRNAs may be decapped by the Dcp1/Dcp2 complex alone. Collectively, our results indicate that yeast cells likely contain many distinct decapping complexes. The notion of a single yeast decapping enzyme is too simplistic and should be replaced by the concept of a decapping enzyme family that shares the core components Dcp1 and Dcp2, similar to the PP1 and PP2A phosphatase families involved in protein dephosphorylation (Shi, 2009; Virshup and Shenolikar, 2009).

ACKNOWLEDGMENTS

AUTHOR CONTRIBUTIONS

F.H. and A.J. conceived and designed the experiments, F.H. carried out the experiments, F.H., A.J., and C.W. analyzed the data, F.H. and A.J. wrote the paper, and A.J. obtained funding for the study.

DECLARATION OF INTERESTS

A.J. is co-founder, director, and SAB chair of PTC Therapeutics Inc. All other authors declare no competing interests.

FIGURE LEGENDS

Figure 1. Consequences of deleting Dcp2's Edc3- and Upf1-binding motifs, and its inhibitory element

(A) Dcp2 schematic depicting its distinct regulatory elements. D1, Dcp1-binding site; E3, Edc3-binding motif; $U1_1$ and $U1_2$, Upf1-binding motifs; L_1-L_9, leucine-rich Pat1-binding motifs; and IE, the inhibitory element.

(B) Two-hybrid assays evaluating the consequences of specific *dcp2* deletions on Dcp2 interactions with Upf1, Edc3, and Pat1. Left, schematics of deletion alleles, with specific element deletions marked by triangles. The letter D in the allele names is used to indicate that a specific element has been deleted, such that *E3D* denotes deletion of the E3 element, *U1D1* denotes deletion of the $U1_1$ element, etc. Right, two-hybrid colony color assays, duplicated horizontally, with blue color indicating interaction and white indicating no interaction.

(C) Northern analyses of individual transcript levels in cells expressing specific *dcp2* deletion alleles or harboring deletions of *UPF1* or *EDC3*. Groupings depict transcripts subject to common regulation.

(D) Northern analyses of Edc3 and Dhh1 substrates in cells expressing *dcp2* alleles deleted for E3-1 or E3-2, or harboring deletions of *EDC3* or *DHH1*.

Further analyses of the transcripts considered in (C) and (D) are presented in Figures S1 and S2. In all blots lower case letters denote *SCR1* blots duplicated for clarity of presentation.

Figure 2. Consequences of deleting Dcp2 leucine-rich Pat1-binding motifs

(A) Two-hybrid assays evaluating the consequences of deleting the leucine-rich motifs (L_1 to L_9) from the Dcp2 C-terminal domain. As in Figure 1B, schematics of the individual *dcp2* alleles are shown on the left (with specific element deletions denoted by triangles) and duplicate two-hybrid assays are on the right.

(B) Northern analyses of individual Pat1/Lsm1 and Pat1/Lsm1/Dhh1 substrate levels in cells harboring individual or combined deletions of Dcp2 leucine-rich motifs.

(C) Bar graphs of average $\pm$ SEM for a subset of the northern analyses depicted in B. The relative levels of each decapping substrate in different strains were determined from

23

three independent experiments, with one representative blot for each transcript shown in panel B.

See also Figure S3.

Figure 3. NMD, Edc3, Dhh1, and Pat1 substrates are still degraded by decapping-dependent 5' to 3' decay in the absence of active decapping enzyme recruitment

(A) Schematics of *dcp2* alleles that eliminate Edc3, Upf1, or Pat1 binding to Dcp2.

(B) Deletion of *XRN1*, but not deletions of *SKI2* or *SKI7*, causes significant stabilization of NMD substrates in *HA-dcp2-U1D1-U1D2* cells, and Edc3 and Dhh1 substrates in *HA-dcp2-E3D* or *E3D1* cells.

(C) Deletion of *XRN1*, but not deletions of *SKI2* or *SKI7*, causes significant stabilization of Pat1 substrates in *HA-dcp2-LD1-9* cells.

Northern analyses in B and C as in Figures 1 and 2. Bar graphs in lower panels of B and C depict relative levels of decapping substrates in different strains determined from average ± SEM of three independent experiments. One representative northern blot for each transcript is shown in the upper panels. In the upper panel of B, lower case letters denote *SCR1* blots duplicated for clarity of presentation. See also Figure S4.

Figure 4. Genetic interactions between the Dcp2 Edc3-, Upf1-, and Pat1-binding motifs, or between the Edc3-binding motif and Edc3, that affect mRNA decapping

(A) Two-hybrid assays examining the effects of different combinations of element deletions on Edc3, Upf1, and Pat1 binding to Dcp2. Allele schematics and two hybrid analyses are as in Figure 1B.

(B) Northern analyses of the consequences of simultaneous loss of the Dcp2 Edc3-binding motif and leucine-rich motifs.

(C) Northern analyses of the consequences of simultaneous loss of the Dcp2 Upf1-binding motifs and leucine-rich motifs, and the roles of single Dcp2 Edc3 or Upf1-binding motifs.

(D) Northern analyses of the consequences for Edc3 and Dhh1 substrates caused by loss of the Dcp2 Edc3-binding motif and *trans* deletion of *EDC3.*

24

Northern analyses as in Figures 1 and 2. Two-hybrid analyses as in Figure 1.

See also Figure S5, S6, S7, S8 and S9.

Figure 5. The Dcp1-Dcp2 decapping enzyme forms distinct decapping complexes in vivo with the decapping activators Edc3, Dhh1, Upf1, and Pat1

Two-hybrid assays, as in Figure 1, were used to dissect the molecular basis of five Dcp2-bridged interactions between Dcp1 and Dhh1, Upf1, or Pat1, and between Edc3 and Upf1 or Pat1.

(A) Dcp1:Dhh1, Dcp1:Upf1, Dcp1:Pat1, Edc3:Upf1, and Edc3:Pat1 interactions in tester strains harboring different gene deletions or truncations of decapping factors.

(B) Dcp1:Dhh1, Dcp1:Upf1, and Dcp1:Pat1 interactions in tester strains harboring Dcp2 C-terminal truncations in *EDC3* and *edc3Δ* cells.

(C) Edc3:Upf1 and Edc3:Pat1 interactions in tester strains harboring Dcp2 C-terminal truncations in *EDC3* and *edc3Δ* cells.

(D) Three different decapping complexes inferred from two-hybrid analyses in A and B.

(E) Two different decapping complexes inferred from two-hybrid analyses in A and C.

Figure 6. Xrn1 binds to Dcp2 and is directly recruited to different decapping complexes by Dcp2.

(A) Two-hybrid analyses of Xrn1 interactions with Dcp1, Edc3, Pat1, Upf1, and an N-terminally truncated Dcp2 fragment in WT cells.

(B) Two-hybrid analyses of Dcp2-bridged interactions between Xrn1 and Dcp1, Edc3, or Upf1.

(C) Two-hybrid analyses of interactions between Xrn1 and Pat1 or N-terminally truncated Dcp2.

(D) Two-hybrid analyses of Xrn1 binding to an internal Dcp2 fragment.

(E) Dcp1:Xrn1, Edc3:Xrn1, and Upf1:Xrn1 interactions in tester strains harboring Dcp2 C-terminal truncations and *EDC3* or *edc3Δ* alleles.

(F)Two different Xrn1-containing decapping complexes inferred from two-hybrid analyses in B and E.

Allele schematics and two-hybrid analyses as in Figure 1.

Figure 7. A New Model: Formation of Target-specific Decapping Complexes Controls mRNA Decapping

In brief, the Dcp1-Dcp2 decapping enzyme interacts with Edc3 and then Xrn1, forming a pre-assembled inactive Dcp1-Dcp2-Edc3-Xrn1 complex. The resulting complex binds to individual targeting components, forming target-specific decapping complexes. The final assembly and enzymatic activation of these complexes is postulated to occur on mRNPs destined for degradation.

RESOURCE AVAILABILITY

Lead Contact

Further information and requests for resources and reagents should be directed to the Lead Contact, Feng He (feng.he@umassmed.edu).

Materials Availability

Strains and plasmids generated in this study are available from the Lead Contact without restriction.

Data and code availability

All data generated in this study are available from the Lead Contact.

EXPERIMENTAL MODEL AND SUBJECT DETAILS

The experiments described in this study used the yeast *Saccharomyces cerevisiae* as a model system. Yeast strains used for phenotypic analyses of mRNA decay were

derived from the W303 background (*MATa ade2-1 his3-11,15 leu2-3,112 trp1-1 ura3-1 can1-100*). Yeast strains used for two-hybrid analyses were all derived from the GGY1::171 background (*his3 leu2 URA3::GAL1-lacZ gal4Δ gal80Δ*) (Fields and Song, 1989). All yeast strains used in this study are listed in Table S1.

Yeast cells used for RNA isolation and transformation were all grown at 30°C in YEPD media (1% yeast extract, 2% peptone, 2% D-glucose). For integrative yeast transformation, transformants were selected at 30°C on different media depending on the selection markers of the transforming DNA fragments. For the drug resistance genes *KanMX* and *HygroR*, G418 (Gibco #11811-023) and hygromycin (Roche #10843555001) were included in YEPD media (1% yeast extract, 2% peptone, 2% D-glucose, 30g agar/L, 400µg/ml G418 or 200µg/ml hygromycin). For the auxotrophic markers, *URA3* and *ADE2*, synthetic *-ura* or *-ade* drop-out media (6.7 g/L of yeast nitrogen base without amino acids, 2g/L *-ura* or *-ade* drop-out mix, 30g/L of agar, 100 ml/L of 20% D-glucose) were used. For yeast two-hybrid analyses, transformants were first selected on synthetic *-leu-his* drop-out media and then replica-plated on SSX media [6.7 g/L of yeast nitrogen base without amino acids, 2 g/L *-leu-his* drop-out mix, 30 g/L of agar, 100 ml/L of 20% sucrose, 100 ml/L of 1 M potassium phosphate buffer pH 7.0, 2 ml/L of 20 mg/ml of 5-bromo4-chloro-3-indolyl ß-D-galactoside (X-gal) (USB #7240-90-6) in formamide] for color development.

METHOD DETAILS

Methodological overview: generation and functional analysis of Dcp2 element deletion mutants

To dissect the roles of different Dcp2 regulatory elements (Figure 1A) in mRNA decapping, we generated specific deletions in the C-terminal domain of *DCP2* that eliminated either a single element or combinations of different elements and analyzed the consequences of these deletions on Dcp2 interactions with specific decapping activators and decay of different decapping substrates. In total, we constructed three sets of element deletions and generated 50 *dcp2* mutant alleles. The first set of *dcp2* alleles contains single deletions as well as double, triple, and quadruple deletions in all possible combinations of the inhibitory element and the Edc3 and Upf1-binding motifs. The second set of *dcp2* alleles contains consecutive deletions of the nine leucine-rich Pat1-binding motifs, proceeding either from the N-terminal end of this set of motifs or from its C-terminus. The third set of *dcp2* alleles contains deletions of different combinations of Edc3, Upf1, and Pat1-binding motifs.

To link the potential defect in mRNA decapping to a specific Dcp2 interaction, we analyzed each of the *dcp2* element mutant alleles in two parallel assays. In the first assay, each *dcp2* allele was fused to the *GAL4* DNA-binding domain and the encoded fusion proteins were tested for interactions with those encoded by *EDC3*, *UPF1*, and *PAT1* fused

to the *GAL4* activation domain in the yeast two-hybrid system. In the second assay, each *dcp2* allele was N-terminally tagged with a triple HA epitope and integrated at the genomic locus of *DCP2* for functional analysis. Using quantitative northern blotting analyses, we measured the steady-state levels of different decapping substrates in each *dcp2* element mutant. Decapping substrates analyzed in this study include the NMD substrates *CYH2* pre-mRNA and *ade2-1*, *can1-100*, and *trp1-1* mRNAs; the Edc3 substrates *YRA1* pre-mRNA and *RPS28B* mRNA; the Dhh1 substrates *EDC1* and *SDS23* mRNAs; the Pat1/Lsm1 substrates *AGA1*, *BUR6*, *DIF1,* and *LSM3* mRNAs; and the Pat1/Lsm1/Dhh1 substrates *CHA1*, *HSP12,* and *HXT6* mRNAs. It should be noted that the presence of the HA-tag at the N-terminus of Dcp2 had no effect on its function in mRNA decay (Figure 1C, compare *HA-DCP2* to *WT*).

Plasmid construction

Plasmids used in this study are listed in the Table S2. Plasmids containing the original WT *DCP2* allele, *HA-DCP2* allele, and *dcp2* alleles with different C-terminal truncations were previously described (He and Jacobson, 2015). A plasmid containing the *edc3::URA3* allele was described in Dong *et al.* (2007). Plasmids containing the *xrn1::ADE2*, *ski2::URA3*, *ski7::URA3*, and *scd6::KanMX6* alleles were described in He et al. (2018). Plasmids containing the full-length *DCP1*, *UPF1*, *EDC3*, *PAT1*, and *DHH1* alleles fused to either *GAL4(AD)* or *GAL4(DB)* were described in He and Jacobson (2015). Plasmids constructed in this study are described below.

Construction of the *dcp2* element deletion alleles

dcp2 alleles harboring regulatory element deletions were all constructed in Bluescript by using the plasmid HFSE1645 either as an initial template or as a cloning vector (see Table S2). This plasmid contains the WT *HA-DCP2* allele as a 3.7kb *SalI-BglII/NotI* fragment, including 320 bp from the promoter/5'-UTR region and 401bp from the 3'-UTR region. Specific element deletions were all generated by using the QuikChange Site-Directed Mutagenesis Kit from Agilent Technologies (cat# 200519) according to the manufacturer's instructions. PCR primers used to generate specific Dcp2 element deletions are listed in Table S3. *dcp2* alleles containing single element deletions were generated by using plasmid HFSE1645 as a template. *dcp2* alleles containing two or more element deletions were generated by two different strategies. One strategy used sequential rounds of site-direct mutagenesis and the other used molecular cloning to combine pre-existing element deletions from different *DCP2* regions. Details on construction of each *dcp2* element deletion allele are provided in Table S2. Specific element deletions in individual *dcp2* mutant alleles were all confirmed by DNA sequencing. Each of these *dcp2* alleles can be isolated from the corresponding plasmids as a *SalI-BglII* DNA fragment. For clarity, we use the following matched pairs of abbreviations for each specific element and its deletion: the inhibitory element: IE/ID; the Edc3-binding motif: E3/E3D, E3-1/E3D1, and

28

E3-2/E3D2; the Upf1-binding motifs U1$_1$/U1D1 and U1$_2$/U1D2; and the nine leucine-rich motifs L$_1$ to L$_9$/LD1 to LD9. Analysis of *dcp2* alleles harboring different deletions of the inhibitory element and the Edc3 and Upf1-binding motifs revealed that loss of the inhibitory element affected neither the binding of Edc3, Upf1, and Pat1 to Dcp2, nor the steady-state levels of different decapping substrates (Figures 1B and 1C). Thus, *dcp2* alleles harboring a deletion of the inhibitory element are not discussed further and we focused our analysis on deletions of the Edc3, Upf1, and Pat1-binding motifs.

Construction of C-terminally truncated *dcp2* alleles

To facilitate the construction of the *dcp2-KanMX6* knock-in alleles harboring different *DCP2* C-terminal truncations, we generated modified versions of the *dcp2-N925*, *N770*, *N635*, *N475*, *N400*, and *N300* alleles in pRS315. These modified *dcp2* alleles are identical to those that were described in He and Jacobson (2015) except that each has a shorter 3'-UTR fragment and two additional restriction sites *BamHI* and *NotI* added to the 3'-end. The modified *dcp2* alleles were constructed in two steps. In the first step, a 5' *XbaI-NcoI* fragment isolated from the original WT *DCP2* allele and a 3' *NcoI-SalI* fragment amplified from the *DCP2* 3'-UTR region were ligated to pRS315 digested by *XbaI* and *XhoI*, generating pRS315-*DCP2-WT-M1*(HFSE1632). In the second step, the individual *SalI-NcoI dcp2* fragments were isolated from each of the original *dcp2* truncation alleles and these DNA fragments were then ligated to HFSE1632 digested by *SalI* and *NcoI*. Each of the modified *dcp2* truncation alleles can be isolated as either a *XbaI-BamHI* or a *SalI-BamHI* fragment.

Construction of the *dcp2-KanMX6 knock-in* alleles

All *dcp2-KanMX6* knock-in alleles were constructed in Bluescript by using the plasmid HFSE1636 as the cloning vector (see Table S2). This plasmid contains the previously described *dcp2-N245-KanMX6* allele as a 3.5 kb *NotI-BamHI/NotI/SalI* fragment, including 925 bp from the *DCP2* promoter/5'-UTR region and 401 bp from the 3'-UTR region (He and Jacobson, 2015). In this *dcp2* allele, the 1452 bp *BglII-EcoRI* KanMX6 selection cassette was inserted into the promoter region 588 bp upstream from the first base of the *DCP2* initiation codon. Two classes of *dcp2* knock-in alleles were constructed. One class contains different *dcp2* element deletions and the other contains different *dcp2* C-terminal truncations. For construction of the *dcp2* element deletion knock-in alleles, individual *SalI-BglII* DNA fragments were isolated from each of the original *dcp2* element deletion alleles in Bluescript and ligated to HFSE1636 previously digested by *SalI* and *BamHI*. For construction of the *dcp2* truncation knock-in alleles, individual *SalI-BamHI* DNA fragments were isolated from each of the modified *dcp2* truncation alleles in pRS315 and ligated to HFSE1636 previously digested by *SalI* and *BamHI*. Each of the *dcp2* knock-in alleles can be isolated as a *NotI-NotI* fragment for integrative yeast transformation.

Construction of the *Gal4(DB)-dcp2 fusion* alleles

Coding sequences from each of the *dcp2* element deletion alleles were fused to the *GAL4* DNA-binding domain by using plasmid pMA424 as the cloning vector (see Table S2). To facilitate the construction of these fusion alleles, we first used the plasmid HFSE1718 as a cloning vector to generate an intermediate allele from each of the original *dcp2* element deletion alleles. Plasmid HFSE1718 contains the entire WT *DCP2* coding region and 222bp from the 3'-UTR region as a *BamHI-NcoI/SalI* DNA fragment. To generate the intermediate *dcp2* alleles, depending on specific cases, either a 5' PCR amplified *BamHI-XhoI* fragment, or a 3' restriction *XhoI-NcoI* fragment, or both of these fragments were obtained from the *dcp2* element deletion alleles in Bluescript and then ligated to plasmid HFSE1718 previously digested by *BamH-XhoI*, *XhoI-NcoI*, or *BamH-NcoI*, respectively. To generate the final *Gal4(DB)-dcp2* fusion alleles, each of the *dcp2* intermediate alleles was isolated from the corresponding plasmid as a *BamHI-SalI* DNA fragment and then ligated to pMA424 previously digested by *BamHI-SalI*. All *Gal4(DB)-dcp2* fusion alleles were confirmed by DNA sequencing.

Construction of the *Gal4(DB)-XRN1 and Gal4(AD)-XRN1 fusion* alleles

The entire *XRN1* coding sequence was fused to the *GAL4* DNA-binding domain and activation domain by using plasmids pMA424 and pGAD-C2 as cloning vectors, respectively. Both fusion alleles were constructed through a three-piece ligation reaction by making use of the unique S*acI* restriction site located at nt 293 to 298 of the *XRN1* coding region. The *XRN1* coding sequences from nt 1 to 309 were amplified by PCR using oligonucleotide pair *XRN1-5'-BamHI-F* and *XRN1-5'-SacI-R* (Table S3). The resulting PCR product was digested by *BamHI* and *SacI*, yielding a *5' BamHI-SacI XRN1* fragment encompassing the first 297 nts of its coding sequences. A 3' *SacI-SalI XRN1* fragment encompassing the coding sequences from nt 298 to 4584 was isolated from plasmid HFSE1532. The 5' *BamHI-SacI* and 3' *SacI-SalI XRN1* fragments were then ligated to pMA4242 and pGAD-C2 digested by *BamHI* and *SalI* to generate the final *XRN1* fusion alleles. Both *XRN1* fusion alleles were confirmed by DNA sequencing.

Construction of the *upf1::KanMX6 and edc3::Hygro* alleles

The *upf1::KanMX6* and *edc3::Hygro* alleles were constructed in Bluescript. To construct Bs-ks-*upf1::KanMX6*, a PCR-amplified 417bp *NotI-BglII/NcoI* fragment from the *UPF1* 5'-UTR region and a PCR-amplified 416 bp *NcoI/EcoRI-SalI* fragment from the *UPF1* 3'-UTR region were ligated to Bluescript digested by *NotI* and *SalI* in a three-piece ligation reaction (*NotI-NcoI/NcoI-SalI*) to generate an intermediate plasmid containing a *upf1* allele lacking its entire CDS. The resulting intermediate plasmid was digested by *BglII* and *EcoRI* and then ligated to a 1452bp *BglII-EcoRI* KanMX6 selection cassette. To

construct Bs-ks-*edc3::Hygro*, a 455 bp PCR-amplified *NotI-XbaI*/*BamHI* fragment from the *EDC3* 5'-UTR region and a 512 bp PCR-amplified *BamHI/EcoRI-SalI* fragment from the *EDC3* 3'-UTR region were ligated to Bluescript digested by *NotI* and *SalI* in a three-piece ligation reaction (*NotI-BamHI*/*BamHI-SalI*) to generate an intermediate plasmid containing an *edc3* allele lacking its entire CDS. The resulting plasmid was digested by *BamHI* and *SalI* and then ligated to a 1666bp *BglII-SacI* Hygromycin resistant gene and a 508 bp PCR-amplified *SacI-SalI* fragment from the *EDC3* 3'-UTR region. The *upf1::KanMX6* and *edc3::Hygro* alleles can each be isolated as a *NotI-SalI* fragment for integrative yeast transformation.

Strain construction

Yeast strains used in this study are listed in the Table S1. The WT strain (HFY114) and its isogenic derivative harboring a deletion *of UPF1* were described previously (He et al., 1997), as were isogenic strains harboring deletions of *EDC3* (CFY25), *PAT1* (SYY2674), *LSM1* (SYY2680), or *DHH1* (SYY2686) (He and Jacobson, 2015). The yeast two-hybrid tester strain (GGY1::171) and its isogenic derivatives harboring deletions of *EDC3* (SYY1774), *PAT1* (SYY2451), and *DHH1* (SYY2467), or the *dcp2-N245* truncation of the Dcp2 C-terminal domain (SYY2390) were described previously (He and Jacobson, 2015). Yeast strains constructed in this study are described below.

Construction of yeast strains harboring *dcp2* element deletions

To assess the consequences of deleting specific Dcp2 regulatory elements on mRNA decay, we constructed a set of yeast strains with the W303 background that harbor different *dcp2* element deletion alleles. Each of these alleles was tagged by a triple-HA epitope at the 5'-end of its coding sequence and was integrated at the genomic locus of *DCP2* by gene replacement (Guthrie and Fink, 1991). As a control, we also constructed a yeast strain harboring the HA-tagged WT *DCP2* allele. Plasmids harboring different *dcp2-KanMX6* alleles were digested by *NotI* to release the DNA fragments harboring specific *dcp2* element deletion knock-in alleles. About 2 μg of each digested plasmid was transformed into the WT yeast strain HFY114 by the high-efficiency LiOAC method (Schiestl and Gietz, 1989). After transformation, cells were cultured in 1 ml YEPD media at room temperature for 90 minutes and then plated on G418-containing YEPD plates to select for integration events. Plates were incubated at 30°C for 3 to 4 days. Individual stable transformants were isolated from the plates and patched again on G418-containing YEPD plates. The patched transformants served as master cells for both genotyping and long-term storage. The correct integration and deletion of specific elements for each *dcp2-kanMX* knock-in allele were confirmed by genomic DNA PCR and sequencing. The primers used for genomic DNA PCR and sequencing are listed in Table S3. Approximately ten transformants were screened for each integrative yeast transformation.

To assess the decay mechanisms of different decapping substrates, we also introduced an *EDC3* deletion into yeast cells harboring *dcp2-E3D* or *E3D1* alleles, as well as deletions *of XRN1, SKI2,* or *SKI7* into yeast cells harboring *dcp2-E3D, E3D1, U1D1-U1D2,* and *LD1-9* alleles. Plasmids harboring the *edc3::URA3, xrn1::ADE2, ski2::URA3,* and *ski7::URA3* null alleles were used for yeast transformation. In each case, *a NotI-SalI* DNA fragment harboring the respective null allele was used for gene replacement. Each of the knock-out alleles was confirmed by genomic DNA PCR.

Construction of yeast strains expressing different Dcp2 C-terminal truncations

To assess the roles of the Dcp2 C-terminal domain in the formation of different decapping complexes, we constructed a set of two-hybrid tester strains harboring different C-terminal truncations of Dcp2 in both *EDC3* and *edc3Δ* backgrounds. These strains were also constructed by gene replacement. The transformation and selection procedures were identical to those described for the construction of yeast strains harboring different *dcp2* element deletion alleles except that : 1) plasmids harboring different *dcp2* C-terminal truncation knock-in alleles were used, and 2) each digested plasmid was transformed into the GGY1::171 and GGY1::171 *edc3::HygroR* (SYY3064) stains. The correct integration and C-terminal truncation for each *dcp2-kanMX* knock-in allele was confirmed by genomic DNA PCR and sequencing.

To assess the roles of Edc3, Upf1, Pat1, and Scd6 in the formation of different decapping complexes, we constructed additional yeast two-hybrid tester strains harboring single gene deletions of *EDC3, UPF1,* or *SCD6*; double gene deletions of *UPF1, PAT1,* or *SCD6* and *EDC3;* and the *dcp2-N245* C-terminal truncation of Dcp2 and *EDC3* deletion. Strains harboring the single *EDC3, UPF1,* or *SCD6* deletions were constructed by transforming a DNA fragment containing either the *edc3::HygroR* or the *upf1::KanMX6* or the *scd6::KanMX6* null allele into the GGY1::171 strain. Strains harboring the double deletions of *UPF1, PAT1,* or *SCD6* and *EDC3,* and strains harboring the *dcp2-N245* C-terminal truncation and *EDC3* deletion were constructed by transforming a DNA fragment containing the *edc3::HygroR* null allele into the single *UPF1, PAT1,* or *SCD6* deletion strains *upf1::KanMX6* (SYY2973), *pat11::KanMX6* (SYY2451), *scd6::KanMX6* (SYY2976) strains or the *dcp2-N245* truncation strain *dcp2-N245::KanMX6* (SYY2390), respectively. The *edc3::HygroR* and *scd6::KanMX6* knock-out alleles in the respective strains were confirmed by genomic DNA PCR.

Yeast Two-hybrid Interaction Assay

Two-hybrid assays employed previously described procedures (Fields and Song, 1989) and all tester strains used were in the GGY1::171 background. In each case, a *GAL4(DB)* fusion construct (1.5 μg) was co-transformed with a *GAL4(AD)* construct (1.5 μg) into a tester strain using the high-efficiency LiOAc method. Transformants were plated on

standard synthetic *-leu-his* drop-out media, incubated for 3 to 5 days at 30°C, and then replica-plated on X-Gal-containing SSX plates to observe the color development of the transformant population. The color phenotypes of two independent transformants from each interaction assay are presented in the figures. To assess the potential for self-activation, each of the *GAL4(DB)* fusions was also co-transformed with a GAL4(AD) empty vector into the GGY1::171 strain. In this study only *GAL4(DB)-DHH1* exhibited weak self-activation (He and Jacobson, 2015).

Cell samples for RNA isolation

Cells used for RNA isolation were all grown in YEPD media at 30°C. In each case, 15 ml YEPD in a 50 ml tube was inoculated with 1.5 OD_{600} overnight culture and the resulting culture was grown in a shaking incubator (200 rpm) to an OD_{600} of 0.7. Yeast cells in the 50-ml tube were pelleted by centrifugation in a benchtop centrifuge at 5000 rpm for 5 min. Cell pellets were resuspended in 0.5 ml fresh YEPD liquid medium and the cell suspension was then transferred to a 2-ml micro-centrifuge tube. Cells were pelleted by centrifugation in a micro-centrifuge at 12,000 rpm for one minute and the liquid medium was removed from the tube. Cell pellets were frozen on dry ice and then stored at -80°C until RNA isolation.

RNA isolation

Total RNA was isolated from yeast cells by using the hot phenol method described previously (Herrick et al., 1990). Briefly, each cell pellet from a 15 ml culture was resuspended in 500 µl buffer A (50 mM NaOAc pH5.2, 10 mM EDTA, 1% SDS, 1% DEPC) and mixed with 500 µl phenol pre-saturated with 50 mM NaOAc pH5.2, 10 mM EDTA (Fisher, Cat# A92-500) pre-warmed to 65°C. RNA was extracted by six cycles of 10 sec of vortexing followed by a 50 sec water bath incubation at 65°C. Samples were centrifuged in a micro-centrifuge at 12,000 rpm for three minutes. After centrifugation, the phenol layer from each sample was removed with a Pasteur pipette and 500µl pre-warmed buffer-saturated phenol was then added to each sample, followed by another six cycles of RNA extraction. After the final extraction cycle, samples were centrifuged in a micro-centrifuge at 12,000 rpm for 10 minutes and the aqueous layer from each sample was recovered and transferred to a new micro-centrifuge tube. Additional (400 µl) phenol/chloroform/isoamyl alcohol (25:24:1) (Ambion, Cat# AM9732) was added to the sample and the mixture was vortexed for two min followed by a 10 min centrifugation at 12,000rpm. The aqueous layer was recovered and subjected to another round of phenol/chloroform extraction. The aqueous layer was recovered and 40 µl NaOAc (3 M, pH 5.2) and 1 ml ethanol were added to each sample. RNA was precipitated at -70°C for 1h. Samples were centrifuged at 12,000 rpm for 15 min and pellets were washed two times with 70% ethanol. RNA pellets were air-dried for 15 min and dissolved in 80-100 µl RNase free distilled water. The RNA concentration of each sample was determined by measuring the A_{260} value of a diluted sample.

Northern blotting analysis

Procedures for northern blotting were described previously (He and Jacobson, 1995) . In brief, 15µg total RNA from each sample was loaded onto a formaldehyde-containing 1% agarose gel that was electrophoresed in 1x MOPS buffer (40 mM MOPS, 10 mM NaoAc, 1mM EDTA, pH7.0) overnight (1h at 70 volts and 16 hrs at 23 volts). RNA separated on the gel was transferred a cellulose membrane (Bio-Rad, Zeta-probe #1620159) by vacuum blotting with a sequence of 5 min in 50 mM NaOH/100 mM NaCl, 5 min in 100 mM Tris-HCl pH7.0, and 1h in 20X SSC buffer. After the transfer, the membrane was cross-linked with a UV Stratalinker 2400 and washed with a RPDW buffer (0.1X SSC, 0.1% SDS) at 58°C for 30 min. For random primed DNA probes, pre-hybridization of the membrane was carried out in Pre-Hyb buffer (50% formamide, 5X SSPE, 10X Denhardt's solution, 1% SDS, 0.5mg/ml sheared salmon sperm DNA) at 42°C for 2h, and hybridization was carried out in Hyb buffer (50% formamide, 5X SSPE, 2X Denhardt's solution, 5% dextran sulfate, 1% SDS, 0.25 mg/ml sheared salmon sperm DNA) at 42°C overnight. The membrane was washed with RPDW buffer 2X at room temperature for 10 min each, and then 2X at 58°C for 30 min each. Transcript-specific hybridization signals on the membrane were detected and imaged with a FUJI BAS-2500 analyzer. The images of northern blots were analyzed with MultiGauge software.

Random primed DNA probes were generated by using the Random Primed DNA Labeling Kit from Roche (cat# 11-004-760-001). Generally, 25-50 ng of purified DNA fragment was used to make the probe. The reaction was carried out in a total volume of 20µl, containing 10µl denatured DNA fragment, 2µl 10X concentrated reaction mixture, 1µl 10 mM dATP, 1µl 10 mM dGTP, 1µl 10 mM dTTP, 3µl α-^{32}P-dCTP (6000Ci/mmol, Perkin Elmer, Blu513Z), and 2µl Klenow enzyme. The reaction was incubated at 37°C for 1 to 4 h and stopped by heating at 65°C for 5 min. The reactions were then diluted to 80µl with sterile distilled water and purified with a mini-Quick-Spin Column (Roche #11814427001) according to the manufacturer's instructions.

DNA fragments used as template for making α-^{32}P-dCTP-labeled probes were isolated from plasmids. Depending on the specific gene, the DNA fragment covered part of the coding region, the entire coding region, both exon and intron, the entire 3'-UTR, or the entire gene. DNA sequences for each of these template DNA fragments are listed in Table S4. DNA probes used in this study included those that are specific for NMD substrates (*CYH2*, *CAN1*, *ADE2*, *TRP1*, *CPA1*, and *EST1*), Edc3 substrates (*YRA1* and *RPS28B*), Dhh1 substrates (*EDC1* and *SDS23*), Pat1/Lsm1 substrates (*LSM3*, *DIF1*, *BUR6,* and *AGA1*), and Pat1/Lsm1/Dhh1 substrates (*HXT6*, *HSP12*, and *CHA1*). Each northern blot was also hybridized with an *SCR1* probe to serve as a loading control. With a few exceptions, each experiment was repeated independently two or three times.

QUANTIFICATION AND STATISTICAL ANALYSIS

34

The transcript-specific image signals from each northern blot were quantified with MultiGauge software. The band intensity data were saved as txt files and then exported to and analyzed in Microsoft Excel. To determine the relative expression levels of a specific transcript in different strains, transcript-specific signals in these strains were first normalized to the corresponding *SCR1* signals and the resulting normalized signals in different strains were then divided by those from the WT strain. With a few exceptions, each northern blotting experiment was repeated independently at least two times. Bar graphs in relevant figures were generated by GraphPad Prism 9, mostly using the average ± SEM data.

REFERENCES

Aglietti, R.A., Floor, S.N., McClendon, C.L., Jacobson, M.P., and Gross, J.D. (2013). Active site conformational dynamics are coupled to catalysis in the mRNA decapping enzyme Dcp2. Structure *21*, 1571-1580.

Arribere, J.A., Doudna, J.A., and Gilbert, W.V. (2011). Reconsidering movement of eukaryotic mRNAs between polysomes and P bodies. Mol. Cell *44*, 745-758.

Badis, G., Saveanu, C., Fromont-Racine, M., and Jacquier, A. (2004). Targeted mRNA degradation by deadenylation-independent decapping. Mol. Cell *15*, 5-15.

Beelman, C.A., Stevens, A., Caponigro, G., LaGrandeur, T.E., Hatfield, L., Fortner, D.M., and Parker, R. (1996). An essential component of the decapping enzyme required for normal rates of mRNA turnover. Nature *382*, 642-646.

Behm-Ansmant, I., Rehwinkel, J., Doerks, T., Stark, A., Bork, P., and Izaurralde, E. (2006). mRNA degradation by miRNAs and GW182 requires both CCR4:NOT deadenylase and DCP1:DCP2 decapping complexes. Genes Dev. *20*, 1885-1898.

Borja, M.S., Piotukh, K., Freund, C., and Gross, J.D. (2011). Dcp1 links coactivators of mRNA decapping to Dcp2 by proline recognition. RNA *17*, 278-290.

Bouveret, E., Rigaut, G., Shevchenko, A., Wilm, M., and Seraphin, B. (2000). A Sm-like protein complex that participates in mRNA degradation. EMBO J. *19*, 1661-1671.

Braun, J.E., Truffault, V., Boland, A., Huntzinger, E., Chang, C.T., Haas, G., Weichenrieder, O., Coles, M., and Izaurralde, E. (2012). A direct interaction between DCP1 and XRN1 couples mRNA decapping to 5' exonucleolytic degradation. Nat. Struct. Mol. Biol. *19*, 1324-1331.

Celik, A., Baker, R., He, F., and Jacobson, A. (2017). High-resolution profiling of NMD targets in yeast reveals translational fidelity as a basis for substrate selection. RNA *23*, 735-748.

Chang, C.T., Muthukumar, S., Weber, R., Levdansky, Y., Chen, Y., Bhandari, D., Igreja, C., Wohlbold, L., Valkov, E., and Izaurralde, E. (2019). A low-complexity region in human XRN1 directly recruits deadenylation and decapping factors in 5'-3' messenger RNA decay. Nucleic Acids Res. *47*, 9282-9295.

Charenton, C., Gaudon-Plesse, C., Fourati, Z., Taverniti, V., Back, R., Kolesnikova, O., Seraphin, B., and Graille, M. (2017). A unique surface on Pat1 C-terminal domain directly interacts with Dcp2 decapping enzyme and Xrn1 5'-3' mRNA exonuclease in yeast. Proc. Natl. Acad. Sci. USA *114*, E9493-E9501.

Charenton, C., and Graille, M. (2018). mRNA decapping: finding the right structures. Phil. Trans. R. Soc. B *373*, 20180164

Charenton, C., Taverniti, V., Gaudon-Plesse, C., Back, R., Seraphin, B., and Graille, M. (2016). Structure of the active form of Dcp1-Dcp2 decapping enzyme bound to m^{7}GDP and its Edc3 activator. Nat. Struct. Mol. Biol. *23*, 982-986.

Coller, J., and Parker, R. (2005). General translational repression by activators of mRNA decapping. Cell *122*, 875-886.

Coller, J.M., Tucker, M., Sheth, U., Valencia-Sanchez, M.A., and Parker, R. (2001). The DEAD box helicase, Dhh1p, functions in mRNA decapping and interacts with both the decapping and deadenylase complexes. RNA *7*, 1717-1727.

Decker, C.J., and Parker, R. (1993). A turnover pathway for both stable and unstable mRNAs in yeast: evidence for a requirement for deadenylation. Genes Dev. *7*, 1632-1643.

Decker, C.J., Teixeira, D., and Parker, R. (2007). Edc3p and a glutamine/asparagine-rich domain of Lsm4p function in processing body assembly in *Saccharomyces cerevisiae*. J. Cell Biol. *179*, 437-449.

Deshmukh, M.V., Jones, B.N., Quang-Dang, D.U., Flinders, J., Floor, S.N., Kim, C., Jemiely, J., Kalek, M., Darzynkiewicz, E., and Gross, J.D. (2008). mRNA decapping is promoted by an RNA-binding channel in Dcp2. Mol. Cell *29*, 324-336.

Dong, S., Li, C., Zenklusen, D., Singer, R.H., Jacobson, A., and He, F. (2007). YRA1 autoregulation requires nuclear export and cytoplasmic Edc3p-mediated degradation of its pre-mRNA. Mol. Cell *25*, 559-573.

Dunckley, T., and Parker, R. (1999). The DCP2 protein is required for mRNA decapping in *Saccharomyces cerevisiae* and contains a functional MutT motif. EMBO J. *18*, 5411-5422.

Dunckley, T., Tucker, M., and Parker, R. (2001). Two related proteins, Edc1p and Edc2p, stimulate mRNA decapping in *Saccharomyces cerevisiae*. Genetics *157*, 27-37.

Fenger-Gron, M., Fillman, C., Norrild, B., and Lykke-Andersen, J. (2005). Multiple processing body factors and the ARE binding protein TTP activate mRNA decapping. Mol. Cell *20*, 905-915.

Fields, S., and Song, O. (1989). A novel genetic system to detect protein-protein interactions. Nature *340*, 245-246.

Fischer, N., and Weis, K. (2002). The DEAD box protein Dhh1 stimulates the decapping enzyme Dcp1. EMBO J. *21*, 2788-2797.

Floor, S.N., Borja, M.S., and Gross, J.D. (2012). Interdomain dynamics and coactivation of the mRNA decapping enzyme Dcp2 are mediated by a gatekeeper tryptophan. Proc. Natl. Acad. Sci. US A *109*, 2872-2877.

Floor, S.N., Jones, B.N., Hernandez, G.A., and Gross, J.D. (2010). A split active site couples cap recognition by Dcp2 to activation. Nat. Struct. Mol. Bio.l *17*, 1096-1101.

Fromm, S.A., Truffault, V., Kamenz, J., Braun, J.E., Hoffmann, N.A., Izaurralde, E., and Sprangers, R. (2012). The structural basis of Edc3- and Scd6-mediated activation of the Dcp1:Dcp2 mRNA decapping complex. EMBO J. *31*, 279-290.

Gaudon, C., Chambon, P., and Losson, R. (1999). Role of the essential yeast protein PSU1 in transcriptional enhancement by the ligand-dependent activation function AF-2 of nuclear receptors. EMBO J. *18*, 2229-2240.

Grudzien-Nogalska, E., and Kiledjian, M. (2017). New insights into decapping enzymes and selective mRNA decay. WIREs RNA *8, e1379*.

Guthrie, C., and Fink, G.R. (1991). Methods in Enzymology: Molecular Biology of *Saccharomyces cerevisiae*., Vol 194 (NY: Academic Press).

Hatfield, L., Beelman, C.A., Stevens, A., and Parker, R. (1996). Mutations in trans-acting factors affecting mRNA decapping in *Saccharomyces cerevisiae*. Mol. Cell. Biol. *16*, 5830-5838.

He, F., Brown, A.H., and Jacobson, A. (1997). Upf1p, Nmd2p, and Upf3p are interacting components of the yeast nonsense-mediated mRNA decay pathway. Mol. Cell. Biol. *17*, 1580-1594.

He, F., Celik, A., Wu, C., and Jacobson, A. (2018). General decapping activators target different subsets of inefficiently translated mRNAs. Elife *7,* e34409.

He, F., and Jacobson, A. (1995). Identification of a novel component of the nonsense-mediated mRNA decay pathway by use of an interacting protein screen. Genes Dev. *9*, 437-454.

He, F., and Jacobson, A. (2001). Upf1p, Nmd2p, and Upf3p regulate the decapping and exonucleolytic degradation of both nonsense-containing mRNAs and wild-type mRNAs. Mol. Cell. Biol. *21*, 1515-1530.

He, F., and Jacobson, A. (2015). Control of mRNA decapping by positive and negative regulatory elements in the Dcp2 C-terminal domain. RNA *21*, 1633-1647.

He, F., Li, C., Roy, B., and Jacobson, A. (2014). Yeast Edc3 targets RPS28B mRNA for decapping by binding to a 3' untranslated region decay-inducing regulatory element. Mol. Cell. Biol. *34*, 1438-1451.

He, F., Li, X., Spatrick, P., Casillo, R., Dong, S., and Jacobson, A. (2003). Genome-Wide Analysis of mRNAs Regulated by the Nonsense-Mediated and 5' to 3' mRNA Decay Pathways in Yeast. Mol. Cell *12*, 1439-1452.

Herrick, D., Parker, R., and Jacobson, A. (1990). Identification and comparison of stable and unstable mRNAs in *Saccharomyces cerevisiae*. Mol. Cell. Biol. *10*, 2269-2284.

Kshirsagar, M., and Parker, R. (2004). Identification of Edc3p as an enhancer of mRNA decapping in *Saccharomyces cerevisiae*. Genetics *166*, 729-739.

Lobel, J.H., Tibble, R.W., and Gross, J.D. (2019). Pat1 activates late steps in mRNA decay by multiple mechanisms. Proc. Natl. Acad. Sci. USA *116*, 23512-23517.

Mugridge, J.S., Tibble, R.W., Ziemniak, M., Jemielity, J., and Gross, J.D. (2018). Structure of the activated Edc1-Dcp1-Dcp2-Edc3 mRNA decapping complex with substrate analog poised for catalysis. Nat. Commun. *9*, 1152.

Nissan, T., Rajyaguru, P., She, M., Song, H., and Parker, R. (2010). Decapping activators in *Saccharomyces cerevisiae* act by multiple mechanisms. Mol. Cell *39*, 773-783.

Paquette, D.R., Tibble, R.W., Daifuku, T.S., and Gross, J.D. (2018). Control of mRNA decapping by autoinhibition. Nucleic Acids Res. *46*, 6318-6329.

Parker, R. (2012). RNA degradation in *Saccharomyces cerevisae*. Genetics *191*, 671-702.

Pedro-Segura, E., Vergara, S.V., Rodriguez-Navarro, S., Parker, R., Thiele, D.J., and Puig, S. (2008). The Cth2 ARE-binding protein recruits the Dhh1 helicase to promote the decay of succinate dehydrogenase SDH4 mRNA in response to iron deficiency. J. Biol. Chem. *283*, 28527-28535.

Radhakrishnan, A., Chen, Y.H., Martin, S., Alhusaini, N., Green, R., and Coller, J. (2016). The DEAD-Box Protein Dhh1p Couples mRNA Decay and Translation by Monitoring Codon Optimality. Cell *167*, 122-132 e129.

Rehwinkel, J., Behm-Ansmant, I., Gatfield, D., and Izaurralde, E. (2005). A crucial role for GW182 and the DCP1:DCP2 decapping complex in miRNA-mediated gene silencing. RNA *11*, 1640-1647.

Schiestl, R.H., and Gietz, R.D. (1989). High efficiency transformation of intact yeast cells using single stranded nucleic acids as a carrier. Curr. Genet. *16*, 339-346.

Sharif, H., Ozgur, S., Sharma, K., Basquin, C., Urlaub, H., and Conti, E. (2013). Structural analysis of the yeast Dhh1-Pat1 complex reveals how Dhh1 engages Pat1, Edc3 and RNA in mutually exclusive interactions. Nucleic Acids Res. 41, 8377-90

She, M., Decker, C.J., Chen, N., Tumati, S., Parker, R., and Song, H. (2006). Crystal structure and functional analysis of Dcp2p from *Schizosaccharomyces pombe*. Nat. Struct. Mol. Biol. *13*, 63-70.

She, M., Decker, C.J., Sundramurthy, K., Liu, Y., Chen, N., Parker, R., and Song, H. (2004). Crystal structure of Dcp1p and its functional implications in mRNA decapping. Nat. Struct. Mol. Biol. *11*, 249-256.

She, M., Decker, C.J., Svergun, D.I., Round, A., Chen, N., Muhlrad, D., Parker, R., and Song, H. (2008). Structural basis of dcp2 recognition and activation by dcp1. Mol. Cell *29*, 337-349.

Shi, Y. (2009). Serine/threonine phosphatases: mechanism through structure. Cell *139*, 468-484.

Steiger, M., Carr-Schmid, A., Schwartz, D.C., Kiledjian, M., and Parker, R. (2003). Analysis of recombinant yeast decapping enzyme. RNA *9*, 231-238.

Sweet, T., Kovalak, C., and Coller, J. (2012). The DEAD-box protein Dhh1 promotes decapping by slowing ribosome movement. PLoS Biol. *10*, e1001342.

Tharun, S., He, W., Mayes, A.E., Lennertz, P., Beggs, J.D., and Parker, R. (2000). Yeast Sm-like proteins function in mRNA decapping and decay. Nature *404*, 515-518.

Valkov, E., Jonas, S., and Weichenrieder, O. (2017). Mille viae in eukaryotic mRNA decapping. Curr. Opin. Struct. Biol. *47*, 40-51.

Valkov, E., Muthukumar, S., Chang, C.T., Jonas, S., Weichenrieder, O., and Izaurralde, E. (2016). Structure of the Dcp2-Dcp1 mRNA-decapping complex in the activated conformation. Nat. Struct. Mol. Biol. *23*, 574-579.

Virshup, D.M., and Shenolikar, S. (2009). From promiscuity to precision: protein phosphatases get a makeover. Mol. Cell *33*, 537-545.

Webster, M.W., Chen, Y.H., Stowell, J.A.W., Alhusaini, N., Sweet, T., Graveley, B.R., Coller, J., and Passmore, L.A. (2018). mRNA Deadenylation Is Coupled to Translation Rates by the Differential Activities of Ccr4-Not Nucleases. Mol. Cell *70*, 1089-1100, e1088.

Wurm, J.P., Holdermann, I., Overbeck, J.H., Mayer, P.H.O., and Sprangers, R. (2017). Changes in conformational equilibria regulate the activity of the Dcp2 decapping enzyme. Proc. Natl. Acad. Sci. USA *114*, 6034-6039.

Zeidan, Q., He, F., Zhang, F., Zhang, H., Jacobson, A., and Hinnebusch, A.G. (2018). Conserved mRNA-granule component Scd6 targets Dhh1 to repress translation initiation and activates Dcp2-mediated mRNA decay in vivo. PLoS Genet. *14*, e1007806.

KEY RESOURCES TABLE

REAGENT or RESOURCE	SOURCE	IDENTIFIER
Bacterial and virus strains		
ElectroMax DH5a-E competent cells	Invitrogen	11319-019
Chemicals, peptides, and recombinant proteins		
[α-^{32}P]-dCTP	Perkin Elmer	Blu513Z
5-Bromo-4-chloro-3-indolyl-beta-D-galactopyranoside (X-GAL)	USB	7240-90-6
Phenol	Fisher	A92-500
Phenol:Choroform:IAA (25:24:1)	Ambion	AM9732
Taq DNA polymerase	Roche	04-728-874-001
Herring Sperm DNA	Promega	D1815
Geneticin Selective Antibiotic (G418 Sulfate)	Gibco	11811-023
Hygromycin B	Roche	10843555001
Critical commercial assays		
QuikChange XL Site-Directed Mutagenesis Kit	Agilent Technologies	200519
Random Primed DNA labeling Kit	Roche	11-004-760-001
Experimental models: Organisms/strains		
See Table S1	This paper	N/A
Oligonucleotides		
See Table S3	This paper	N/A
Recombinant DNA		
See Table S2	This paper	N/A
See Table S4	This paper	N/A
Software and algorithms		
MultiGauge software	Fujifilm	Science lab 2005
GraphPad Prism 9 for Windows	GraphPad Software, LLC	https://www.graphpad.com/
Other		
Zeta-Probe Blotting Membranes	Bio-Rad	1620159
Mini Quick Spin RNA Columns	Roche	11-814-427-001

Figure 1

Figure 2

Figure 3

Figure 4

Figure 5

Figure 6

Figure 7

Supplemental Text and Figures

Figure S1. Loss of the Upf1- and Edc3-binding motifs respectively causes selective stabilization of NMD or Edc3/Dhh1 substrates (related to Figure 1)

(A) Schematics of *dcp2* alleles harboring specific deletions of the inhibitory element and the Edc3- and Upf1-binding motifs. Each of the *dcp2* alleles contains a triple HA-tag at its N-terminus and was integrated at the *DCP2* genomic locus for phenotypic analysis of mRNA decay. Specific element deletions are marked by filled triangles. The lower part of the panel displays the amino acid sequences and conservation patterns of the originally designated Edc3-binding site and its composite motifs, E3-1 and E3-2. Our data indicate that Edc3 binds to the E3-1 motif (see Figure 1B).

(B) Northern analyses of individual transcript levels in cells expressing specific *dcp2* deletion alleles or harboring deletions of *UPF1* or *EDC3*. Groupings depict transcripts subject to common regulation. The northern blots shown here are the same as those in Figure 1C but contain their respective matched loading control *SCR1* blots. In all blots lower case letters denote *SCR1* blots duplicated for clarity of presentation.

(C) Bar graphs of average ± SEM for the northern analyses depicted in Figure 1D. The relative levels of each decapping substrate in different strains were determined from three independent experiments, with one representative blot for each transcript shown in Figure 1D. In each case, the relative RNA levels in different mutants were calculated by comparisons to the levels of the respective transcripts in wild-type cells.
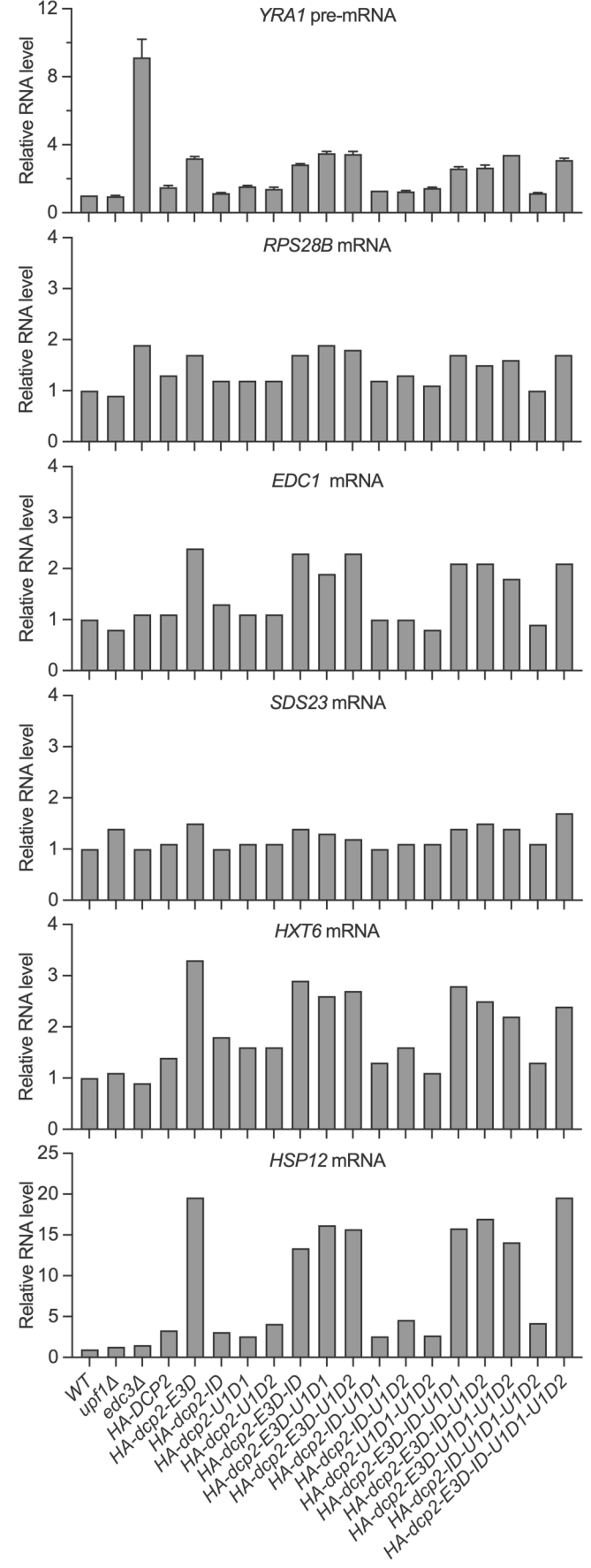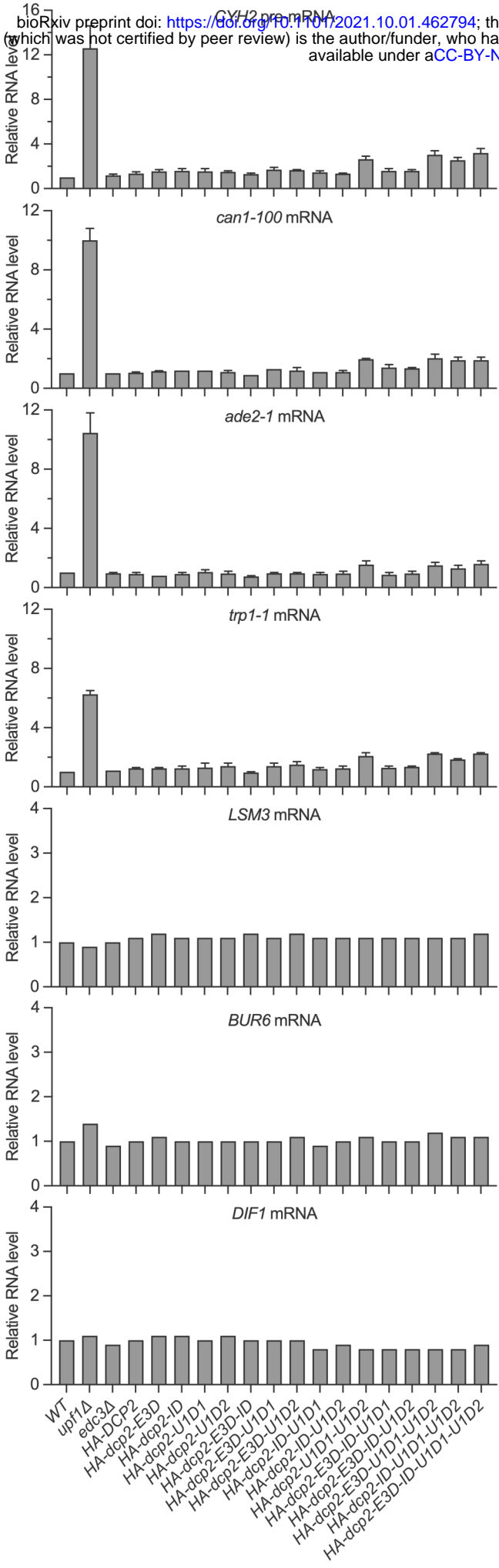
Figure S2. Loss of the Upf1- and Edc3-binding motifs respectively causes selective stabilization of NMD or Edc3/Dhh1 substrates (related to Figure 1)

Bar graphs for the northern analyses depicted in Figure 1C and for additional blots for *CYH2* and *YRA1*-pre-mRNAs, and *can1-100, ade2-1*, *trp1-1*, and *LSM3* mRNAs from independent experiments. In each case, relative RNA levels in different mutants were determined by comparisons to the levels of the same transcripts in wild-type cells. The graphs depict either single measurements or the average $\pm$ SEM.
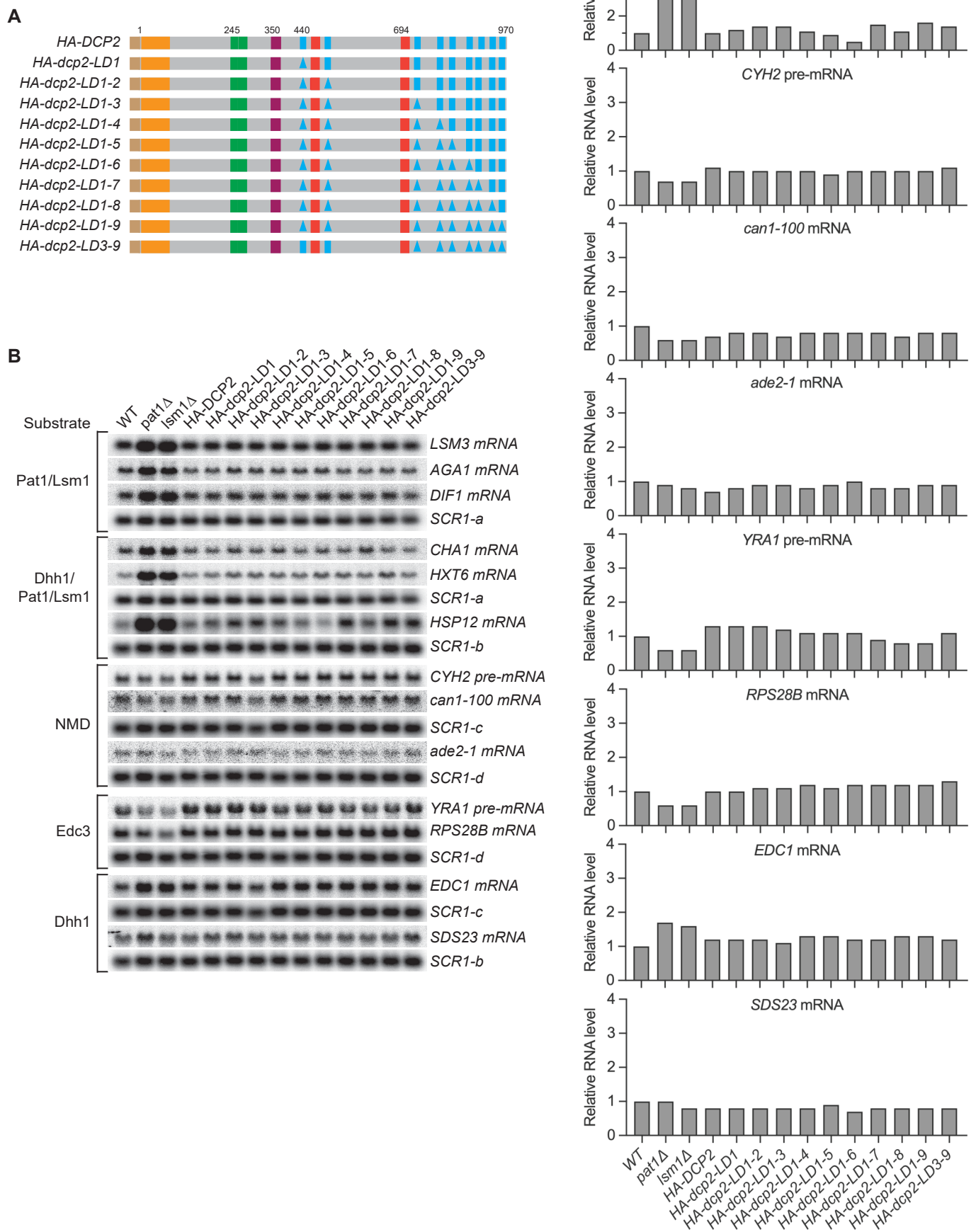
Figure S3. Loss of single, multiple, or even all nine leucine-rich motifs has no effect on decay of Pat1/Lsm1 and Pat1/Lsm1/Dhh1 substrates (related to Figure 2)

(A) Schematics of *dcp2* alleles harboring specific deletions of the leucine-rich Pat1-binding motifs. Each *dcp2* allele contains a triple HA-tag at its N-terminus and was integrated at the *DCP2* genomic locus for phenotypic analysis of mRNA decay. Specific element deletions are marked by filled triangles.

(B) Northern analyses of individual Pat1/Lsm1 and Pat1/Lsm1/Dhh1 substrate levels in cells harboring individual or combined deletions of Dcp2 leucine-rich motifs. The northern blots shown here are the same as those in Figure 2B but contain matched loading control *SCR1* blots. In all blots lower case letters denote *SCR1* blots duplicated for clarity of presentation.

(C) Bar graphs for a subset of the northern analyses depicted in Figure 2B. In each case, the relative RNA levels in different mutants were determined by comparison to the levels of the same transcripts in wild-type cells. The graphs depict data from single measurements.
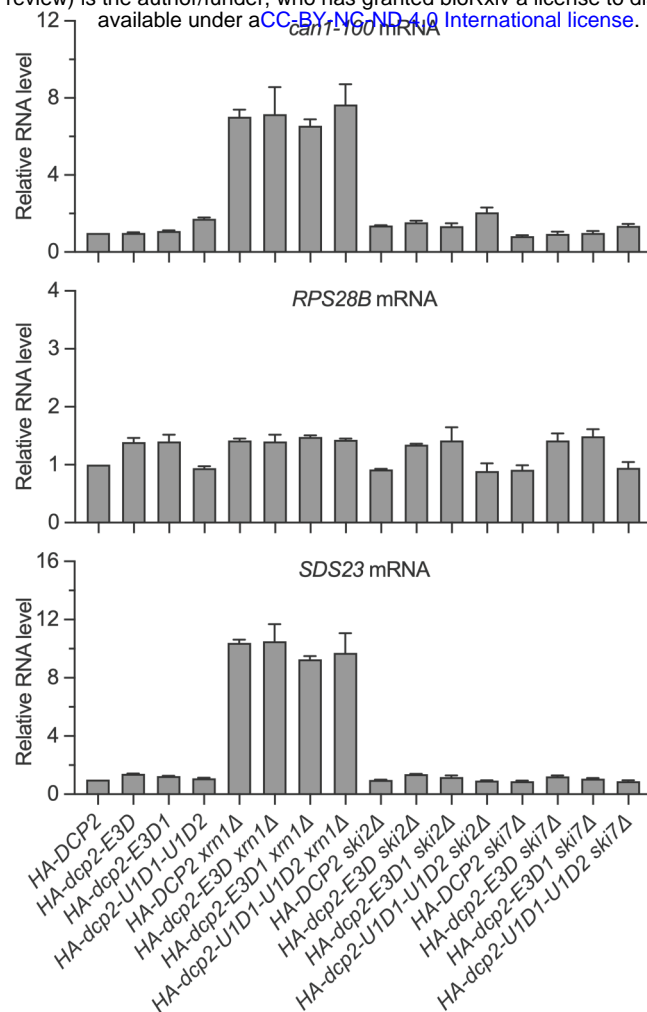
Figure S4. NMD, Edc3, and Dhh1 substrates are still degraded by decapping-dependent 5' to 3' decay in the absence of active recruitment of the decapping enzyme (related to Figure 3)

Bar graphs of average ± SEM for a subset of the northern analyses depicted in Figure 3B. The relative levels of each decapping substrate in different strains were determined from three independent experiments, with one representative blot for each transcript shown in Figure 3B. In each case, the relative RNA levels in different mutants were determined by comparison to the levels of the same transcripts in wild-type cells.
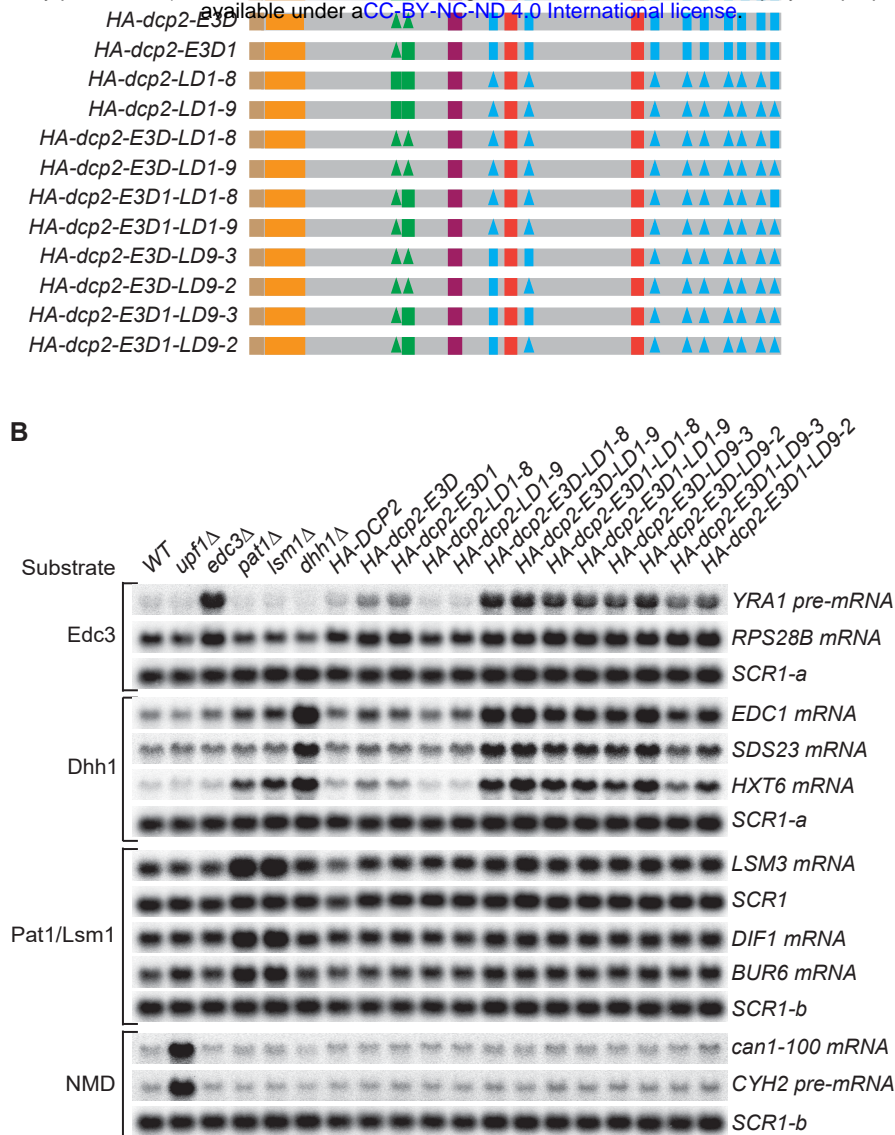
Figure S5. Simultaneous loss of the Edc3-binding motif and the leucine-rich motifs has synergistic effects and causes substantial stabilization of both Edc3 and Dhh1 substrates (related to Figure 4)

(A) Schematics of *dcp2* alleles harboring different combinations of deletions of the Edc3-binding motif and the leucine-rich Pat1-binding motifs. Each of the *dcp2* alleles contains a triple HA-tag at its N-terminus and was integrated at the *DCP2* genomic locus for phenotypic analysis of mRNA decay. Specific element deletions are marked by filled triangles.

(B) Northern analyses of the consequences of simultaneous loss of the Dcp2 Edc3-binding motif and leucine-rich motifs. The northern blots shown here are the same as those in Figure 4B but contain matched loading control *SCR1* blots. In all blots lower case letters denote *SCR1* blots duplicated for clarity of presentation.
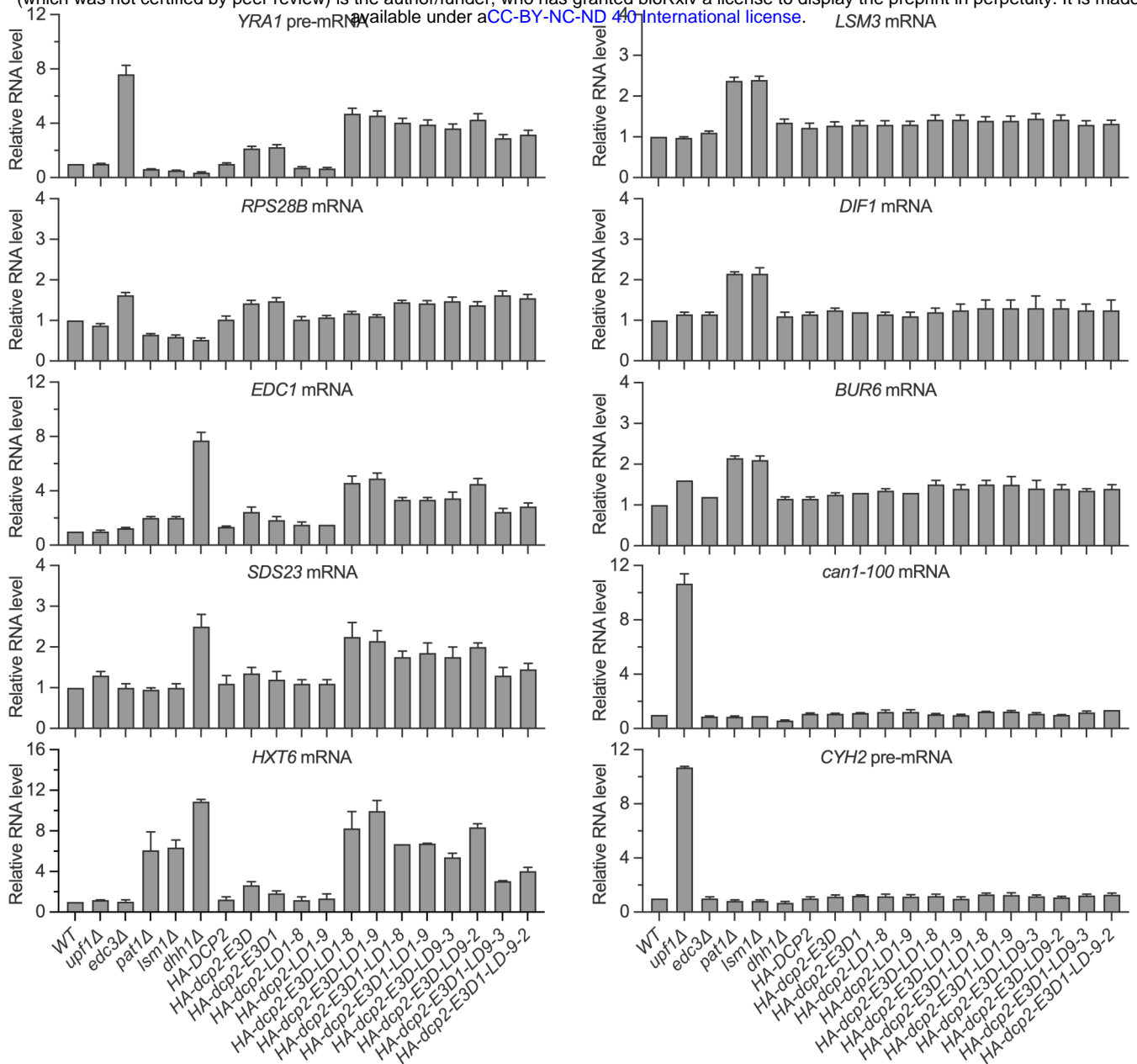
Figure S6. Simultaneous loss of the Edc3-binding motif and the leucine-rich motifs has synergistic effects and causes substantial stabilization of both Edc3 and Dhh1 substrates (related to Figure 4)

Bar graphs of average ± SEM for the northern analyses depicted in Figure 4B. The relative levels of each decapping substrate in different strains were determined from two or three independent experiments, with one representative blot for each transcript shown in Figure 4B. In each case, the relative RNA levels in different mutants were determined by comparison to the levels of the same transcripts in wild-type cells.
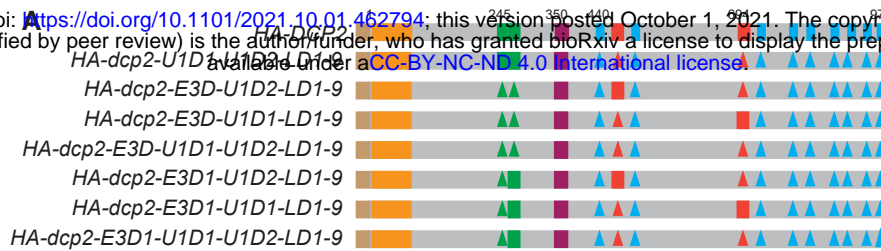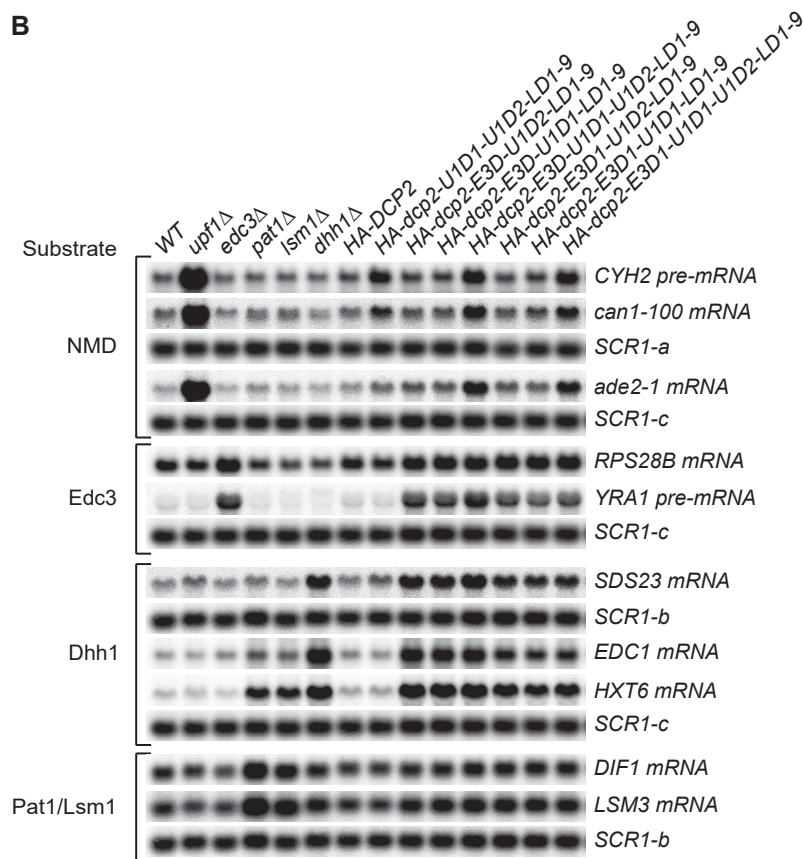
Figure S7. Simultaneous loss of the Upf1-binding motifs and the leucine-rich motifs has no synergistic effects on mRNA decapping, and a single Edc3- or Upf1-binding motif alone can promote efficient decapping of Edc3 or NMD substrates (related to Figure 4)

A) Schematics of *dcp2* alleles harboring different combinations of deletions of the Upf1-binding motifs, the Edc3-binding motif, and the leucine-rich Pat1-binding motifs. Each of these *dcp2* alleles contains a triple HA-tag at its N-terminus and was integrated at the *DCP2* genomic locus for phenotypic analysis of mRNA decay. Specific element deletions are marked by filled triangles.

(B) Northern analyses of the consequences of simultaneous loss of the Dcp2 Upf1-binding motifs and leucine-rich motifs, and the roles of single Dcp2 Edc3- or Upf1-binding motifs. The northern blots shown here are same as those in Figure 4C but contain matched loading control *SCR1* blots. In all blots lower case letters denote *SCR1* blots duplicated for clarity of presentation.
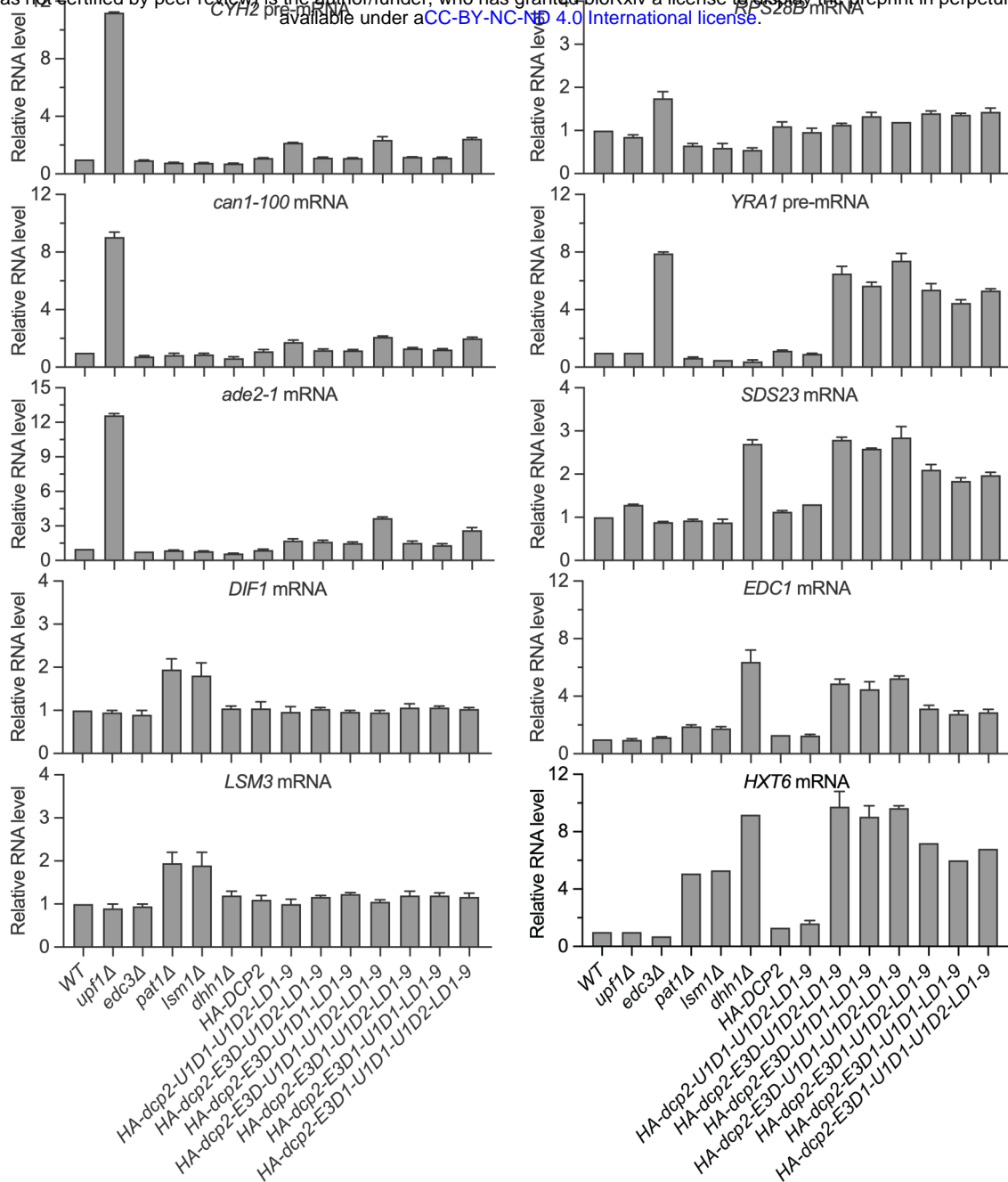
Figure S8. Simultaneous loss of the Upf1-binding motifs and the leucine-rich motifs has no synergistic effects on mRNA decapping, and a single Edc3- or Upf1-binding motif alone can promote efficient decapping of Edc3 or NMD substrates (related to Figure 4)

Bar graphs of average ± SEM for the northern analyses depicted in Figure 4C. The relative levels of each decapping substrate in different strains were determined from three or four independent experiments, with one representative blot for each transcript shown in Figure 4C. In each case, the relative RNA levels in different mutants were determined by comparison to the levels of the same transcripts in wild-type cells.
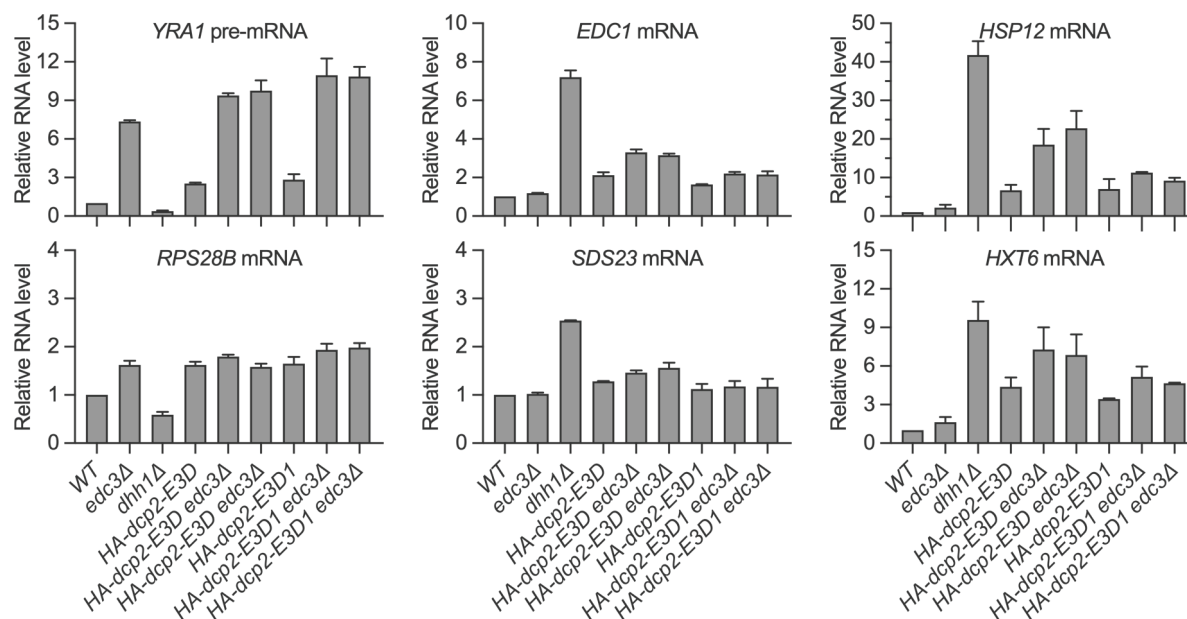
Figure S9. Loss of the Edc3-binding motif and *trans* deletion of *EDC3* have additive effects on decapping of both Edc3 and Dhh1 substrates (related to Figure 4)

Bar graphs of average ± SEM for the northern analyses depicted in Figure 4D. The relative levels of each decapping substrate in different strains were determined from two to four independent experiments, with one representative blot for each transcript shown in Figure 4D. In each case, the relative RNA levels in different mutants were determined by comparison to the levels of the same transcripts in wild-type cells.

Figure S10. Xrn1 binds to an internal region of Dcp2 (related to Figure 6)

(A) Xrn1 binds to specific Dcp2 fragments. A panel of Dcp2 fragments was tested for interaction with Xrn1 in two-hybrid assays. The *ND244* and *ND315* fragments exhibited weak interaction and the F5-C6 fragment exhibited strong interaction. The Xrn1-binding site on the F5-C6 was mapped further in Figure 6D.

(B) Interactions between Xrn1 and two internal fragments of Dcp2, F5-C6 or F5-C5, are independent of Edc3, Upf1, or Pat1. Two-hybrid interactions between Xrn1 and the Dcp2 F5-C6 or F5-C5 fragments were assessed in the wild-type tester strain and in tester strains containing single or double deletions of *EDC3*, *UPF1*, and *PAT1*.

SUPPLEMENTAL TABLE LEGENDS

Table S1. Yeast strains used in this study

Table S2. Plasmids used in this study

Table S3. Oligonucleotides used in this study

Table S4. DNA fragments used as probes in this study

Table S1. Yeast strains used in this study

Strain	Genotype	Reference
HFY114(W303)	*MATa ade2-1 his3-11,15 leu2-3,112 trp1-1 ura3-1 can1-100*	He et *al.*, 1997
HFY871	*MATa ade2-1 his3-11,15 leu2-3,112 trp1-1 ura3-1 can1-100 upf1::HIS3*	He et *al.*, 1997
CFY25	*MATa ade2-1 his3-11,15 leu2-3,112 trp1-1 ura3-1 can1-100 edc3::URA3*	He and Jacobson, 2015
SYY2674	*MATa ade2-1 his3-11,15 leu2-3,112 trp1-1 ura3-1 can1-100 pat1::KanMX6*	He and Jacobson, 2015
SYY2680	*MATa ade2-1 his3-11,15 leu2-3,112 trp1-1 ura3-1 can1-100 lsm1::KanMX6*	He and Jacobson, 2015
SYY2686	*MATa ade2-1 his3-11,15 leu2-3,112 trp1-1 ura3-1 can1-100 dhh1::KanMX6*	He and Jacobson, 2015
SYY2990	*MATa ade2-1 his3-11,15 leu2-3,112 trp1-1 ura3-1 can1-100 HA-DCP2-KanMX6*	This study
SYY3013	*MATa ade2-1 his3-11,15 leu2-3,112 trp1-1 ura3-1 can1-100 HA-dcp2-E3D-KanMX6*	This study
SYY3016	*MATa ade2-1 his3-11,15 leu2-3,112 trp1-1 ura3-1 can1-100 HA-dcp2-ID-KanMX6*	This study
SYY3019	*MATa ade2-1 his3-11,15 leu2-3,112 trp1-1 ura3-1 can1-100 HA-dcp2-U1D1-KanMX6*	This study
SYY3022	*MATa ade2-1 his3-11,15 leu2-3,112 trp1-1 ura3-1 can1-100 HA-dcp2-U1D2-KanMX6*	This study
SYY3025	*MATa ade2-1 his3-11,15 leu2-3,112 trp1-1 ura3-1 can1-100 HA-dcp2-E3D-ID-KanMX6*	This study
SYY3028	*MATa ade2-1 his3-11,15 leu2-3,112 trp1-1 ura3-1 can1-100 HA-dcp2-E3D-U1D1-KanMX6*	This study
SYY3031	*MATa ade2-1 his3-11,15 leu2-3,112 trp1-1 ura3-1 can1-100 HA-dcp2-E3D-U1D2-KanMX6*	This study
SYY3034	*MATa ade2-1 his3-11,15 leu2-3,112 trp1-1 ura3-1 can1-100 HA-dcp2-ID-U1D1-KanMX6*	This study
SYY3037	*MATa ade2-1 his3-11,15 leu2-3,112 trp1-1 ura3-1 can1-100 HA-dcp2-ID-U1D2-KanMX6*	This study
SYY3040	*MATa ade2-1 his3-11,15 leu2-3,112 trp1-1 ura3-1 can1-100 HA-dcp2-U1D1-U1D2-KanMX6*	This study
SYY3043	*MATa ade2-1 his3-11,15 leu2-3,112 trp1-1 ura3-1 can1-100 HA-dcp2-E3D-ID-U1D1-KanMX6*	This study
SYY3046	*MATa ade2-1 his3-11,15 leu2-3,112 trp1-1 ura3-1 can1-100 HA-dcp2-E3D-ID-U1D2-KanMX6*	This study
SYY3049	*MATa ade2-1 his3-11,15 leu2-3,112 trp1-1 ura3-1 can1-100 HA-dcp2-E3D-U1D1-U1D2-KanMX6*	This study
SYY3052	*MATa ade2-1 his3-11,15 leu2-3,112 trp1-1 ura3-1 can1-100 HA-dcp2-ID-U1D1-U1D2-KanMX6*	This study
SYY3055	*MATa ade2-1 his3-11,15 leu2-3,112 trp1-1 ura3-1 can1-100 HA-dcp2-E3D-ID-U1D1-U1D2-KanMX6*	This study
SYY3097	*MATa ade2-1 his3-11,15 leu2-3,112 trp1-1 ura3-1 can1-100 HA-dcp2-LD1-KanMX6*	This study
SYY3100	*MATa ade2-1 his3-11,15 leu2-3,112 trp1-1 ura3-1 can1-100 HA-dcp2-LD1-2-KanMX6*	This study
SYY3103	*MATa ade2-1 his3-11,15 leu2-3,112 trp1-1 ura3-1 can1-100 HA-dcp2-LD1-3-KanMX6*	This study
SYY3106	*MATa ade2-1 his3-11,15 leu2-3,112 trp1-1 ura3-1 can1-100 HA-dcp2-LD1-4-KanMX6*	This study
SYY3109	*MATa ade2-1 his3-11,15 leu2-3,112 trp1-1 ura3-1 can1-100 HA-dcp2-LD1-5-KanMX6*	This study
SYY3112	*MATa ade2-1 his3-11,15 leu2-3,112 trp1-1 ura3-1 can1-100 HA-dcp2-LD1-6-KanMX6*	This study
SYY3115	*MATa ade2-1 his3-11,15 leu2-3,112 trp1-1 ura3-1 can1-100 HA-dcp2-LD1-7-KanMX6*	This study
SYY3118	*MATa ade2-1 his3-11,15 leu2-3,112 trp1-1 ura3-1 can1-100 HA-dcp2-LD1-8-KanMX6*	This study
SYY3121	*MATa ade2-1 his3-11,15 leu2-3,112 trp1-1 ura3-1 can1-100 HA-dcp2-LD1-9-KanMX6*	This study
SYY3124	*MATa ade2-1 his3-11,15 leu2-3,112 trp1-1 ura3-1 can1-100 HA-dcp2-LD3-9-KanMX6*	This study
SYY3091	*MATa ade2-1 his3-11,15 leu2-3,112 trp1-1 ura3-1 can1-100 HA-dcp2-E3D1-KanMX6*	This study
SYY3094	*MATa ade2-1 his3-11,15 leu2-3,112 trp1-1 ura3-1 can1-100 HA-dcp2-E3D2-KanMX6*	This study
SYY3127	*MATa ade2-1 his3-11,15 leu2-3,112 trp1-1 ura3-1 can1-100 HA-dcp2-E3D-KanMX6 edc3::URA3*	This study
SYY3128	*MATa ade2-1 his3-11,15 leu2-3,112 trp1-1 ura3-1 can1-100 HA-dcp2-E3D-KanMX6 edc3::URA3*	This study
SYY3131	*MATa ade2-1 his3-11,15 leu2-3,112 trp1-1 ura3-1 can1-100 HA-dcp2-E3D1-KanMX6 edc3::URA3*	This study
SYY3132	*MATa ade2-1 his3-11,15 leu2-3,112 trp1-1 ura3-1 can1-100 HA-dcp2-E3D1-KanMX6 edc3::URA3*	This study
SYY3171	*MATa ade2-1 his3-11,15 leu2-3,112 trp1-1 ura3-1 can1-100 HA-dcp2-E3D-LD1-8-KanMX6*	This study
SYY3174	*MATa ade2-1 his3-11,15 leu2-3,112 trp1-1 ura3-1 can1-100 HA-dcp2-E3D-LD1-9-KanMX6*	This study
SYY3177	*MATa ade2-1 his3-11,15 leu2-3,112 trp1-1 ura3-1 can1-100 HA-dcp2-E3D-LD1-8-KanMX6*	This study
SYY3180	*MATa ade2-1 his3-11,15 leu2-3,112 trp1-1 ura3-1 can1-100 HA-dcp2-E3D-LD1-9-KanMX6*	This study
SYY3183	*MATa ade2-1 his3-11,15 leu2-3,112 trp1-1 ura3-1 can1-100 HA-dcp2-E3D-LD9-3-KanMX6*	This study
SYY3186	*MATa ade2-1 his3-11,15 leu2-3,112 trp1-1 ura3-1 can1-100 HA-dcp2-E3D-LD9-2-KanMX6*	This study
SYY3189	*MATa ade2-1 his3-11,15 leu2-3,112 trp1-1 ura3-1 can1-100 HA-dcp2-E3D1-LD9-3-KanMX6*	This study
SYY3192	*MATa ade2-1 his3-11,15 leu2-3,112 trp1-1 ura3-1 can1-100 HA-dcp2-E3D1-LD-9-2-KanMX6*	This study
SYY3237	*MATa ade2-1 his3-11,15 leu2-3,112 trp1-1 ura3-1 can1-100 HA-dcp2-U1D1-U1D2-LD1-9-KanMX6*	This study
SYY3219	*MATa ade2-1 his3-11,15 leu2-3,112 trp1-1 ura3-1 can1-100 HA-dcp2-E3D-U1D2-LD1-9-KanMX6*	This study
SYY3222	*MATa ade2-1 his3-11,15 leu2-3,112 trp1-1 ura3-1 can1-100 HA-dcp2-E3D-U1D1-LD1-9-KanMX6*	This study
SYY3225	*MATa ade2-1 his3-11,15 leu2-3,112 trp1-1 ura3-1 can1-100 HA-dcp2-E3D-U1D1-U1D2-LD1-9-KanMX6*	This study
SYY3228	*MATa ade2-1 his3-11,15 leu2-3,112 trp1-1 ura3-1 can1-100 HA-dcp2-E3D1-U1D2-LD1-9-KanMX6*	This study
SYY3231	*MATa ade2-1 his3-11,15 leu2-3,112 trp1-1 ura3-1 can1-100 HA-dcp2-E3D1-U1D1-LD1-9-KanMX6*	This study

SYY3234	*MATa ade2-1 his3-11,15 leu2-3,112 trp1-1 ura3-1 can1-100 HA-dcp2-E3D1-U1D1-U1D2-LD1-9-KanMX6*	This study
SYY3144	*MATa ade2-1 his3-11,15 leu2-3,112 trp1-1 ura3-1 can1-100 HA-DCP2-KanMX6 xrn1::ADE2*	This study
SYY3135	*MATa ade2-1 his3-11,15 leu2-3,112 trp1-1 ura3-1 can1-100 HA-DCP2-E3D-KanMX6 xrn1::ADE2*	This study
SYY3138	*MATa ade2-1 his3-11,15 leu2-3,112 trp1-1 ura3-1 can1-100 HA-DCP2-E3D1-KanMX6 xrn1::ADE2*	This study
SYY3141	*MATa ade2-1 his3-11,15 leu2-3,112 trp1-1 ura3-1 can1-100 HA-DCP2-U1D1-U1D2-KanMX6 xrn1::ADE2*	This study
SYY3158	*MATa ade2-1 his3-11,15 leu2-3,112 trp1-1 ura3-1 can1-100 HA-DCP2-KanMX6 ski2::URA3*	This study
SYY3149	*MATa ade2-1 his3-11,15 leu2-3,112 trp1-1 ura3-1 can1-100 HA-DCP2-E3D-KanMX6 ski2::URA3*	This study
SYY3152	*MATa ade2-1 his3-11,15 leu2-3,112 trp1-1 ura3-1 can1-100 HA-DCP2-E3D1-KanMX6 ski2::URA3*	This study
SYY3155	*MATa ade2-1 his3-11,15 leu2-3,112 trp1-1 ura3-1 can1-100 HA-DCP2-U1D1-U1D2-KanMX6 ski2::URA3*	This study
SYY3166	*MATa ade2-1 his3-11,15 leu2-3,112 trp1-1 ura3-1 can1-100 HA-DCP2-KanMX6 ski7::URA3*	This study
SYY3160	*MATa ade2-1 his3-11,15 leu2-3,112 trp1-1 ura3-1 can1-100 HA-DCP2-E3D-KanMX6 ski7::URA3*	This study
SYY3163	*MATa ade2-1 his3-11,15 leu2-3,112 trp1-1 ura3-1 can1-100 HA-DCP2-E3D1-KanMX6 ski7::URA3*	This study
SYY3169	*MATa ade2-1 his3-11,15 leu2-3,112 trp1-1 ura3-1 can1-100 HA-DCP2-U1D1-U1D2-KanMX6 ski7::URA3*	This study
SYY3195	*MATa ade2-1 his3-11,15 leu2-3,112 trp1-1 ura3-1 can1-100 HA-dcp2-LD1-9-KanMX6 xrn1::ADE2*	This study
SYY3198	*MATa ade2-1 his3-11,15 leu2-3,112 trp1-1 ura3-1 can1-100 HA-dcp2-LD1-9-KanMX6 ski2::URA3*	This study
SYY3201	*MATa ade2-1 his3-11,15 leu2-3,112 trp1-1 ura3-1 can1-100 HA-dcp2-LD1-9-KanMX6 ski7::URA3*	This study
GGY1::171	*his3 leu2 URA3::GAL1-lacZ gal4Δ gal80Δ*	He and Jacobson, 2015
SYY2390	*his3 leu2 URA3::GAL1-lacZ gal4Δ gal80Δ dcp2-N245::KanMX6*	He and Jacobson, 2015
SYY1774	*his3 leu2 URA3::GAL1-lacZ gal4Δ gal80Δ edc3::KanMX6*	He and Jacobson, 2015
SYY2451	*his3 leu2 URA3::GAL1-lacZ gal4Δ gal80Δ pat1::KanMX6*	He and Jacobson, 2015
SYY2467	*his3 leu2 URA3::GAL1-lacZ gal4Δ gal80Δ dhh1::KanMX6*	He and Jacobson, 2015
SYY2973	*his3 leu2 URA3::GAL1-lacZ gal4Δ gal80Δ upf1::KanMX6*	This study
SYY2976	*his3 leu2 URA3::GAL1-lacZ gal4Δ gal80Δ scd6::KanMX6*	This study
SYY2744	*his3 leu2 URA3::GAL1-lacZ gal4Δ gal80Δ dcp2-N245::KanMX6 edc3::HygroR*	This study
SYY2986	*his3 leu2 URA3::GAL1-lacZ gal4Δ gal80Δ upf1::KanMX6 edc3::HygroR*	This study
SYY2980	*his3 leu2 URA3::GAL1-lacZ gal4Δ gal80Δ pat1::KanMX6 edc3::HygroR*	This study
SYY3060	*his3 leu2 URA3::GAL1-lacZ gal4Δ gal80Δ scd6::KanMX6 edc3::HygroR*	This study
SYY3067	*his3 leu2 URA3::GAL1-lacZ gal4Δ gal80Δ dcp2-N925-KanMX6*	This study
SYY3070	*his3 leu2 URA3::GAL1-lacZ gal4Δ gal80Δ dcp2-N770-KanMX6*	This study
SYY3073	*his3 leu2 URA3::GAL1-lacZ gal4Δ gal80Δ dcp2-N630-KanMX6*	This study
SYY3075	*his3 leu2 URA3::GAL1-lacZ gal4Δ gal80Δ dcp2-N475-KanMX6*	This study
SYY3077	*his3 leu2 URA3::GAL1-lacZ gal4Δ gal80Δ dcp2-N400-KanMX6*	This study
SYY3079	*his3 leu2 URA3::GAL1-lacZ gal4Δ gal80Δ dcp2-N300-KanMX6*	This study
SYY3064	*his3 leu2 URA3::GAL1-lacZ gal4Δ gal80Δ edc3::HygroR*	This study
SYY3081	*his3 leu2 URA3::GAL1-lacZ gal4Δ gal80Δ dcp2-N925-KanMX6 edc3::HygroR*	This study
SYY3083	*his3 leu2 URA3::GAL1-lacZ gal4Δ gal80Δ dcp2-N770-KanMX6 edc3::HygroR*	This study
SYY3085	*his3 leu2 URA3::GAL1-lacZ gal4Δ gal80Δ dcp2-N630-KanMX6 edc3::HygroR*	This study
SYY3087	*his3 leu2 URA3::GAL1-lacZ gal4Δ gal80Δ dcp2-N475-KanMX6 edc3::HygroR*	This study
SYY3090	*his3 leu2 URA3::GAL1-lacZ gal4Δ gal80Δ dcp2-N400-KanMX6 edc3::HygroR*	This study
SYY3089	*his3 leu2 URA3::GAL1-lacZ gal4Δ gal80Δ dcp2-N300-KanMX6 edc3::HygroR*	This study

Table S2. Plasmids used in this study

Name	Vector and allele	5' Restriction site(s)	3' Restriction site(s)	Description
HFSE2095	Bs-xrn1::ADE2	NotI	SalI	Contains the xrn1::ADE2 null allele as a NotI-SalI fragment, described previously in He et al. (2018)
HFE2289	Bs-ski2::URA3	NotI	SalI	Contains the ski2::URA3 null allele as a NotI-SalI fragment, described previously He et al. (2018)
HFSE26	Bs-Ks-ski7::URA3	NotI	SalI	Contains the ski7::URA3 null allele as a NotI-SalI fragment, described previously in He et al. (2018)
HFSE1066	Bs-scd6::KanMX6	NotI	SalI	Contains the scd6::KanMX6 null allele as a NotI-SalI fragment, described previously in He et al. (2018)
HFCE7	Bs-ks-edc3::URA3	NotI	SalI	Contains the edc3::URA3 null allele as a NotI-SalI fragment, described previously in Dong et al. (2007)
HFSE1494	Bs-ks-edc3::HygroR	NotI	SalI	Contains the edc3::HygroR null allele as a NotI-SalI fragment
HFSE814	Bs-ks-upf1::KanMX6	NotI	SalI	Contains the upf1::KanMX6 null allele as a NotI-SalI fragment
HFSE709	pRS315-DCP2	XbaI	Sau3A/BamHI	Contains wild-type DCP2 as a 4.3 kb XbaI-Sau3AI fragment, described previously in He and Jacobson (2015)
HFSE732	pRS315-dcp2-N925	XbaI	Sau3A/BamHI	Same as HFSE709 but contains a deletion of 45 codons from the C-terminus, described previously in He and Jacobson (2015)
HFSE721	pRS315-dcp2-N771	XbaI	Sau3A/BamHI	Same as HFSE709 but contains a deletion of 199 codons from the C-terminus, described previously in He and Jacobson (2015)
HFSE719	pRS315-dcp2-N630	XbaI	Sau3A/BamHI	Same as HFSE709 but contains a deletion of 340 codons from the C-terminus, described previously in He and Jacobson (2015)
HFSE731	pRS315-dcp2-N475	XbaI	Sau3A/BamHI	Same as HFSE709 but contains a deletion of 495 codons from the C-terminus, described previously in He and Jacobson (2015)
HFSE1376	pRS315-dcp2-N400	XbaI	Sau3A/BamHI	Same as HFSE1076 but contains a deletion of 570 codons from the C-terminus, described previously in He and Jacobson (2015)
HFSE729	pRS315-dcp2-N300	XbaI	Sau3A/BamHI	Same as HFSE709 but contains a deletion of 670 codons from the C-terminus, described previously in He and Jacobson (2015)
HFSE1520	pRS315-HA-DCP2	XbaI	Sau3A/BamHI	Same as HFSE709 but contains a triple HA tag at the N-terminus, described previously in He and Jacobson (2015)
HFSE1624	pRS315-HA-dcp2-E153Q-N245	XbaI	SalI	Contains an N-terminal triple HA-tagged dcp2-E153Q-N245 allele as a 2.1kb XbaI-SalI fragment, described previously in He et al. (2018)
HFSE1638	pRS315-HA-DCP2-WT-M1	XbaI	BglII-NotI-SalI/XhoI	Contains the N-terminal triple HA-tagged wild-type DCP2 allele as a 4.3 kb XbaI-BglII fragment, constructed by ligating the BamHI-NcoI DCP2 fragment from HFSE1520 and a PCR amplyfied 3'-UTR Ncol-SalI fragment to HFSE1624 digested by BamHI-XhoI
HFSE1632	pRS315-DCP2-WT-M1	XbaI	BamHI-NotI-SalI/XhoI	contains the wild-type DCP2 allele as a 4.2 kb XbaI-BamHI fragment, constructed by ligating the XbaI-NcoI DCP2 fragment from HFSE709 and a PCR amplified 3'-UTR NcoI-SalI fragment to pRS315 digested by XbaI-XhoI
HFSE1813	pRS315-dcp2-N925-M1	XbaI	BamHI-NotI-SalI/XhoI	same as HFSE1632 but contains a C-terminal 45-codon deletion of DCP2, constructed by ligating the SalI-NcoI dcp2 fragment from HFSE732 to HFSE1632 digested by SalI-NcoI
HFSE1815	pRS315-dcp2-N770-M1	XbaI	BamHI-NotI-SalI/XhoI	same as HFSE1632 but contains a C-terminal 200-codon acid deletion of DCP2, constructed by ligating the SalI-NcoI dcp2 fragment from HFSE721 to HFSE1632 digested by SalI-NcoI
HFSE1817	pRS315-dcp2-N630-M1	XbaI	BamHI-NotI-SalI/XhoI	same as HFSE1632 but contains a C-terminal 340-codon acid deletion of DCP2, constructed by ligating the SalI-NcoI dcp2 fragment from HFSE719 to HFSE1632 digested by SalI-NcoI
HFSE1819	pRS315-dcp2-N475-M1	XbaI	BamHI-NotI-SalI/XhoI	same as HFSE1632 but contains a C-terminal 495-codon deletion of DCP2, constructed by ligating the SalI-NcoI dcp2 fragment from HFSE731 to HFSE1632 digested by SalI-NcoI
HFSE1821	pRS315-dcp2-N400-M1	XbaI	BamHI-NotI-SalI/XhoI	same as HFSE1632 but contains a C-terminal 570-codon deletion of DCP2, constructed by ligating the SalI-NcoI dcp2 fragment from HFSE1376 to HFSE1632 digested by SalI-NcoI
HFSE1823	pRS315-dcp2-N300-M1	XbaI	BamHI-NotI-SalI/XhoI	same as HFSE1632 butcontains a C-terminal 670-codon deletion of DCP2, constructed by ligating the SalI-NcoI dcp2 fragment from HFSE729 to HFSE1632 digested by SalI-NcoI
HFSE1147	Bs-Ks-dcp2-N245-KanMX6	NotI-XbaI	XhoI	contains the dcp2-N245-KanMX6 allele as a 3.5 Kb XbaI-XhoI fragment, described previously in He and Jacobson (2015)
HFSE1636	Bs-ks-dcp2-N245-KanMX6-M1	NotI-XbaI	BamHI-NotI-SalI/XhoI	contains the dcp2-N245-KanMX6 allele as a 3.5 Kb NotI-NotI fragment, constructed by ligating a KanMX6-DCP2 HindIII-NcoI fragment isolated form HFSE1147 and a PCR-amplified DCP2 3'-UTR NcoI-SalI fragment to HFSE1147 digested by HindIII-XhoI
HFSE1825	Bs-ks-dcp2-N925-KanMX6	NotI-XbaI	BamHI-NotI-SalI/XhoI	constructed by ligating the SalI-BamHI dcp2 fragment from HSE1813 to HFSE1636 digested by SalI-BamHI
HFSE1827	Bs-ks-dcp2-N770-KanMX6	NotI-XbaI	BamHI-NotI-SalI/XhoI	constructed by ligating the SalI-BamHI dcp2 fragment from HSE1815 to HFSE1636 digested by SalI-BamHI
HFSE1829	Bs-ks-dcp2-N630-KanMX6	NotI-XbaI	BamHI-NotI-SalI/XhoI	constructed by ligating the SalI-BamHI dcp2 fragment from HSE1817 to HFSE1636 digested by SalI-BamHI
HFSE1831	Bs-ks-dcp2-N475-KanMX6	NotI-XbaI	BamHI-NotI-SalI/XhoI	constructed by ligating the SalI-BamHI dcp2 fragment from HSE1819 to HFSE1636 digested by SalI-BamHI
HFSE1833	Bs-ks-dcp2-N400-KanMX6	NotI-XbaI	BamHI-NotI-SalI/XhoI	constructed by ligating the SalI-BamHI dcp2 fragment from HSE1821 to HFSE1636 digested by SalI-BamHI
HFSE1835	Bs-ks-dcp2-N300-KanMX6	NotI-XbaI	BamHI-NotI-SalI/XhoI	constructed by ligating the SalI-BamHI dcp2 fragment from HSE1823 to HFSE1636 digested by SalI-BamHI
HFSE1643	Bs-ks-HA-DCP2-WT-KanMX6	NotI-XbaI	BglII/BamHI-NotI-SalI/Xhol	constructed by ligating the SalI-BglII DCP2 fragment from HSE1638 to HFSE1636 digested by SalI-BamHI
HFSE1660	Bs-ks-HA-dcp2-E3D-KanMX6	NotI-XbaI	BglII/BamHI-NotI-SalI/XhoI	constructed by ligating the SalI-BglII dcp2 fragment from HSE1647 to HFSE1636 digested by SalI-BamHI
HFSE1663	Bs-ks-HA-dcp2-U1D1-KanMX6	NotI-XbaI	BglII/BamHI-NotI-SalI/XhoI	constructed by ligating the SalI-BglII dcp2 fragment from HSE1648 to HFSE1636 digested by SalI-BamHI
HFSE1678	Bs-ks-HA-dcp2-U1D2-KanMX6	NotI-XbaI	BglII/BamHI-NotI-SalI/XhoI	constructed by ligating the SalI-BglII dcp2 fragment from HSE1651 to HFSE1636 digested by SalI-BamHI
HFSE1681	Bs-ks-HA-dcp2-ID-KanMX6	NotI-XbaI	BglII/BamHI-NotI-SalI/XhoI	constructed by ligating the SalI-BglII dcp2 fragment from HSE1668 to HFSE1636 digested by SalI-BamHI
HFSE1683	Bs-ks-HA-dcp2-ID-U1D1-KanMX6	NotI-XbaI	BglII/BamHI-NotI-SalI/XhoI	constructed by ligating the SalI-BglII dcp2 fragment from HSE1671 to HFSE1636 digested by SalI-BamHI
HFSE1684	Bs-ks-HA-dcp2-ID-U1D2-KanMX6	NotI-XbaI	BglII/BamHI-NotI-SalI/XhoI	constructed by ligating the SalI-BglII dcp2 fragment from HSE1674 to HFSE1636 digested by SalI-BamHI
HFSE1687	Bs-ks-HA-dcp2-U1D1-U1D2-KanMX6	NotI-XbaI	BglII/BamHI-NotI-SalI/XhoI	constructed by ligating the SalI-BglII dcp2 fragment from HSE1677 to HFSE1636 digested by SalI-BamHI
HFSE1688	Bs-ks-HA-dcp2-E3D-U1D1-KanMX6	NotI-XbaI	BglII/BamHI-NotI-SalI/XhoI	constructed by ligating the SalI-BglII dcp2 fragment from HSE1654 to HFSE1636 digested by SalI-BamHI
HFSE1690	Bs-ks-HA-dcp2-E3D-U1D2-KanMX6	NotI-XbaI	BglII/BamHI-NotI-SalI/XhoI	constructed by ligating the SalI-BglII dcp2 fragment from HSE1657 to HFSE1636 digested by SalI-BamHI
HFSE1702	Bs-ks-HA-dcp2-E3D-ID-KanMX6	NotI-XbaI	BglII/BamHI-NotI-SalI/XhoI	constructed by ligating the SalI-BglII dcp2 fragment from HSE1692 to HFSE1636 digested by SalI-BamHI
HFSE1704	Bs-ks-HA-dcp2-E3D-ID-U1D1-KanMX6	NotI-XbaI	BglII/BamHI-NotI-SalI/XhoI	constructed by ligating the SalI-BglII dcp2 fragment from HSE1695 to HFSE1636 digested by SalI-BamHI
HFSE1706	Bs-ks-HA-dcp2-E3D-ID-U1D2-KanMX6	NotI-XbaI	BglII/BamHI-NotI-SalI/XhoI	constructed by ligating the SalI-BglII dcp2 fragment from HSE1697 to HFSE1636 digested by SalI-BamHI
HFSE1708	Bs-ks-HA-dcp2-E3D-U1D1-U1D2-KanMX6	NotI-XbaI	BglII/BamHI-NotI-SalI/XhoI	constructed by ligating the SalI-BglII dcp2 fragment from HSE1698 to HFSE1636 digested by SalI-BamHI
HFSE1711	Bs-ks-HA-dcp2-ID-U1D1-U1D2-KanMX6	NotI-XbaI	BglII/BamHI-NotI-SalI/XhoI	constructed by ligating the SalIBglII dcp2 fragment from HSE1700 to HFSE1636 digested by SalI-BamHI
HFSE1715	Bs-ks-HA-dcp2-E3D-ID-U1D1-U1D2-KanMX6	NotI-XbaI	BglII/BamHI-NotI-SalI/XhoI	constructed by ligating the SalI-BglII dcp2 fragment from HSE1713 to HFSE1636 digested by SalI-BamHI
HFSE1862	Bs-ks-HA-dcp2-E3D1-KanMX6	NotI-XbaI	BglII/BamHI-NotI-SalI/XhoI	constructed by ligating the SalI-BglII dcp2 fragment from HSE1842 to HFSE1636 digested by SalI-BamHI
HFSE1864	Bs-ks-HA-dcp2-E3D2-KanMX6	NotI-XbaI	BglII/BamHI-NotI-SalI/XhoI	constructed by ligating the SalI-BglII dcp2 fragment from HSE1843 to HFSE1636 digested by SalI-BamHI
HFSE1866	Bs-ks-HA-dcp2-LD1-KanMX6	NotI-XbaI	BglII/BamHI-NotI-SalI/XhoI	constructed by ligating the SalI-BglII dcp2 fragment from HSE1844 to HFSE1636 digested by SalI-BamHI
HFSE1868	Bs-ks-HA-dcp2-LD1-2-KanMX6	NotI-XbaI	BglII/BamHI-NotI-SalI/XhoI	constructed by ligating the SalI-BglII dcp2 fragment from HSE1850 to HFSE1636 digested by SalI-BamHI
HFSE1872	Bs-ks-HA-dcp2-LD1-3-KanMX6	NotI-XbaI	BglII/BamHI-NotI-SalI/XhoI	constructed by ligating the SalI-BglII dcp2 fragment from HSE1856 to HFSE1636 digested by SalI-BamHI
HFSE1874	Bs-ks-HA-dcp2-LD1-4-KanMX6	NotI-XbaI	BglII/BamHI-NotI-SalI/XhoI	constructed by ligating the SalI-BglII dcp2 fragment from HSE1858 to HFSE1636 digested by SalI-BamHI
HFSE1885	Bs-ks-HA-dcp2-LD1-5-KanMX6	NotI-XbaI	BglII/BamHI-NotI-SalI/XhoI	constructed by ligating the SalI-BglII dcp2 fragment from HSE1860 to HFSE1636 digested by SalI-BamHI
HFSE1887	Bs-ks-HA-dcp2-LD1-6-KanMX6	NotI-XbaI	BglII/BamHI-NotI-SalI/XhoI	constructed by ligating the SalI-BglII dcp2 fragment from HSE1878 to HFSE1636 digested by SalI-BamHI
HFSE1889	Bs-ks-HA-dcp2-LD1-7-KanMX6	NotI-XbaI	BglII/BamHI-NotI-SalI/XhoI	constructed by ligating the SalI-BglII dcp2 fragment from HSE1880 to HFSE1636 digested by SalI-BamHI
HFSE1922	Bs-ks-HA-dcp2-LD1-8-KanMX6	NotI-XbaI	BglII/BamHI-NotI-SalI/XhoI	constructed by ligating the SalI-BglII dcp2 fragment from HSE1912 to HFSE1636 digested by SalI-BamHI
HFSE1924	Bs-ks-HA-dcp2-LD1-9-KanMX6	NotI-XbaI	BglII/BamHI-NotI-SalI/XhoI	constructed by ligating the SalI-BglII dcp2 fragment from HSE1914 to HFSE1636 digested by SalI-BamHI
HFSE1927	Bs-ks-HA-dcp2-LD3-9-KanMX6	NotI-XbaI	BglII/BamHI-NotI-SalI/XhoI	constructed by ligating the SalI-BglII dcp2 fragment from HSE1910 to HFSE1636 digested by SalI-BamHI
HFSE2040	Bs-ks-HA-dcp2-LD9-KanMX6	NotI-XbaI	BglII/BamHI-NotI-SalI/XhoI	constructed by ligating the SalI-BglII dcp2 fragment from HSE1976 to HFSE1636 digested by SalI-BamHI
HFSE2042	Bs-ks-HA-dcp2-LD9-8-KanMX6	NotI-XbaI	BglII/BamHI-NotI-SalI/XhoI	constructed by ligating the SalI-BglII dcp2 fragment from HSE1978 to HFSE1636 digested by SalI-BamHI
HFSE2054	Bs-ks-HA-dcp2-LD9-7-KanMX6	NotI-XbaI	BglII/BamHI-NotI-SalI/XhoI	constructed by ligating the SalI-BglII dcp2 fragment from HSE1980 to HFSE1636 digested by SalI-BamHI
HFSE2052	Bs-ks-HA-dcp2-LD9-6-KanMX6	NotI-XbaI	BglII/BamHI-NotI-SalI/XhoI	constructed by ligating the SalI-BglII dcp2 fragment from HSE1982 to HFSE1636 digested by SalI-BamHI
HFSE2044	Bs-ks-HA-dcp2-LD9-5-KanMX6	NotI-XbaI	BglII/BamHI-NotI-SalI/XhoI	constructed by ligating the SalI-BglII dcp2 fragment from HSE1984 to HFSE1636 digested by SalI-BamHI
HFSE2046	Bs-ks-HA-dcp2-LD9-4-KanMX6	NotI-XbaI	BglII/BamHI-NotI-SalI/XhoI	constructed by ligating the SalI-BglII dcp2 fragment from HSE1986 to HFSE1636 digested by SalI-BamHI
HFSE2048	Bs-ks-HA-dcp2-LD9-3-KanMX6	NotI-XbaI	BglII/BamHI-NotI-SalI/XhoI	constructed by ligating the SalI-BglII dcp2 fragment from HSE1989 to HFSE1636 digested by SalI-BamHI
HFSE2050	Bs-ks-HA-dcp2-LD9-2-KanMX6	NotI-XbaI	BglII/BamHI-NotI-SalI/XhoI	constructed by ligating the SalI-BglII dcp2 fragment from HSE1990 to HFSE1636 digested by SalI-BamHI
HFSE2092	Bs-ks-HA-dcp2-E3D-LD1-8-KanMX6	NotI-XbaI	BglII/BamHI-NotI-SalI/XhoI	constructed by ligating the SalI-BglII dcp2 fragment from HSE2077 to HFSE1636 digested by SalI-BamHI
HFSE2094	Bs-ks-HA-dcp2-E3D-LD1-9-KanMX6	NotI-XbaI	BglII/BamHI-NotI-SalI/XhoI	constructed by ligating the SalI-BglII dcp2 fragment from HSE2078 to HFSE1636 digested by SalI-BamHI
HFSE2096	Bs-ks-HA-dcp2-E3D-LD9-3-KanMX6	NotI-XbaI	BglII/BamHI-NotI-SalI/XhoI	constructed by ligating the SalI-BglII dcp2 fragment from HSE2081 to HFSE1636 digested by SalI-BamHI
HFSE2098	Bs-ks-HA-dcp2-E3D-LD9-2-KanMX6	NotI-XbaI	BglII/BamHI-NotI-SalI/XhoI	constructed by ligating the SalI-BglII dcp2 fragment from HSE2083 to HFSE1636 digested by SalI-BamHI
HFSE2100	Bs-ks-HA-dcp2-E3D1-LD1-8-KanMX6	NotI-XbaI	BglII/BamHI-NotI-SalI/XhoI	constructed by ligating the SalI-BglII dcp2 fragment from HSE2084 to HFSE1636 digested by SalI-BamHI
HFSE2102	Bs-ks-HA-dcp2-E3D1-LD1-9-KanMX6	NotI-XbaI	BglII/BamHI-NotI-SalI/XhoI	constructed by ligating the SalI-BglII dcp2 fragment from HSE2086 to HFSE1636 digested by SalI-BamHI
HFSE2104	Bs-ks-HA-dcp2-E3D1-LD9-3-KanMX6	NotI-XbaI	BglII/BamHI-NotI-SalI/XhoI	constructed by ligating the SalI-BglII dcp2 fragment from HSE2089 to HFSE1636 digested by SalI-BamHI
HFSE2106	Bs-ks-HA-dcp2-E3D1-LD9-2-KanMX6	NotI-XbaI	BglII/BamHI-NotI-SalI/XhoI	constructed by ligating the SalI-BglII dcp2 fragment from HSE2091 to HFSE1636 digested by SalI-BamHI
HFSE2207	Bs-ks-HA-dcp2-U1D1-LD1-9-KanMX6	NotI-XbaI	BglII/BamHI-NotI-SalI/XhoI	constructed by ligating the SalI-BglII dcp2 fragment from HSE2157 to HFSE1636 digested by SalI-BamHI
HFSE2209	Bs-ks-HA-dcp2-U1D2-LD1-9-KanMX6	NotI-XbaI	BglII/BamHI-NotI-SalI/XhoI	constructed by ligating the SalI-BglII dcp2 fragment from HSE2158 to HFSE1636 digested by SalI-BamHI
HFSE2186	Bs-ks-HA-dcp2-U1D1-U1D2-LD1-9-KanMX6	NotI-XbaI	BglII/BamHI-NotI-SalI/XhoI	constructed by ligating the SalI-BglII dcp2 fragment from HFSE2161 to HFSE1636 digested by SalI-BamHI
HFSE2174	Bs-ks-HA-dcp2-E3D-LD1-LD1-9-KanMX6	NotI-XbaI	BglII/BamHI-NotI-SalI/XhoI	constructed by ligating the SalI-BglII dcp2 fragment from HFSE2162 to HFSE1636 digested by SalI-BamHI
HFSE2176	Bs-ks-HA-dcp2-E3D-U1D2-LD1-9-KanMX6	NotI-XbaI	BglII/BamHI-NotI-SalI/XhoI	constructed by ligating the SalI-BglII dcp2 fragment from HFSE2164 to HFSE1636 digested by SalI-BamHI
HFSE2178	Bs-ks-HA-dcp2-E3D-U1D1-U1D2-LD1-9-KanMX6	NotI-XbaI	BglII/BamHI-NotI-SalI/XhoI	constructed by ligating the SalI-BglII dcp2 fragment from HFSE2166 to HFSE1636 digested by SalI-BamHI
HFSE2180	Bs-ks-HA-dcp2-E3D1-U1D1-LD1-9-KanMX6	NotI-XbaI	BglII/BamHI-NotI-SalI/XhoI	constructed by ligating the SalI-BglII dcp2 fragment from HFSE2168 to HFSE1636 digested by SalI-BamHI
HFSE2182	Bs-ks-HA-dcp2-E3D1-U1D2-LD1-9-KanMX6	NotI-XbaI	BglII/BamHI-NotI-SalI/XhoI	constructed by ligating the SalI-BglII dcp2 fragment from HFSE2170 to HFSE1636 digested by SalI-BamHI
HFSE2184	Bs-ks-HA-dcp2-E3D1-U1D1-U1D2-LD1-9-KanMX6	NotI-XbaI	BglII/BamHI-NotI-SalI/XhoI	constructed by ligating the SalI-BglII dcp2 fragment from HFSE2172 to HFSE1636 digested by SalI-BamHI
HFSE1645	Bs-ks-HA-DCP2-WT-M1(S-N)	SalI	BglII-NotI	HA-DCP2 fragment from HFSE1638 to Bs-ks digested by SalI-NotI
HFSE1647	Bs-ks-HA-dcp2-E3D(S-N)	SalI	BglII-NotI	constructed by site-directed mutagesis using the plasmid HFSE1645 as template and the oligonucleotides DCP2-E3D2-F/DCP2-E3D-R as PCR primers
HFSE1668	Bs-ks-HA-dcp2-ID(S-N)	SalI	BglII-NotI	constructed by site-directed mutagesis using the plasmid HFSE1645 as template and the oligonucleotides DCP2-ID-F/DCP2-ID-R as PCR primers
HFSE1648	Bs-ks-HA-dcp2-U1D1(S-N)	SalI	BglII-NotI	constructed by site-directed mutagesis using the plasmid HFSE1645 as template and the oligonucleotides DCP2-U1D1-F1/DCP2-U1D-R1 as PCR primers
HFSE1651	Bs-ks-HA-dcp2-U1D2(S-N)	SalI	BglII-NotI	constructed by site-directed mutagesis using the plasmid HFSE1645 as template and the oligonucleotides DCP2-U1D-F2/DCP2-U1D-R2 as PCR primers
HFSE1671	Bs-ks-HA-dcp2-ID-U1D1(S-N)	SalI	BglII-NotI	constructed by site-directed mutagesis using the plasmid HFSE1648 as template and the oligonucleotides DCP2-ID-F/DCP2-ID-R as PCR primers
HFSE1674	Bs-ks-HA-dcp2-ID-U1D2(S-N)	SalI	BglII-NotI	constructed by site-directed mutagesis using the plasmid HFSE1651 as template and the oligonucleotides DCP2-ID-F/DCP2-ID-R as PCR primers
HFSE1677	Bs-ks-HA-dcp2-U1D1-U1D2(S-N)	SalI	BglII-NotI	constructed by site-directed mutagesis using the plasmid HFSE1648 as template and the oligonucleotides DCP2-U1D-F2/DCP2-U1D-R2 as PCR primers
HFSE1700	Bs-ks-HA-dcp2-ID-U1D1-U1D2(S-N)	SalI	BglII-NotI	constructed by site-directed mutagesis using the plasmid HFSE1677 as template and the oligonucleotides DCP2-ID-F/DCP2-ID-R as PCR primers
HFSE1654	Bs-ks-HA-dcp2-E3D-U1D1(S-N)	SalI	BglII-NotI	constructed by ligating the 5' NheI-XhoI dcp2 fragment from HFSE1647 and the 3' XhoI-NotI dcp2 fragment from HFSE1648 to HFSE1645 digested by NheI-NotI
HFSE1657	Bs-ks-HA-dcp2-E3D-U1D2(S-N)	SalI	BglII-NotI	constructed by ligating the 5' NheI-XhoI dcp2 fragment from HFSE1647 and the 3' XhoI-NotI dcp2 fragment from HFSE1651 to HFSE1645 digested by NheI-NotI
HFSE1692	Bs-ks-HA-dcp2-E3D-ID(S-N)	SalI	BglII-NotI	constructed by ligating the 5' NheI-XhoI dcp2 fragment from HFSE1647 and the 3' XhoI-NotI dcp2 fragment from HFSE1668 to HFSE1645 digested by NheI-NotI
HFSE1695	Bs-ks-HA-dcp2-E3D-ID-U1D1(S-N)	SalI	BglII-NotI	constructed by ligating the 5' NheI-XhoI dcp2 fragment from HFSE1647 and the 3' XhoI-NotI dcp2 fragment from HFSE1671 to HFSE1645 digested by NheI-NotI
HFSE1697	Bs-ks-HA-dcp2-E3D-ID-U1D2(S-N)	SalI	BglII-NotI	constructed by ligating the 5' NheI-XhoI dcp2 fragment from HFSE1647 and the 3' XhoI-NotI dcp2 fragment from HFSE1674 to HFSE1645 digested by NheI-NotI
HFSE1698	Bs-ks-HA-dcp2-E3D-U1D1-U1D2(S-N)	SalI	BglII-NotI	constructed by ligating the 5' NheI-XhoI dcp2 fragment from HFSE1647 and the 3' XhoI-NotI dcp2 fragment from HFSE1677 to HFSE1645 digested by NheI-NotI
HFSE1713	Bs-ks-HA-dcp2-E3D-ID-U1D1-U1D2(S-N)	SalI	BglII-NotI	constructed by ligating the 5' NheI-XhoI dcp2 fragment from HFSE1647 and the 3' XhoI-NotI dcp2 fragment from HFSE1700 to HFSE1645 digested by NheI-NotI
HFSE1842	Bs-ks-HA-dcp2-E3D1(S-N)	SalI	BglII-NotI	constructed by site-directed mutagesis using the plasmid HFSE1645 as template and the oligonucleotides DCP2-ED1-F/DCP2-ED1-R as PCR primers
HFSE1843	Bs-ks-HA-dcp2-E3D2(S-N)	SalI	BglII-NotI	constructed by site-directed mutagesis using the plasmid HFSE1645 as template and the oligonucleotides DCP2-ED2-F/DCP2-ED2-R as PCR primers
HFSE1844	Bs-ks-HA-dcp2-LD1(S-N)	SalI	BglII-NotI	constructed by site-directed mutagesis using the plasmid HFSE1645 as template and the oligonucleotides DCP2-LD1-F/DCP2-LD1-R as PCR primers
HFSE1850	Bs-ks-HA-dcp2-LD1-2(S-N)	SalI	BglII-NotI	constructed by site-directed mutagesis using the plasmid HFSE1844 as template and the oligonucleotides DCP2-LD2-F/DCP2-LD2-R as PCR primers

HFSE1852	Bs-ks-HA-dcp2-LD3(S-N)	SalI	BglII-NotI	constructed by site-directed mutagesis using the plasmid HFSE1645 as template and the oligonucleotides DCP2-LD3-F/DCP2-LD3-R as PCR primers
HFSE1854	Bs-ks-HA-dcp2-LD3-5(S-N)	SalI	BglII-NotI	constructed by site-directed mutagesis using the plasmid HFSE1852 as template and the oligonucleotides DCP2-LD5-F/DCP2-LD5-R as PCR primers
HFSE1871	Bs-ks-HA-dcp2-LD3-6(S-N)	SalI	BglII-NotI	constructed by site-directed mutagesis using the plasmid HFSE1854 as template and the oligonucleotides DCP2-LD6-F/DCP2-LD6-R as PCR primers
HFSE1877	Bs-ks-HA-dcp2-LD3-7(S-N)	SalI	BglII-NotI	constructed by site-directed mutagesis using the plasmid HFSE1871 as template and the oligonucleotides DCP2-LD7-F/DCP2-LD7-R as PCR primers
HFSE1909	Bs-ks-HA-dcp2-LD3-8(S-N)	SalI	BglII-NotI	constructed by site-directed mutagesis using the plasmid HFSE1877 as template and the oligonucleotides DCP2-LD8-F3/DCP2-LD8-R3 as PCR primers
HFSE1882	Bs-ks-HA-dcp2-LD3-7-9(S-N)	SalI	BglII-NotI	constructed by site-directed mutagesis using the plasmid HFSE1877 as template and the oligonucleotides DCP2-LD9-F/DCP2-LD9-R as PCR primers
HFSE1910	Bs-ks-HA-dcp2-LD3-9(S-N)	SalI	BglII-NotI	constructed by site-directed mutagesis using the plasmid HFSE1882 as template and the oligonucleotides DCP2-LD8-F3/DCP2-LD8-R3 as PCR primers
HFSE1856	Bs-ks-HA-dcp2-LD1-3(S-N)	SalI	BglII-NotI	constructed by ligating the 5' NheI-NdeI dcp2 fragment from HFSE1850 and the 3' NdeI-NotI dcp2 fragment from HFSE1845 to HFSE1645 digested by NheI-NotI
HFSE1858	Bs-ks-HA-dcp2-LD1-4(S-N)	SalI	BglII-NotI	constructed by ligating the 5' NheI-NdeI dcp2 fragment from HFSE1850 and the 3' NdeI-NotI dcp2 fragment from HFSE1852 to HFSE1645 digested by NheI-NotI
HFSE1860	Bs-ks-HA-dcp2-LD1-5(S-N)	SalI	BglII-NotI	constructed by ligating the 5' NheI-NdeI dcp2 fragment from HFSE1850 and the 3' NdeI-NotI dcp2 fragment from HFSE1854 to HFSE1645 digested by NheI-NotI
HFSE1878	Bs-ks-HA-dcp2-LD1-6(S-N)	SalI	BglII-NotI	constructed by ligating the 5' NheI-NdeI dcp2 fragment from HFSE1850 and the 3' NdeI-NotI dcp2 fragment from HFSE1871 to HFSE1645 digested by NheI-NotI
HFSE1880	Bs-ks-HA-dcp2-LD1-7(S-N)	SalI	BglII-NotI	constructed by ligating the 5' NheI-NdeI dcp2 fragment from HFSE1850 and the 3' NdeI-NotI dcp2 fragment from HFSE1877 to HFSE1645 digested by NheI-NotI
HFSE1912	Bs-ks-HA-dcp2-LD1-8(S-N)	SalI	BglII-NotI	constructed by ligating the 5' NheI-NdeI dcp2 fragment from HFSE1850 and the 3' NdeI-NotI dcp2 fragment from HFSE1909 to HFSE1645 digested by NheI-NotI
HFSE1914	Bs-ks-HA-dcp2-LD1-9(S-N)	SalI	BglII-NotI	constructed by ligating the 5' NheI-NdeI dcp2 fragment from HFSE1850 and the 3' NdeI-NotI dcp2 fragment from HFSE1910 to HFSE1645 digested by NheI-NotI
HFSE1976	Bs-ks-HA-dcp2-LD9(S-N)	SalI	BglII-NotI	constructed by site-directed mutagesis using the plasmid HFSE1645 as template and the oligonucleotides DCP2-LD9-F/DCP2-LD9-R as PCR primers
HFSE1978	Bs-ks-HA-dcp2-LD9-8(S-N)	SalI	BglII-NotI	constructed by site-directed mutagesis using the plasmid HFSE1976 as template and the oligonucleotides DCP2-LD8-F3/DCP2-LD8-R3 as PCR primers
HFSE1980	Bs-ks-HA-dcp2-LD9-7(S-N)	SalI	BglII-NotI	constructed by site-directed mutagesis using the plasmid HFSE1978 as template and the oligonucleotides DCP2-LD7-F/DCP2-LD7-R as PCR primers
HFSE1982	Bs-ks-HA-dcp2-LD9-6(S-N)	SalI	BglII-NotI	constructed by site-directed mutagesis using the plasmid HFSE1980 as template and the oligonucleotides DCP2-LD6-F/DCP2-LD6-R as PCR primers
HFSE1984	Bs-ks-HA-dcp2-LD9-5(S-N)	SalI	BglII-NotI	constructed by site-directed mutagesis using the plasmid HFSE1982 as template and the oligonucleotides DCP2-LD5-F/DCP2-LD5-R as PCR primers
HFSE1986	Bs-ks-HA-dcp2-LD9-4(S-N)	SalI	BglII-NotI	constructed by site-directed mutagesis using the plasmid HFSE1984 as template and the oligonucleotides DCP2-LD4-F/DCP2-LD4-R as PCR primers
HFSE1989	Bs-ks-HA-dcp2-LD9-3(S-N)	SalI	BglII-NotI	constructed by site-directed mutagesis using the plasmid HFSE1986 as template and the oligonucleotides DCP2-LD3-R as PCR primers
HFSE1990	Bs-ks-HA-dcp2-LD9-2(S-N)	SalI	BglII-NotI	constructed by site-directed mutagesis using the plasmid HFSE1989 as template and the oligonucleotides DCP2-LD2-F/DCP2-LD2-R as PCR primers
HFSE2077	Bs-ks-HA-dcp2-E3D-LD1-8(S-N)	SalI	BglII-NotI	constructed by ligating the 5' NheI-XhoI dcp2 fragment from HFSE1647 and the 3' XhoI-NotI dcp2 fragment from HFSE1912 to HFSE1645 digested by NheI-NotI
HFSE2078	Bs-ks-HA-dcp2-E3D-LD1-9(S-N)	SalI	BglII-NotI	constructed by ligating the 5' NheI-XhoI dcp2 fragment from HFSE1647 and the 3' XhoI-NotI dcp2 fragment from HFSE1914 to HFSE1645 digested by NheI-NotI
HFSE2081	Bs-ks-HA-dcp2-E3D-LD9-3(S-N)	SalI	BglII-NotI	constructed by ligating the 5' NheI-XhoI dcp2 fragment from HFSE1647 and the 3' XhoI-NotI dcp2 fragment from HFSE1989 to HFSE1645 digested by NheI-NotI
HFSE2083	Bs-ks-HA-dcp2-E3D-LD9-2(S-N)	SalI	BglII-NotI	constructed by ligating the 5' NheI-XhoI dcp2 fragment from HFSE1647 and the 3' XhoI-NotI dcp2 fragment from HFSE1990 to HFSE1645 digested by NheI-NotI
HFSE2084	Bs-ks-HA-dcp2-E3D1-LD1-8(S-N)	SalI	BglII-NotI	constructed by ligating the 5' NheI-XhoI dcp2 fragment from HFSE1842 and the 3' XhoI-NotI dcp2 fragment from HFSE1914 to HFSE1645 digested by NheI-NotI
HFSE2086	Bs-ks-HA-dcp2-E3D1-LD1-9(S-N)	SalI	BglII-NotI	constructed by ligating the 5' NheI-XhoI dcp2 fragment from HFSE1842 and the 3' XhoI-NotI dcp2 fragment from HFSE1914 to HFSE1645 digested by NheI-NotI
HFSE2089	Bs-ks-HA-dcp2-E3D1-LD9-3(S-N)	SalI	BglII-NotI	constructed by ligating the 5' NheI-XhoI dcp2 fragment from HFSE1842 and the 3' XhoI-NotI dcp2 fragment from HFSE1989 to HFSE1645 digested by NheI-NotI

Table S3 Oligonucleotides used in this study

Name	Sequence
DCP2-NcoI-F(4032)	ATATCCATGGTATCGACTTTTGGCCAAACC
DCP2-DS4(B-N-S)	GATCGTCGACGCGGCCGCAGATCTGCAAGATTCAAAATTAGGGCAATCTCACACA
DCP2-DS4(BH-N-S)	GATCGTCGACGCGGCCGCGGATCCGCAAGATTCAAAATTAGGGCAATCTCACACA
DCP2-E3D-F	CAGAGGCAAATAAAAAATGAAGATGCTAACAGTAATAATAATGCGGTC
DCP2-E3D-R	GACCGCATTATTATTACTGTTAGCATCTTCATTTTTTATTTGCCTCTG
DCP2-U1D-F1	AATTCGAAAAAGCCTGACAGCAACATCAAGCAAAACAATAATGATGAA

DCP2-U1D-F2	ACTGTCGGGTTATCATCAACAACACTGGCGAATGATAAAAAAGCTTTT
DCP2-U1D-R2	AAAAGCTTTTTTATCATTCGCCAGTGTTGTTGATGATAACCCGACAGT
DCP2-ID-F	CCGTTTGCTAACAATAAGAATGTTAACAATAGTAATAGCGCTAACCCT
DCP2-ID-R	AGGGTTAGCGCTATTACTATTGTTAACATTCTTATTGTTAGCAAACGG
DCP2-ED1-F	CAGAGGCAAATAAAAAATGAAGATAAGGAGGAGCAGATTGATCCCGGT
DCP2-ED1-R	ACCGGGATCAATCTGCTCCTCCTTATCTTCATTTTTTATTTGCCTCTG
DCP2-ED2-F	TTGAAATTGTTGTTGGGTATCACTGCTAACAGTAATAATAATGCGGTC
DCP2-ED2-R	GACCGCATTATTATTACTGTTAGCAGTGATACCCAACAACAATTTCAA
DCP2-LD1-F	TACAGCAGCTCCTCCCCTGGGCAGAATTCGAAAAAGCCTGACAGCAAC
DCP2-LD1-R	GTTGCTGTCAGGCTTTTTCGAATTCTGCCCAGGGGAGGAGCTGCTGTA
DCP2-LD2-F	ACTGCTCATTCAAACTCTCAAGCTAAAAAACCAACATCATCGCAGAAG
DCP2-LD2-R	CTTCTGCGATGATGTTGGTTTTTTAGCTTGAGAGTTTGAATGAGCAGT
DCP2-LD3-F	TCCAATGTGTCTTCATCAAAAGATAGAAACCCAATTTCCTCTACTGTA
DCP2-LD3-R	TACAGTAGAGGAAATTGGGTTTCTATCTTTTGATGAAGACACATTGGA
DCP2-LD4-F	ATAAACGATGCGAATGCAAGCGAAAAACAAAAGGAAAAAGACATTACA
DCP2-LD4-R	TGTAATGTCTTTTTCCTTTTGTTTTTCGCTTGCATTCGCATCGTTTAT
DCP2-LD5-F	TCGCAGAAAAATTCAGCTAAAGGAAAAAGAACGACTCTACCGGGTAC
DCP2-LD5-R	GTACCCGGTAGAGTCGTTCTTTTTTCCTTTAGCTGAATTTTTCTGCGA
DCP2-LD6-F	GAATTAGATAAGAATTCAACAGAGAAGCCCAAGCCTCTTAATGATGGG
DCP2-LD6-R	CCCATCATTAAGAGGCTTGGGCTTCTCTGTTGAATTCTTATCTAATTC
DCP2-LD7-F	TCAAATAAGGACAGTTCTCATGAACATGGTAATAAAAACAGCAGCGCC
DCP2-LD7-R	GGCGCTGCTGTTTTTATTACCATGTTCATGAGAACTGTCCTTATTTGA
DCP2-LD9-F	AATGGAACTTCAGGGTCTAATGAACATAGGAAGTGAAAGAATAAGTGT
DCP2-LD9-R	ACACTTATTCTTTCACTTCCTATGTTCATTAGACCCTGAAGTTCCATT
DCP2-LD9-F2	TCGAATGGAACTTCAGGGTCTAATGAACATAGGAAGTGAAAGAATAAGTGTTAT
DCP2-LD9-R2	ATAACACTTATTCTTTCACTTCCTATGTTCATTAGACCCTGAAGTTCCATTCGA
DCP2-LD8-F3	GCATCTGATAACAACGAAAATTCCTCAAATAAACAAAACAGGTCTAGTGCAATAAATGAGCCCAAC
DCP2-LD8-R3	GTTGGGCTCATTTATTGCACTAGACCTGTTTTGTTTATTTGAGGAATTTTCGTTGTTATCAGATGC
DCP2-F598	GATAAGATAGAATGGTTCGATTTT
DCP2-F1198	CCGAATCCGATGGCTTTTGGTGTT
DCP2-F1798	TCGACTCAGAGTAAACAGAATTCA
DCP2-F2398	AAACAAAAGGAAAAAGACATTACA
DCP2-R700	ACATTGATAAGGGTCTCATCATGG
DCP2-R1300	CAGAGTCCCTCGGTAAAGGAGCAG
DCP2-R1900	AACTGCTTTCGAAGACTTCATATG
DCP2-R2500	TCTTTTTCAAAATATTCAACAATC
DCP2-R3000	TTATTTATTTAGCAATGTATTTTA
DCP2-F1171	CCGGTCCCCCCTAATTTTAATGCTCCT
DCP2-F2047	ATAAACGAAACTGTCGGGTTATCATCA
DCP2-F2074	ACAACAAATACTGTAAAAAGGTA
DCP2-F2557	TCAATGAAACGCAACGACGCTACAAAT
DCP2-R1551	ATTTGGTAAAAAGGAAGTATCTGGTTT
DCP2-R2556	CGTTGACATTTCACTTGACGGTCCACC
DCP2-R2964	TCGGCTGCCTTCATTTACAGTGTGTCT
DCP2-XbaI-F	GATCTCTAGAGCATCCTTGGTAAGAATATCTCCC
DCP2-NcoI-R	TACTCCATGGTCTAATGCGAAGGTACTTTTATTTTTTTC
DCP2-N210-E1-R	GATCGAATTCAATTTTCTTAAAATCGAACCATTCTATCTT
DCP2-TH-F1	GATCGGATCCATATGTCACTGCCGCTACGACACGCATTGGAG
DCP2-TH-C1	GATCGTCGACCCATGGTTACTCTTGGCTCGAGGGTACCTGTCCGTTGGA

DCP2-DS5	TGATTAACCTGGGGGTTACCTAAAGAGAACA
DCP2-DS6	AATCCATCCAATTGGTTAAATAGGATCACA
YEL015W-1	AATTGCGGCCGCGGTCAACAGGTTGCTCGAAAAGAAGCA
YEL015W-4	AATTGTCGACGCTCAGTTCCTGTCTTCGTAGGATTGG
XRN1-DS5	CGCCACCGCAGAGCAAGTAACAACAGAGAC
XRN1-DS6	ACTGCCTCGAGTCTGACGATAGAAGACCCT
SKI2-DS1	ATTATCTTCAACGACTGAGAAGAATGAGCA
SKI2-DS4	AATACCATTTTCGCCTATCTTACCGACAGT
SKI7-atg-up500	AACTGGATATTGTAGCGCCTAGCGTCCTCA
PAT1-DS5	AATTTATCGGCTAACAACTGTGACAGTTGC
PAT1-DS6	TGTAACCCACCACACATGCCATGGTGATCG
SCD6-DS5	CAGACTCTAGAGTTAACATTGATGATATGCT
SCD6-DS6	GCCGAATATCGCTAGCTTCGAAGTTATGTAA
CYH2-NotI-F	GATCGCGGCCGCATGCCTTCCAGATTCACTAAGACTAGAAAG
CYH2-SalI-R	GATCGTCGACTTAAGCGATCAATTCAACAACACCACCAGC
XRN1-DS3A	AAAAAGATCTGAATTCAACATACGACTAAAAACGAAGTATATT
XRN1-DS4	AAAAGTCGACAGAAGACCCTGCAATAACATTTACACA
XRN1-5'-BamHI-F	CCCTGCTAGCGGATCCATATGGGTATTCCAAAATTTTTCAGGTACA
XRN1-5'-SacI-R	TCTGAATCTACGAGCTCTTTGTTGATTCAT

Table S4. Sequences of DNA probes used in this study

CYH2

gcggccgcatgccttccagattcactaagactagaaagcacagaggtcacgtctcaggtatgtagttccatttggaagag
ggaatgaaagaaccaagacggtgactttttttttagtgttgtgcaaccaatatgtcgtgtgtatatcatggtacaggaga
atgtcaatcagctaagtgtactcaacatatttctttgtgttttgattgcgaactttgtattaccatctcactgttgagac
ggcttatttgaggtaatagctcgagtaaatgtactcttccatcgcaaactgagcaaaaagaaagtgtgcatagcctttgt
catacttctcctttattataccatgatattcagaacagtcatactgtctactcattttacggctataaaaggtaactttc
atttagattatggaaagcactaattatcgctgtatcaaatggttgtagagagcgcaattatgaaaaagagttaccacgtt
tcttttgtttcgataaaatgtccagttgaaaacctgttttactaacgatttaaaaattgtatttcattacaatatttttt
ttgtacagccggtaaaggtcgtatcggtaagcacagaaagcaccccggtggtagaggtatggccggtggtcaacatcacc
acagaattaacatggataaataccatccaggttatttcggtaaggttggtatgagatacttccacaagcaacaagctcat
ttctggaagccagtcttgaacttggacaaattgtggacattgatcccagaagacaagagagaccaatacttgaaatctgc
ttctaaggaaactgctccagttattgacactttggcagccggttacggtaagatcttgggtaagggtagaattccaaatg
ttccagttatcgtcaaagctagattcgtctccaagttggctgaagaaaaaatcagagctgctggtggtgttgttgaattg
atcgcttagtcgaca

CAN1

ggatccagtttttaatctgtcgtcaatcgaaagtttatttcagagttcttcagacttcttaactcctgtaaaaacaaaaa
aaaaaaaaggcatagcaatgacaaattcaaaagaagacgccgacatagaggagaagcatatgtacaatgagccggtcaca
accctctttcacgacgttgaagcttcacaaacacaccacagacgtgggtcaataccattgaaagatgagaaaagtaaaga
attgtatccattgcgctctttcccgacgagagtaaatggcgaggatacgttctctatggaggatggcataggtgatgaag
atgaaggagaagtacagaacgctgaagtgaagagagagcttaagcaaagacatattggtatgattgcccttggtggtact
attggtacaggtcttttcattggtttatccacacctctgaccaacgccggcccagtgggcgctcttatatcatatttatt
tatgggttctttggcatattctgtcacgcagtccttgggtgaaatggctacattcatccctgttacatcctctttcacag
ttttctcacaaagattcctttctccagcatttggtgcggccaatggttacatgtattggttttcttgggcaatcactttt
gccctggaacttagtgtagttggccaagtcattcaattttggacgtacaaagttccactggcggcatggattagtatttt
ttgggtaattatcacaataatgaacttgttccctgtcaaatattacggtgaattcgagttctgggtcgcttccatcaaag
ttttagccattatcgggtttctaatatactgtttttgtatggtttgtggtgctggggttaccggcccagttggattccgt
tattggagaaacccaggtgcctggggtccaggtataatatctaaggataaaaacgaaggggaggttcttaggttgggtttc
ctctttgattaacgctgccttcacatttcaaggtactgaactagttggtatcactgctggtgaagctgcaaaccccagaa
aatccgttccaagagccatcaaaaaagttgtttttccgtatcttaaccttctacattggctctctattattcattggactt
ttagttccatacaatgaccctaaactaacacaatctacttcctacgtttctacttctcccctttattattgctattgagaa
ctctggtacaaaggtttttgccacatatcttcaacgctgttatcttaacaaccattatttctgccgcaaattcaaatattt
acgttggttcccgtatttttatttggtctatcaaagaacaagttggctcctaaattcctgtcaaggaccaccaaaggtggt
gttccatacattgcagttttcgttactgctgcatttggcgctttggcttacatggagacatctactggtggtgacaaagt
tttcgaatggctattaaatatcactggtgttgcaggctttttttgcatggttatttatctcaatctcgcacatcagattta
tgcaagctttgaaataccgtggcatctctcgtgacgagttaccatttaaagctaaattaatgcccggcttggcttattat
gcggccacatttatgacgatcattatcattattcaaggtttcacggcttttgcaccaaaattcaatggtgttagctttgc
tgccgcctatatctctattttcctgttcttagctgtttggatcttatttcaatgcatattcagatgcagatttatttgga
agattggagatgtcgac

ADE2

agatctgaattaattcggattcatgcttatgggttagctatttcgcccaatgtgtccatctgacattactattttgcatt
ttaatttaattagaacttgactagcgcactaccagtatatcatctcatttccgtaaataccaaatgtattatatattgaa
agcttttgaccaggttattataaaagaaacttcatgctcgaaaaagatcatttcgaaaagttgcctagtttcatgaaatt

ttaaaagcagtttatataaattttacctttttgatgcggaattgactttttcttgaataatacataactttttcttaaaagaa
tcaaagacagataaaatttaagagatattaaatattagtgagaagccgagaattttgtaacaccaacataacactgacat
ctttaacaacttttaattatgatacatttcttacgtcatgattgattattacagctatgctgacaaatgactcttgttgc
atggctacgaaccgggtaatactaagtgattgactcttgctgaccttttattaagaactaaatggacaatattatggagc
atttcatgtataaattggtgcgtaaaatcgttggatctctcttctaagtacatcctactataacaatcaagaaaaacaag
aaaatcggacaaaacaatcaagtatggattctagaacagttggtatattaggaggggggacaattgggacgtatgattgtt
gaggcagcaaacaggctcaacattaagacggtaatactagatgctgaaaattctcctgccaaacaaataagcaactccaa
tgaccacgttaatggctcctttccaatcctcttgatatcgaaaaactagctgaaaaatgtgatgtgctaacgattgaga
ttgagcatgttgatgttcctacactaaagaatcttcaagtaaaacatcccaaattaaaaatttacccttctccagaaaca
atcagattgatacaagacaaatatattcaaaaagagcatttaatcaaaaatggtatagcagttacccaaagtgttcctgt
ggaacaagccagtgagacgtccctattgaatgttggaagagatttgggtttttccattcgtcttgaagtcgaggactttgg
catacgatggaagaggtaacttcgttgtaaagaataaggaaatgattccggaagctttggaagtactgaaggatcgtcct
ttgtacgccgaaaaatgggcaccatttactaaagaattagcagtcatgattgtgagatctgttaacggtttagtgttttc
ttacccaattgtagagactatccacaaggacaatatttgtgacttatgttatgcgcctgctagagttccggactccgttc
aacttaaggcgaagttgttggcagaaaatgcaatcaaatcttttcccggttgtggtatatttggtgtggaaatgttctat
ttagaaacaggggaattgcttattaacgaaattgccccaaggcctcacaactctggacattataccattgatgcttgcgt
cacttctcaatttgaagctcatttgagatcaatattggatttgccaatgccaaagaatttcacatctttctccaccatta
caacgaacgccattatgctaaatgttcttggagacaaacatacaaaagataaagagctagaaacttgcgaaagagcattg
gcgactccaggttcctcagtgtacttatatggaaaagagtctagacctaacagaaaagtaggtcacataaatattattgc
ctccagtatggcggaatgtgaacaaaggctgaactacattacaggtagaactgatattccaatcaaaatctctgtcgctc
aaaagttggacttggaagcaatggtcaaaccattggttggaatcatcatgggatcagactctgacttgccggtaatgtct
gccgcatgtgcggttttaaaagatttggcgttccatttgaagtgacaatagtctctgctcatagaactccacataggat
gtcagcatatgctatttccgcaagcaagcgtggaattaaaacaattatcgctggagctggtggggctgctcacttgccag
gtatggtggctgcaatgacaccacttcctgtcatcggtgtgcccgtaaaaggttcttgtctagatggagtagattcttta
cattcaattgtgcaaatgcctagaggtgttccagtagctaccgtcgctattaataatagtacgaacgctgcgctgttggc
tgtcagactgcttggcgcttatgattcaagttatacaacgaaaatggaacagttttattaaagcaagaagaagaagttc
ttgtcaaagcacaaaagttagaaactgtcggttacgaagcttatctagaaaacaagtaatatataagtttattgatatac
ttgtacagcaaataattataaaatgatatacctatttttttaggctttgttatgattacatcaaatgtggacttcatacat
agaaatcaacgcttacaggtgtcctttttttaagaatttcatacataagatct

TRP1

atgtctgttattaatttcacaggtagttctggtccattggtgaaagtttgcggcttgcagagcacagaggccgcagaatg
tgctctagattccgatgctgacttgctgggtattatatgtgtgcccaatagaaagagaacaattgacccggttattgcaa
ggaaaatttcaagtcttgtaaaagcatataaaaatagttcaggcactccgaaatacttggttggcgtgtttcgtaatcaa
cctaaggaggatgtttggctctggtcaatgattacggcattgatatcgtccaactgcatggagatgagtcgtggcaaga
ataccaagagttcctcggtttgccagttattaaaagactcgtatttccaaaagactgcaacatactactcagtgcagctt
cacagaaacctcattcgtttattcccttgtttgattcagaagcaggtgggacaggtgaactttggattggaactcgatt
tctgactgggttggaaggcaagagagccccgaaagcttacattttatgttagctggtggactgacgccagaaaatgttgg
tgatgcgcttagattaaatggcgttattggtgttgatgtaagcggaggtgtggagacaaatggtgtaaaagactctaaca
aaatagcaaatttcgtcaaaaatgctaagaaatag

YRA1

agatctaaaaatctccctcgttctatttgaaactttaagaaatccatattaagaaaatacctacatctgctaaatgtctg
ctaacttagataaatccttagacgaaatcattggctctaacaaagcaggaagtaatagagcccgtgtcggtggtactcgt
ggtaacggtccaagaagagttggtaagcaagttggtagccaacgtaggagccttccaaacagaagaggccctatcagaaa
aaatactagggcacctccaaacgcagtcgctagagttgccaagctcttggacaccactagagaggtcaaggtcaacgtcg
aaggtttgccaagggacattaagcaggatgctgtaagagtatgttaatacgtgaaatgagagctatttgtttagttactc

gcatcgtctcgtgtggatacgagaaatattctttgtaaggaaggatatggcacacgcttttgatcaagaattctcttttt
agagatgaagaaagagtccgaaatacttcgctagagaaatacaaaaagagtatcgttttcataagccaaccataccaat
tttttttcaatacttcaaatcatggcctataaggttggaattaccagctaccactgagaatgggtttgttcttattggctg
ggttaactcaaatcaatctgactatctgctaatctgtcaatcttacattttttaagctggcgtattgtgtcgcctcgaccg
tgatagttagttcctatttttaataagcgtatcatccaatactgaagttgtggaaggatcaattaattttgtatcctttc
aagagggagtagctttcagtttcgaatggcaccattttcaaaaaatagctatgggaaacatgtctttcatgaacgttcga
aaagatatgagtgcatcgcttcattttttttattatgatagttacaaaaatatttgatttgagacacctaatgaaaccaaa
gaggaactcacccatcgtggtacatgtttatttgagggtttattttttcctacgcaatggtatactttttaatactctcaac
tccttgattgtttgtgtattgtcccttccttctttgattttatatcatagagatatatgactaacttttttttttttttatt
ataggaattttttgcatctcaagtaggtggtgttcaaagagtttttgttgagttataacgaaaggggccaatctactggta
tggctaacatcacattcaaaaacggtgaattggccagaagggctgttgaaagatttaacggctctccaatcgatggaggc
agatcaagattgagacttaacctaatcgttgatccaaaccaacgcccagtcaaaagtttagccgacaggatcaaggctat
gccacaaaaaggcggaaacgctccaagaccagtaaagaggggtccaaatagaaaagctgctatggcaaaatcccaaaaca
aaccaaagagagaaaagcctgctaagaaaagtcttgaagatct

RPS28B

gctagcatggattctaagaccccagtcaccttagctaaagtcatcaaagtttttaggccgtaccggttctcgtggtggtgttacca
agttcgtgttgagttcttggaagacacttcccgtaccattgtcagaaatgtcaagggtccagttagagaaaacgacatttt
tggtcttgatggaatctgaacgtgaagctcgtcgtttgcgttaaaggtatattaaaaaatttactattggtgctcttcga
gcattgtttttttttctatatttacaaacaacagcttattttttaatatttctcaaaaaatgaagttcgaatgattatttt
aattgagtttagtgatgaaatcgattgcaaataatataaacgttggtaagctcatctaaacaatcgaaaggagggataga
agacagtaggtgtttgtgctttggtcggtttttccattcggtgaattcatacatctcctttattaattttaatggattct
ttacaagggattttcggttgccaaaaacagagaacaaatgcgtagaaatactcaatgatgtcaattttcaaaaaatgaa
ttaaatgattgaagtcacttaattttgtggtttttggaggtgggttgagtgtacaactcactataattgatgagatat
tcgacgaacttgttactttttggattccagaatgtttactgaattttaagaattaattaatttgaggctaacctgtatg
gcatggaataacgaatcgacaagaagtctcttactgtaactttctttttttttttggtgcatctatcgttaaatacaattta
aatattacattcatgtacttactcaatataataatctgattacttcatacaatagaagagaaagaaacagtctctaaaac
tgctgtcataacgcgt

EDC1

atgtcgacggataccatgtatttcaacagctccaggctgttgccatcggctggcaggaacaagacaaataatctaatcaa
acaaaaaactagaaataatcgtgcgaggggaaatgctgctaagaacgccaataataacaactatatcacagatataccac
ctcctcaaactcttcctaacggtcagaaacctaacttcggccattcttccaacaagaaaccatcatttaatcaaaagaag
cactctccaccttcttccccttcctctacaactactttaggtaaaaaaaacagacagaataataaagaaacgccacgaca
gaacaacaaagatgatactcgtttactgagtcagaacctaaagaatctgcttctgaaccagaaacaatccccgcatggct
ctcaagggataataccaatgggttgtaatggcagtgccaaaaaactcagtcactcttatgcaggctccactttcgccact
aatggtccaagggaggctaaaaacttgcccaaaccaagtt

SDS23

atgcctcaaaatacaagacacacgtccatcgtagaaatgctttctaccccacctcaattaccgaattccacagatttaaa
tagtttgagcgaacagacagacaagaacactgaagcaaacaaaagcgacacagaatcactacataaatctatttcgaaat
cgtcatcttcatcttctctctccacgctggataacacggaatactcaaacaataatggcaactccttgtccaccttgaat
tcacagaatctgttatctgttcataggcaggagtggcaacacactcctctgtcaaatttggtggaacagaacaaattgat
tttcatcagaggttctatttccgtagaggaagcattcaacacgctggtcaagcaccagctaacgtctttgcctgtggaga
attttccgggagacatgaattgtttaacattcgactataatgatctcaatgcgtaccttcttcttgtattaaacaggatc
aaggtgagcaacgacaagat

HXT6

atgtcacaagacgctgctattgcagagcaaactcctgtggagcatctctctgctgttgactcagcctcccactcggtttt
atctacaccatcaaacaaggctgaaagagatgaaataaaagcttatggtgaaggtgaagagcacgaacctgtcgttgaaa
ttccaaagagaccagcttctgcctatgtcactgtctctattatgtgtatcatgatcgcctttggtggtttcgttttcggt
tgggatactggtaccatttctggtttcatcaatcaaaccgatttcatcagaagatttggtatgaagcataaagatggtac
taattatttgtctaaggttagaactggtttgattgtctccattttcaacattggttgtgccattggtggtattattcttt
ccaaattgggtgatatgtacggtcgtaaggtgggtttgattgtcgttgttgtcatctacatcatcggtat

HSP12

atgtctgacgcaggtagaaaaggattcggtgaaaaagcttctgaagctttgaagccagactctcaaaagtcatacgctga
acaaggtaaggaatacatcactgacaaggccgacaaggtcgctggtaaggttcaaccagaagacaacaagggtgtcttcc
aaggtgtccacgactctgccgaaaaaggcaaggataacgctgaaggtcaaggtgaatctttggcagaccaagctagagat
tacatgggagccgccaagtccaagttgaacgatgccgtcgaatatgtttccggtcgtgtccacggtgaagaagacccaac
caagaagtaa

HSP26

agaggctacgcaccaagacgtcagttagcaaacacacccgcaaaggattctactggcaaggaagttgctagaccaaataa
ctatgctggcgctctttatgatcccagagatgaaaccttagatgattggttcgacaatgacttgtccctgttcccatctg
gtttcggtttccctagaagtgtcgcagttccagttgatattttggaccatgacaacaactacgagttgaaagtcgtggtt
cctggtgtcaaaagcaagaaggacattgatattgagtaccatcaaaacaagaaccaaattttggtttctggtgaaattcc
atctaccttgaatgaagagagtaaagacaaggtcaaggtcaaggagagcagctctggtaagttcaagagagtcatcactt
tgccagactacccaggtgtggatgcagacaacattaaagcagactacgcaaatggtgtttttgacattaacagttccaaaa
ttgaagcctcagaaggatggtaagaaccacgtcaagaagattgaggtttcttctcaagaatcgtggggta

LSM3

atggagacacctttggatttattgaaactcaatctcgatgagagggtgtacatcaagctgcgcggggccaggacgctggt
gggcacactgcaagcgttcgactcacactgcaacatcgtgctgagtgatgcagtagagaccatataccaattaaacaacg
aggagttgagtgagtccgaaagacgatgtgaaatggtgttcatcagaggagacacagtgactctaatcagcacgccctct
gaagatgacgatggcgcagtggagatataa

BUR6

atggcagatcaagtaccagttacaacacaactaccaccaataaaacctgaacatgaggtaccacttgatgctggagggag
tccagtaggtaacatgggtaccaactcgaataacaacaacgagctaggtgatgtattcgacagaataaagacacacttcc
ctccggccaaggtaaagaaaataatgcagacagacgaggatataggaaaagtttcacaagccacgcccgtaatagcgggc
aggtccctagagtttttttatagcgttattggtgaaaaaaagcggggagatggcaagaggacaaggaaccaagagaataac
cgccgaaatactaaaaaaaacaattttaaacgacgaaaaattcgatttcttaagggaaggtctatgcgtagaagaaggcc
aaacacaaccggaggaagagagtgcctga

DIF1

atggacgcacaactggaatgggcaagcagcctcgtcccaaagagacagcttcaacaacaacaacaacaacaggagcagca
gcagcagcagcaacaggatttccacaaggaccagttgatgactgtgggtatgcgaatcagacagcgggtcgaccagggtt
atgcatcgaggacgccgagcacctcggacgcttcactacagccgggtgtcattagagattactcgagcgttattgttccg
caatttacaaggtcgcccttgcccactgctaactcgctaccacctatgctgataaaccagagaacaatgtcgaccgaggc
gtcctcgctcgagaaatgggacgtcgcggaacctgccgcggagcacgaaacaatggttaatggatccaagagaagacttt

CHA1

atgtcgatagtctacaataaaacaccattattacgtcaattcttccccggaaaggcttctgcacaattttttcttgaaata

tgaatgccttcaaccaagtggctccttcaaaagtagaggaatcggtaatctcatcatgaaaagtgccattcgaattcaaa
aggacggtaaaagatctcctcaggttttcgctagttctggcggtaatgccggttttgctgctgcaacagcatgtcaaaga
ctgtctctaccatgtacagtcgtggttcctacagcgacaaagaagagaatggtagataaaatcaggaacaccggtgccca
ggttatcgtgagtggtgcctactggaaagaagcagatactttttaaaaacaaatgtcatgaataaaatagactctcagg
tcattgagcccatttatgttcatcccttcgataatccggatatttgggaaggacattcatctatgatagatgaaatagta
caagatttgaaatcgcaaca

AGA1

atgacattatctttcgctcattttacctacctgttcacaatattgttgggattaactaatattgccttggcatctgatcc
agaaacgattctagtgacgataaccaagacaaacgatgcaaatggggttgttacaactacagtttcacccgcgctagtct
ccacatccactatcgttcaagctggcactacgacattgtatacgacttggtgtccattgacggtatccacttcatctgct
gccgaaataagtccttcaatatcgtacgctactaccctatccagatttagtactttgacattatctacagaagtctgctc
ccatgaggcatgtccttcgtcatcgacgttgccaaccaccaccttatctgtgacttccaagttcacttcatatatttgcc
ctacttgtcacacaaccgctatcagctcattatccgaagtaggaactacaaccgtggtatcatccagcgccattgaacca
tcaagtgcctctataatctc

CPA1

tatgattacagaattcaagatgttgcttctgaattcgacggtattttcttatccaatggaccaggcaacccagaactatg
ccaagctacaatttccaacgtcagggaattactaaataaccctgtttatgactgtatccctattttgggatttgtctag
gccatcaactcttggctctggcctccggtgcctctactcacaaattgaaatatggtaatagggctcacaacatccctgcc
atggatttgactaccggccagtgccacattacatctcaaaatcatggctatgcagttgatcctgagaccctaccaaagga
ccaatggaaaccttattttgttaatttaaacgacaaatcaaacgaaggcatgatacaccttcaaagacccatattttcta
cccaatttcacccagaggcaaaaggtggtcccttagacacagctattctttttgacaaattcttcgataatatagaaaaa
taccaattacaatctcaggcaaaaagttcaatctcactaaaagtaacatacagtaccgataaatcgagattgcagagtat
aaatgttactaagttggccaaggaaagagtgttgttctaa

EST1

gaatgtgttctgcgaattagatcaataatattttctggcatgaaattttagagaaaaatgacaccggcgtcatatggaa
tgccagcaaatataagtttgatttaataagcccaaatattaaaataaaacgccaaatagcattatcggaaatttcctcca
aaataaatgtaaaaacacaacaggaaagagtagtctcttcgagaaaagttgaggccaaaagagatgaacaacagcgcaaa
agagccgggaaaatagctgtgacagaactggaaaaacaatttgcaaatgtccggagaacaaaaaaattgtctccgctccc
agaaaaagatggcgtttcttctgagttggtaaaacatgctgcttcacgagggagaaaaactatcactggcccactatcct
ctgattttctctcatatccagacgaagcaattgatgctgatgaggacatcaccgtccaagtgccagatactcct

RPS9A

gagcccccaagaacatattccaagacttactctaccccaaagagaccttacgaatcttctcgtttggacgcagaattgaag
ttggccggtgaattcggtttgaagaacaagaaggaaatttacagaatttccttccagttatctaagattcgtcgtgctgc
aagagacttgttgacaagagacgaaaaggacccaaagagattgttcgaaggtaatgctttgattaggagactagttagag
tcggtgtttatccgaagataagaagaagttagattatgttttagccttgaaggtcgaagatttcttggaaagaagattg
caaactcaagtctacaagctaggtttagccaagtctgtccaccatgcaagagtttaatcactcaaaggcacattgctgt
tggtaagcaaattgtcaacatcccctctttcatggtcagattggactctgagaagcacattgactttgctccaacatctc
cattcggtggtgctagaccaggcagagttgctagaagaaatgctgcaaggaaggcggaagcttctggtgaagctgctgat
gaagctgatgaggccgatgaagaataa